

CHAPTER 11

SUMMARY OF THE PRESENT WORK AND THE FUTURE SCOPE

11.1 SUMMARY

Modern technology needs perfect single crystals for various applications. Progress in solid-state sciences depends upon the availability of perfect crystalline materials. The gel method holds substantial promise in obtaining single crystals suitable for scientific investigations. This method is found to be the most appropriate one to grow single crystals of tartrate compounds and so has been employed to grow rare earth ($R = \text{Ho, Gd, Yb}$) tartrate crystals.

The growth of well defined single crystals of holmium tartrate trihydrate, gadolinium tartrate trihydrate and ytterbium tartrate trihydrate single crystals was achieved by controlled diffusion of the respective rare earth ions through organic (agar-agar) as well as in inorganic (silica) gels impregnated with tartrate ions. The effects of various growth parameters like gel concentration, gel pH, gel age and concentration of reactants on the growth kinetics were studied. It is reported that the pH of silica gel had a profound effect on the morphology of the grown crystals. In case of holmium tartrate, silica gel pH ≤ 3.75 leads to single crystal growth whereas for gadolinium tartrate, single crystals are observed to grow at gel pH ≤ 3.5 . In both the cases crystals assumed spherulitic morphology for gel pH ≥ 4 . In case of ytterbium tartrate, single crystal growth occurs at silica gel pH ≤ 3 whereas for gel pH ≥ 3.5 crystals assume spherulitic morphology. Use of agar-agar gel at pH = 2 yields single crystals in all the three types of rare earth tartrates. The morphological form of single crystals is dipyramidal with the major habit faces as $\{111\}$ and $\{001\}$ irrespective of the rare earth ($R = \text{Ho, Gd, Yb}$) involved in the growth of their corresponding tartrates. The experimental results obtained for the crystal count on the variation of growth parameters (gel pH, gel age, upper reactant concentration and gel concentration) suggests that the crystals grown in silica gel follow classical laws of three-dimensional nucleation. Spherulitic growth of holmium, ytterbium and gadolinium tartrates is also studied in the present work.

Scanning electron microscopic studies reveal that the spherulitic formation of holmium and ytterbium nitro-tartrates result due to crystal fibres diverging radially from multiple nuclei originating from the centrally located amorphous/non-crystalline base

The grown crystals are characterized by various methods. The crystallinity of samples is confirmed by X-ray powder diffraction. Single crystal X-ray diffraction experiments carried out on single crystals of holmium and gadolinium tartrate trihydrate show that both the crystals belong to tetragonal system bearing non-centrosymmetric space group $P4_1$. The cell parameters for holmium and gadolinium tartrate trihydrate crystals are respectively, $a = 5.9701 \text{ \AA}$, $c = 36.089 \text{ \AA}$ and $V = 1286.28 \text{ \AA}^3$ and $a = 6.0201 \text{ \AA}$, $c = 36.3719 \text{ \AA}$ and $V = 1318.17 \text{ \AA}^3$. In case of ytterbium tartrate trihydrate the cell parameters were worked out from their X-ray powder diffraction results. The cell parameters of ytterbium tartrate trihydrate are computed to be; $a = 5.885 \text{ \AA}$, $c = 35.80 \text{ \AA}$, $\alpha = \beta = \gamma = 90^\circ$ and $V = 1239.86 \text{ \AA}^3$. Fourier transform infra red spectroscopic studies carried out on the grown crystals of holmium, gadolinium and ytterbium tartrate trihydrate show the presence of tartrate ligands and it establishes that one of the tartrate ions is singly ionized. Elemental and thermogravimetric analysis supplemented by energy dispersive analysis of X-rays suggests the stoichiometric composition of the grown crystals to be $R(C_4H_4O_6)(C_4H_5O_6) \cdot 3H_2O$ (where $R = Ho, Gd, Yb$). The thermal studies, using thermoanalytical techniques, support the proposed chemical formula and it is concluded that the single crystals of holmium, gadolinium and ytterbium tartrates contain three coordinated water molecules. Scanning electron microscopic studies reveal that the single crystals grown in the present work maintain their growth by two dimensional 'layer by layer' mechanisms.

The thermal behaviour of single crystals of holmium, gadolinium and ytterbium tartrate trihydrates is studied using thermoanalytical techniques like TGA/DTG and DTA. The experimental results show that single crystals of holmium, gadolinium and ytterbium tartrate trihydrate are thermally stable up to a temperature of about 220°C , 205°C and 200°C respectively. Non-isothermal decomposition kinetics of holmium and ytterbium tartrate trihydrate has been used to determine the values of kinetic parameters viz, activation energy and frequency factor and the same is described and discussed in the thesis.

Studies are extended to some physical properties of the grown samples. The dielectric studies are carried out and it is found that the crystals of holmium gadolinium and ytterbium tartrate trihydrates show anomalous dielectric behaviour. The dielectric constant increases with the temperature and attains a peak value near about 240 °C (for gadolinium tartrate trihydrate), 250 °C (for holmium tartrate trihydrate) and 215 °C (for ytterbium tartrate trihydrate) after which it decreases, suggesting these crystals to be ferroelectric in nature. A vibration sample magnetometer is used to determine the magnetic susceptibility of all the three variety of crystals by measuring the magnetic moments. The effective magnetic moment is calculated for each sample of the rare earth tartrate trihydrate crystals and the values are observed to be in good agreement with the theoretical values of the respective free rare earth ions. It also establishes that the tartrate ligands make negligible contribution to the magnetic moment of the crystals.

11.2 Scope for further research

The present work describes and discusses the growth, characterization and some properties of rare earth tartrates of the type $R(C_4H_4O_6)(C_4H_5O_6) \cdot 3H_2O$ (where $R = Ho, Gd, Yb$) as has been summarized above. The studies on single crystals of rare earth tartrates reveal that they have a lot of potential in various applications due to their ferroelectric, magnetic and non-linear optical properties. The anomalous behaviour of the dielectric constant of gadolinium, holmium and ytterbium tartrate trihydrate crystals near the transition temperature as described in the concerned chapters of this thesis, indicate the possibility of these materials being ferroelectric. The results on the study of thermal behaviour of these crystals also support this argument. However, in order to further confirm the ferroelectric property of these materials, it is required that hysteresis curves (saturation polarization versus electric field) of the samples are recorded and studied. Therefore, there is a further scope in investigating the ferroelectric behaviour of these materials. Preliminary single crystal X-ray diffraction results have indicated that the crystals of rare earth tartrate trihydrates grown in the present work belong to tetragonal system bearing the non-centrosymmetric space group $P4_1$. However, detailed study of crystal structure leading to knowledge regarding position of constituent atoms in the lattice is required to be worked out.

Recent advances in nonlinear optics (NLO) have created a new frontier for applied optics. This technology requires nonlinear optical materials, i.e., materials which alter the frequency of laser light, materials which have an index of refraction that varies with light intensity or with applied electrical field, or (in the case of photorefractive nonlinear optical materials) materials which have a local index of refraction that is changed by the spatial variation of light intensity. Rare earth tartrate trihydrate crystals grown in the present work (in which a rare earth ion is coordinated to asymmetric conjugate organic molecules i.e. tartrate ions) bear the non-centrosymmetric space $P4_1$. Therefore, there is a possibility of these types of materials to show non-linear optical properties like second harmonic generation. Such materials have the potential for their use in the optical nonlinear devices. The non-linear optical properties of these materials are required to be studied in detail which has a scope for further research work on these materials. Perfection of the crystals grown during the present investigation is another area of study, wherein surface (viz., etching) and bulk (X-ray topography) methods may be used for detection and study of defects.

REPRINTS OF PUBLISHED/ACCEPTED PAPERS

1. Crystal growth and characterization of gadolinium tartrate trihydrate: $Gd(C_4H_4O_6)(C_4H_5O_6) \cdot 3H_2O$.
Basharat Want, Farooq Ahmad and P.N. Kotru (2006)
Mater. Sci. and Engg A, **431**, 237-247. **A1**
2. Growth of ytterbium tartrate trihydrate crystals in silica and agar-agar gels and their characterization
Basharat Want, Farooq Ahmad and P. N. Kotru, (2006)
Cryst.Res.Technol, **41**,1167-1173. **A2**
3. Dielectric characterization of gadolinium tartrate trihydrate crystals
Basharat Want, Farooq Ahmad and P.N. Kotru (2007)
Mater. Sci. and Engg. A, **443**, 270-276. **A3**
4. Magnetic moment measurements of gadolinium, holmium and ytterbium tartrate trihydrate crystals.
Basharat Want, Farooq Ahmad and P.N. Kotru (2007)
J. Alloys Comp., **In Press, Corrected Proof**. **A4**
5. Single crystal growth and characterization of holmium tartrate trihydrate
Basharat Want, Farooq Ahmad and P.N. Kotru (2007)
J. Cryst. Growth, **299**, 336-343. **A5**
6. Dielectric and thermal characteristics of holmium tartrate trihydrate crystals.
Basharat Want, Farooq Ahmad and P. N. Kotru, (2007)
Cryst. Res. Technol.,**42**,822-828. **A6**
7. Dielectric and thermal behaviour of gel grown ytterbium tartrate trihydrate crystals.
Basharat Want, Farooq Ahmad and P. N. Kotru,
J. Mater. Sci. (2007) **Accepted** **A7**



Crystal growth and characterization of gadolinium tartrate trihydrate: $Gd(C_4H_4O_6)(C_4H_5O_6) \cdot 3H_2O$

Basharat Want^{a,1}, Farooq Ahmad^a, P.N. Kotru^{b,*}

^a Department of Physics, University of Kashmir, Srinagar 190006, J&K, India

^b Department of Physics and Electronics, University of Jammu, Jammu 180006, India

Received 15 March 2006; received in revised form 26 May 2006; accepted 2 June 2006

Abstract

The growth of gadolinium tartrate trihydrate crystals is achieved in silica and agar-agar gels. The crystals are grown by diffusion of gadolinium ions through silica and agar-agar gels impregnated with *t*-tartaric acid. The type of medium influences the morphology of grown crystals: silica gel yielding single crystals and spherulites whereas agar-agar gel leads to growth of only single crystals. The grown crystals are characterized using energy dispersive analysis of X-rays (EDAX), carbon and hydrogen analysis (CHN), X-ray powder diffraction (XRD), Fourier transform infrared (FT-IR) spectroscopy, thermogravimetric (TG), differential thermogravimetric (DTG) and differential thermal analysis. The chemical formula of the grown crystals is suggested to be $Gd(C_4H_4O_6)(C_4H_5O_6) \cdot 3H_2O$. The infrared spectrum indicates the presence of tartrate ligands and suggests that one of the tartrate ions is singly ionized. The thermal analysis shows that the material is thermally stable up to about 205 °C.
© 2006 Elsevier B.V. All rights reserved.

Keywords: Gadolinium tartrate trihydrate crystals; Gel method; Crystal morphology; Spherulitic growth; Thermal stability

1. Introduction

Crystal growth from gels [1,2] is an inexpensive and simple technique for growing single crystals of materials that show poor solubility in water. The method involves diffusion of two reagents in a gel at a reasonably slow and controlled rate to yield a sparingly soluble reaction product. By preventing convection currents or turbulences and remaining chemically inert, the gel medium provides a three-dimensional structure in which the crystal nuclei are delicately held in the position of their formation. Moreover, as the crystals grow at low temperature, there is reason to believe the presence of minimum equilibrium defects.

Most tartrate compounds have shown to exhibit interesting physical properties such as ferroelectricity, piezoelectricity and optical second harmonic generation, etc. [3–8]. Consequently, some of them are used in transducers and several linear and non-linear mechanical devices [3,4,6]. Many investigators have grown single crystals of tartrate compounds by gel method and

studied their characteristics [9–11]. Rare earth tartrates bearing the general formula $R_2(C_4H_4O_6)_x \cdot xH_2O$ ($R = Nd, Dy, Gd, La, Di, Pr, Sm$ and Y) have been grown by gel diffusion method using silica hydrogel as a medium of growth [12–18]. In the present study, we report the growth and characterization of single as well as spherulitic crystals of gadolinium tartrate trihydrate bearing the chemical formula $Gd^{3+}(C_4H_4O_6)^{2-}(C_4H_5O_6)^{1-} \cdot 3H_2O$, which suggests that there are three water molecules bonded to gadolinium and the tartrate is disordered between a doubly and singly ionized species. Therefore, the gadolinium tartrate trihydrate crystals grown here are different from those reported in the literature [19,13]. Pastorek [19] reported the material to have five waters of hydration whereas Kotru et al. [13] reported the growth of dihydrated gadolinium tartrate spherulites by gel method bearing the formula $Gd_2(C_4H_4O_6)_3 \cdot 2H_2O$. The crystals grown during the present study are isomorphous with erbium ditartrate trihydrate, yttrium tartrate hydrate and samarium tartrate trihydrate reported in the literatures [20–22]. In this paper, we also present the results obtained by powder X-ray diffraction, EDAX, FT-IR spectroscopy, elemental analysis (CHN), thermo-analytical techniques such as thermogravimetry (TG), differential thermogravimetry (DTG) and differential thermal analysis (DTA) of gadolinium tartrate trihydrate crystals.

* Corresponding author. Tel.: +91 191 2450939; fax: +91 191 2453079.

E-mail address: pn.kotru@yahoo.com (P.N. Kotru).

¹ Present address: Crystal Growth and Materials Research Laboratory, Department of Physics and Electronics, University of Jammu, Jammu 180006, India

2. Experimental procedure

2.1. Growth

Rare earth tartrates show poor solubility in water, they decompose before melting, and do not vaporize or sublime. Consequently, the only alternative to grow single crystals of these materials is by chemical reaction at a controlled rate using gel diffusion method. Therefore, crystallization of gadolinium tartrate trihydrate was accomplished using the gel diffusion technique. The crystallizer consisted of a single glass tube of length 20 cm and diameter 2.5 cm. The crystals were grown in two types of gels: an inorganic (silica) gel and an organic (agar-agar) gel. The silica gel was prepared by adding a solution of sodium metasilicate (0.5–1 M) to *t*-tartaric acid (0.25–1 M), drop by drop with continuous stirring to avoid excessive local ion concentration, which may cause premature local gelling and make the final solution inhomogeneous. The pH of the gel was adjusted between a value of 3–6 by mixing the tartaric acid and sodium metasilicate solutions in various proportions by volume. The solution with the desired value of pH was then transferred to several glass tubes. The gel was found to set in 30 min to 20 days, depending upon its pH and the environmental temperature. Once gelled, an aqueous solution of gadolinium nitrate (0.5–2 M) was carefully poured with the help of a pipette over the set gel in order to avoid any gel breakage. The Gd^{3+} ions diffuse slowly through the narrow pores of the gel to react with the tartrate ions, giving rise to the formation of spherulites and single crystals of $Gd(C_4H_4O_6)(C_4H_5O_6) \cdot 3H_2O$. Experiments were also carried out to grow single crystals of gadolinium tartrate trihydrate from organic agar-agar gel. The agar-agar gel was prepared by dissolving 0.8–1.6% (w/v) of agar-agar in water. The agar-agar solution was then mixed with *t*-tartaric acid (0.25–1 M) in various proportions by volume. The mixed solution, whose pH was kept at a value of 2 by adding few drops of dilute nitric acid, was then transferred to several glass tubes. After the setting of gel, an aqueous solution of gadolinium nitrate (0.5–2 M) was carefully poured over it. The tubes were allowed to stand for a period of about 4 weeks, after which small single crystals of $Gd(C_4H_4O_6)(C_4H_5O_6) \cdot 3H_2O$ grew in the whole gel column. All the experiments were carried out in the temperature range of 35–37 °C.

2.2. Characterization

The single crystals of $Gd(C_4H_4O_6)(C_4H_5O_6) \cdot 3H_2O$ were characterized by using X-ray powder diffraction, EDAX, carbon and hydrogen analysis (CHN), optical and scanning electron microscopy (SEM), FT-IR spectroscopy, and thermo-analytical techniques such as TG, DTG and DTA.

The powder XRD patterns of $Gd(C_4H_4O_6)(C_4H_5O_6) \cdot 3H_2O$ were obtained using a Bruker D8 advance X-ray diffractometer with Cu K α radiation ($\lambda = 1.5406 \text{ \AA}$). The C and H contents in the obtained crystals were determined by using Vario-EL III CHNS-analyzer. An energy dispersive spectrometer (OXFORD ISIS-300 system) attached to a scanning electron microscope JEOL JSM-5800 was used to identify the presence of gadolinium.

The FT-IR spectra of the material in the wave number range of 400–4000 cm^{-1} were recorded on a Bruker Vector 22 spectrometer using KBr pellet technique. The thermal behavior (TGA, DTG and DTA) of the crystals was recorded on a Shimadzu DTG 60 thermal analyzer in N_2 atmosphere at a heating rate of 10 °C/min. The morphology of the grown crystals was examined using an optical microscope (EpiGnost of Carl Zeiss, Germany), a large incident light microscope (Neophot-2 of Carl Zeiss, Germany) and a scanning electron microscope (HITACHI S-3000H).

3. Results and discussion

3.1. Growth

The type of medium influences the morphology of grown crystals: silica gel yielding single and spherulitic crystals whereas agar-agar gel leading to growth of only single crystals. The results on growth and morphology of crystals grown in silica and agar-agar gel are described as follows:

3.1.1. Growth in silica gel

Table 1 gives a detailed summary of the experiments and results on morphology, size and nucleation density of spherulites of $Gd(C_4H_4O_6)(C_4H_5O_6) \cdot 3H_2O$ grown in silica gel. The results in Table 1 show that for silica gel, a gel pH of 3 and 3.5 yields single crystals and for a pH ≥ 4 , the crystals attain spherulitic morphology.

3.1.1.1. Spherulitic growth. Spherulites are spherical aggregates of crystallites. They consist of radially oriented micro crystals arranged at non-crystallographic angles within a spherical envelope. A typical spherulite is described as needles, fibers, or ribbons fanning out from the centre with extensive branching. They are commonly observed in the freezing of viscous melts at high undercoolings and in solution growth involving chemical reactions (including gel growth) at high supersaturations. They occur in a variety of materials, including polymers [23,24], elemental selenium [25,26], liquid crystals [27,28] and inorganic materials [29,30]. However, there is no generally accepted theory of spherulite crystallization, a number of phenomenological models and necessary physical conditions for this process have been suggested by many authors. The first conception of spherulitic growth was given by Keith and Padden [31]. They proposed that spherulitic growth is connected to diffusion fields that arise during segregation of impurities into the melt. According to them high viscosity and presence of impurities are the basic requirement for spherulitic crystal growth in melts. According to Bolotov and Maravev [32], a spherulite grows from a single crystal nucleus, drawn out in a direction perpendicular to c -axis lying in the plane of the crystal, the circular shape arising due to surface tension forces acting on the different faces. Felton and Griffiths [33] showed that spherulitic crystallization results due to lamellas or crystalline fibers growing radially from a common centre or a nucleus. The occurrence of "secondary" nucleation at the growth front has also been emphasized as an essential feature of spherulite formation in polymeric fluids [34].

Table 1
Detailed summary of experiments^a for the growth of spherulites of $\text{Gd}_2(\text{C}_2\text{O}_4)_3 \cdot 3\text{H}_2\text{O}$ in silica gel

Experiment	Constant parameters	Variable parameters	Results
1 Variation of gel pH	Gel concentration: 0.5 M, UR ^b concentration: 1 M, LR ^c concentration: 0.5 M, gel age ^d : 3 days	Gel pH: 3, 3.5, 4, 5 and 6	Morphology: (i) single crystals with well-developed {001} and {111} faces at pH 3 and 3.5; (ii) normal and coalesced spherulites for gel pH = 4. Size: (i) maximum size of spherulites at pH 4 (diameter ~3 mm); Nucleation density: maximum at pH 3 and minimum at gel pH 6
2 Variation of UR concentration	Gel concentration: 0.5 M, LR concentration: 0.5 M, gel pH: 4, gel age: 3 days	Upper reactant concentration: 0.5, 0.75, 1 and 2 M	Morphology: (i) normal and coalesced spherulites. Size: maximum size of normal spherulites at the UR concentration of 1 M (diameter ~4 mm); Nucleation density: maximum at UR concentration of 2 M and minimum at 0.5 M
3 Variation of LR concentration	Gel concentration: 0.5 M, UR concentration: 1 M, gel pH: 4, gel age: 3 days	Lower reactant concentration: 0.25, 0.5, 0.75 and 1 M	Morphology: normal and coalesced spherulites. Size: maximum size of spherulites at LR concentration 1 M (diameter ~3 mm); Nucleation density: maximum at LR concentration 1 M and minimum at 0.25 M
4 Variation of gel concentration	LR concentration: 0.5 M, UR concentration: 1 M, gel pH: 4, gel age: 3 days	Gel concentration: 0.5, 0.75 and 1 M	Morphology: normal and coalesced spherulites. Size: maximum size of spherulites at gel concentration of 0.5 M (diameter ~3 mm); Nucleation density: maximum at gel concentration of 0.5 M and minimum at 1 M
5 Variation of gel age	Gel concentration: 0.5 M, UR concentration: 1 M, LR concentration: 0.5 M, gel pH: 4	Gel age: 1, 2, 3, 5, and 10 days	Morphology: normal and coalesced spherulites. Size: maximum size of spherulites at a gel age of 3 days (diameter ~3 mm); Nucleation density: maximum at gel age of 1 day and minimum at 10 days

^a All experiments were performed in the temperature range of 35–37 °C.

^b UR = upper reactant (gadolinium nitrate).

^c LR = lower reactant (L-tartaric acid).

^d The time between the setting of gel and pouring of upper reactant.

Random lamellar branching with preferred crystallographic misorientation ("non-crystallographic branching") is also observed to be responsible for spherulitic growth [35]. In gel diffusion method, the growth of crystals takes place due to the chemical reaction between the reagents at a controlled rate. However, if the value of supersaturation at any point in the gel becomes very high, it results in the formation of spherulites. Under isothermal conditions, the supersaturation in gels depends on many factors like concentration of reactants, gel pH and gel age. Among these factors, the gel pH has a profound effect on the formation of spherulites. Although, supersaturation could be controlled by taking low concentration of reactants, but it was observed that the decrease in concentration of reactants, to control supersaturation, had an adverse effect on the growth. For instance, at low concentration of reactants (0.1 and 0.2 M) the nucleation and consequent growth of crystals of reasonable size took over 6

months. The formation of spherulites of gadolinium tartrate may be discussed as follows. As soon as the upper reactant (gadolinium nitrate) is poured over the set gel containing tartrate ions, there is an instantaneous reaction between the gadolinium and tartrate ions resulting in the spontaneous formation of a precipitate. It was observed that the strength of precipitation depends on the gel pH, higher the pH stronger is the precipitation (other parameters of growth like upper and lower reactant concentrations, gel age and gel concentration remaining the same). Under the conditions of strong precipitation, the supersaturation available for three-dimensional nucleation and growth becomes very high which results in the formation of spherulites in gels. The most important contributing factor is the increased concentration of precipitant ions ($\text{C}_2\text{H}_4\text{O}_6^{2-} \rightleftharpoons \text{C}_4\text{H}_4\text{O}_6^{4-}$) at high pH values (here for $\text{pH} \geq 4$) [36]. In addition, as the pH increases the gel structure changes from a box like network to a structure

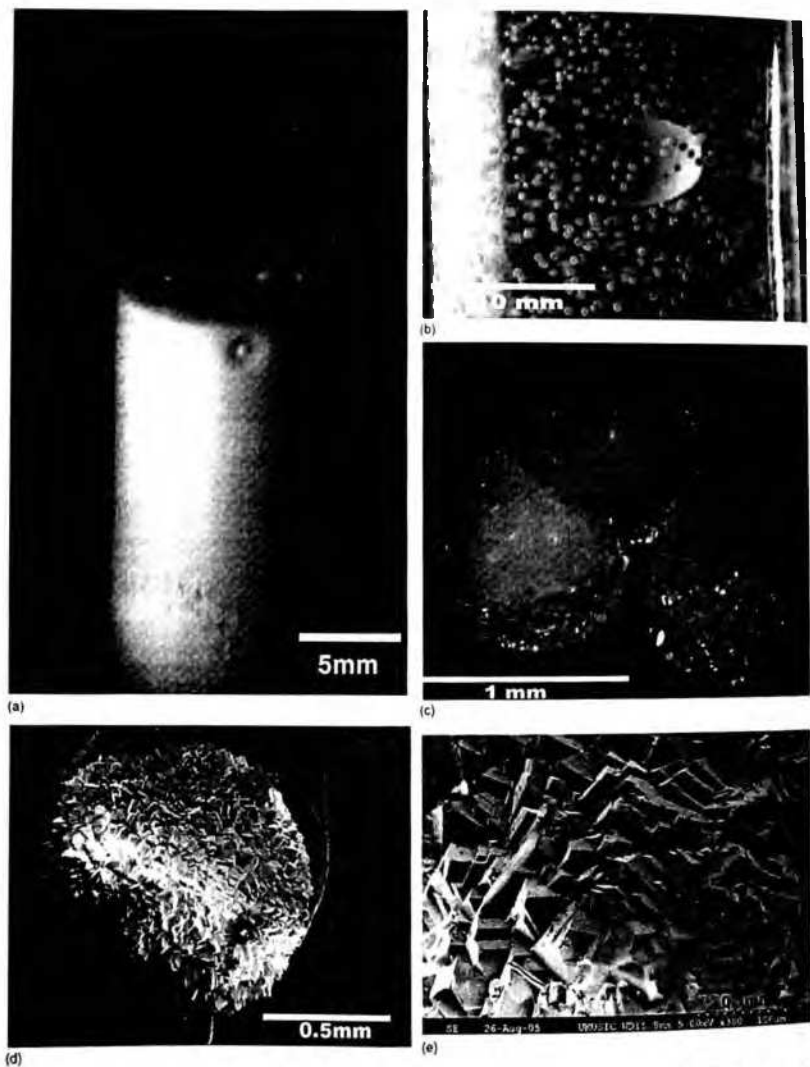


Fig. 1. (a) Photograph showing gadolinium tartrate spherulites growing out of precipitate with the creation of a halo; (b) photograph showing the spherulites of gadolinium tartrate trihydrate grown in silica gel after complete dissolution of the precipitate; (c) optical micrograph of a single and a coalesced spherulite of gadolinium tartrate trihydrate; (d) SEM micrograph of the normal spherulite of (c) at a higher magnification, showing aggregation of tiny single crystals orienting themselves into a spherical envelope; (e) a region of (d) at a much higher magnification suggesting each tiny crystal to have a pyramidal morphology.

consisting of loosely bound platelets that lacks cross linkage [37]. After the formation of precipitate, it begins to advance into the gel with the result that the precipitate column is formed whose length depends on concentrations of the upper and lower reactants and pH of the gel. The advancement of the precipitate continues until a maximum size is obtained which takes about 10–15 days. At this stage, further advancement of the precipitate column stops. Each nucleation site is associated with a halo (a spherical region) which is depleted of colloidal particles as shown in Fig. 1(a). The colloidal particles surrounding the crystal nucleation site tend to migrate radially towards it from all directions. In this way, a spherical region of greater volume than that of growing spherulite is depleted of colloidal

particles. Due to this, the surrounding space is cleared from any precipitate with the result a halo is formed. The process of crystallization continues until the colloidal particles within the precipitate are consumed in building the crystal. After a period of 20–30 days, the whole gel column was impregnated with the spherulites of gadolinium tartrate. The halo formation is a result of diffusion processes involved in the growth of more stable phase (here spherulite) by dissolution of a less stable or metastable phase precipitated in the entire gel column before the nucleation and growth of the stable phase. This observation follows from Oswald's supersaturation theory [38]. According to this theory, the diffusion of electrolyte A into a gel impregnated with electrolyte B forms a layer of supersaturated solution

Table 2
Detailed summary of experiments^a for the growth of single crystals of $Gd(C_2H_3O_4)_2 \cdot (C_2H_3O_4)_2 \cdot 3H_2O$ crystals in silica gel

Experiment	Constant parameters	Variable parameters	Results
1 Variation of gel pH	Gel concentration: 0.5 M; UR concentration: 1 M; LR concentration: 0.5 M; gel age: 3 days	Gel pH: 3, 3.5, 4, 5 and 6	Morphology: single crystals with well-developed {001} and {111} faces at pH 3 and 3.5; (ii) normal and coalesced spherulites for gel pH ≥ 4 Size: maximum size of single crystals at gel pH 3.5 (~1 mm \times 1 mm \times 2 mm) Nucleation density: maximum at gel pH 3 and minimum at pH 6
2 Variation of UR concentration	Gel concentration: 0.5 M; LR concentration: 0.5 M; gel pH: 3.5; gel age: 3 days	Upper reactant concentration: 0.5, 0.75, 1 and 2 M	Morphology: single crystals with well-developed faces at all conditions of growth Size: maximum size of single crystals at UR concentration 1 M (~0.5 mm \times 0.5 mm \times 1 mm) Nucleation density: maximum at UR concentration of 2 M and minimum at 0.5 M
3 Variation of LR concentration	Gel concentration: 0.5 M; UR concentration: 1 M; gel pH: 3.5; gel age: 3 days	Lower reactant concentration: 0.25, 0.5, 0.75 and 1 M	Morphology: single crystals with well-developed {001} and {111} faces under all conditions of growth Size: maximum size of single crystals at LR concentration 0.5 M (~1 mm \times 1 mm \times 2 mm) Nucleation density: maximum at LR concentration 1 M and minimum at 0.25
4 Variation of gel concentration	LR concentration: 0.5 M; UR concentration: 1 M; gel pH: 3.5; gel age: 3 days	Gel concentration: 0.5, 0.75 and 1 M	Morphology: single crystals with well-developed faces under all conditions of growth except at gel concentration of 1.5 M Size: maximum size of single crystals at gel concentration of 0.5 M (~1 mm \times 1 mm \times 2 mm) Nucleation density: maximum at gel concentration 0.5 M and minimum at 1 M
5 Variation of gel age	Gel concentration: 0.5 M; UR concentration: 1 M; LR concentration: 0.5 M; gel pH: 3.5	Gel age: 1, 2, 3, 5, and 10 days	Morphology: single crystals with well-developed faces at all conditions of growth Size: maximum size of single crystals at gel age of 3 days (~1 mm \times 1 mm \times 2 mm) Nucleation density: maximum at gel age of 1 day and minimum at 10 days

^a All experiments were performed in the temperature range of 35–37 °C.

near the initial boundary between the two. Precipitation of the reaction product is assumed to occur once a critical degree of supersaturation is exceeded. By serving as active site for further precipitation, the crystals in the initial precipitate (here crystals at the centre of the halo) rob ions from the neighborhood by diffusion. Consequently, no precipitation occurs in the depleted zone surrounding the halo. This kind of feature is frequently observed in the different polymorphs of calcium carbonate [39] and in different phases of calcium oxalate [40]. Fig. 1(b) illustrates a typical crystallizer with spherulites growing in the gel medium and Fig. 1(c) is an optical micrograph showing a single and a coalesced spherulite. Fig. 1(d) is a scanning electron micrograph of the normal spherulite of Fig. 1(c) revealing it to be just an aggregate of tiny crystallites of gadolinium tartrate trihydrate, orienting themselves in a spherical envelop. Fig. 1(e), which shows a region of Fig. 1(d) at a higher magnification under SEM, suggests the spherulite to be just an aggregate of tiny single crystallites, with each crystal exhibiting a pyramidal morphology. It may be mentioned here that the morphology of the tiny crystallites, which form a spherulite of gadolinium tartrate, has been reported as cuboids in the literature [13]. This is quite different from what has been observed in the present investigation. Each tiny crystal has dipyrnidal morphology with one of the pyramids protruding out of the surface of the spherulite. It may also be noted that the single crystals grown from both agar-agar and silica gel have the same morphology as that of the tiny crystals forming the spherulite.

3.1.1.2. Single crystal growth. Table 2 gives a detailed summary of the experiments and results on morphology, nucleation density and size of single crystals of $Gd(C_4H_4O_6)(C_4H_5O_6) \cdot 3H_2O$ grown in silica gel. Unlike in a gel with $pH \geq 4$, at a lower gel pH of 3 and 3.5, negligible precipitation occurs at the gel/solution interface upon pouring of upper reactant. After a period of about 7 days, very small single crystals of $Gd(C_4H_4O_6)(C_4H_5O_6) \cdot 3H_2O$ start appearing at different sites near the gel/solution interface. The formation of single crystals at $pH \leq 3.5$ may be explained as follows: Firstly, in a low pH medium the solubility of salts of tartaric acid (here gadolinium tartrate) gets raised with the result that the local concentration product $[Gd^{3+}][C_4H_4O_6^{2-}]$ does not exceed more than the solubility product K_{sp} [41]. Due to this, the value of supersaturation developed at different sites inside the gel changes and becomes as low as appropriate for growth of single crystals. Secondly, at low gel pH, the gel structure and hence the average pore size changes, making conditions favorable for the growth of single crystals. However, the pore size may further change during the crystal growth involving reaction between reactants in the gel volume. It could be because of the fact as the reaction proceeds for the formation of a stable product (gadolinium tartrate), there is release of HNO_3 as a by-product, which further reduces the pH of the gel medium. This observation was confirmed by measuring the pH of the gel medium at the time of gelling and at the time of taking out the crystals from the gel. Further, it was observed that even few single crystals grew near the bottom of some tubes, which were set initially at gel pH 5 and were kept for about 1 year. This is because after such a

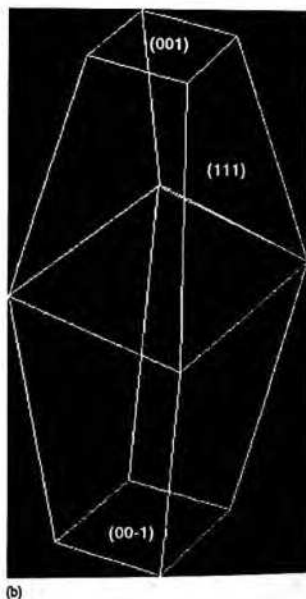
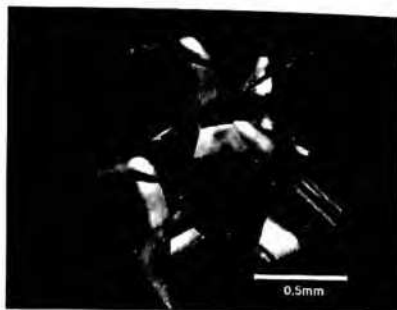


Fig. 2. (a) Single crystals of $Gd(C_4H_4O_6)(C_4H_5O_6) \cdot 3H_2O$ grown in silica gel at gel pH 3 and (b) a schematic diagram, showing the dipyrnidal morphology and habit faces of $Gd(C_4H_4O_6)(C_4H_5O_6) \cdot 3H_2O$ crystals.

long period the pH of the medium is reduced to much lower values (in this case $pH=2$). Fig. 2(a) shows an optical micrograph of some single crystals of $Gd(C_4H_4O_6)(C_4H_5O_6) \cdot 3H_2O$ grown in silica gel. Fig. 2(b) is a schematic diagram illustrating the form and habit faces of the crystals. The single crystals of $Gd(C_4H_4O_6)(C_4H_5O_6) \cdot 3H_2O$ grow with $\{001\}$ and $\{111\}$

Table 3
Detailed summary of experiments for the growth of $Gd(C_4H_4O_6)_3 \cdot 3H_2O$ crystals in agar-agar gel

Experiment	Constant parameters ^a	Variable parameters	Results
1. Variation of gel concentration ^b	LR concentration: 1 M, UR concentration: 2 M, AA:TA = 4:1 ^c	Gel concentration (%) w/v: 0.8, 1, 1.2, 1.4, and 1.6	Morphology: single crystal of dipyramidal class with {111} and {001} dominant faces in all the cases. Size: maximum size of single crystals at gel concentration of 1.2% (w/v) (size ~1 mm × 1 mm × 2 mm)
2. Variation of AA:TA ratio	LR concentration: 1 M, UR concentration: 2 M, gel concentration: 1.2% (w/v)	AA:TA ratio: 1:1, 2:1, 3:1, 4:1, and 5:1	Morphology: (i) single crystal of dipyramidal class with well-developed faces in all cases; (ii) twinned crystals. Size: maximum size of single crystals at AA:TA ratio of 4:1 (size ~0.7 mm × 0.7 mm × 1 mm)
3. Variation of LR concentration	UR concentration: 2 M, AA:TA = 4:1, gel concentration: 1.2% (w/v)	Lower reactant concentration: 0.25, 0.5, 1 and 2 M	Morphology: (i) single crystal of dipyramidal class with well-developed faces in all cases; (ii) twinned crystals. Size: maximum size of single crystals at a lower reactant concentration of 1 M (size ~1 mm × 1 mm × 2 mm)
4. Variation of UR concentration	LR concentration: 1 M, AA:TA = 4:1, gel concentration: 1.2% (w/v)	Upper reactant concentration: 0.5, 1, 1.5 and 2 M	Morphology: (i) single crystal of dipyramidal class with well-developed faces in all cases; (ii) twinned crystals. Size: maximum size of single crystals at an upper reactant concentration of 2 M (size ~1 mm × 1 mm × 2 mm)

^a In all these experiments the agar-agar gel pH was initially adjusted to a value of 2.

^b Concentration of agar-agar gel (% w/v), sp=0.25/>= agar-agar, TA = tartaric acid, ratio of agar-agar and tartaric acid solutions.

as dominant faces, the morphology being that of a dipyramidal class.

3.1.2. Growth in agar-agar gel

The growth of single crystals at pH value of 3 and 3.5 in silica gel led us to carry out further experiments at much lower values of pH. However, experiments on gelation of silica gel showed that at a pH of 1.5 the gel did not set at all, whereas at a pH of 2 the gel was so loosely set that it could not support the upper reactant. Therefore, to grow single crystals of gadolinium tartrate at low values of pH, agar-agar gel was used. Being a physical gel, it can be made to set at much lower values of pH. In the present case, the pH of the agar-agar gel was adjusted to a value of 2 by adding few drops of dilute nitric acid to the agar-agar/tartaric acid solution. In this case, negligible precipitation occurred at the gel/solution interface upon pouring of upper reactant and after a period of about 1 month, the whole gel column was impregnated with single and twinned crystals of gadolinium tartrate trihydrate. The single crystals grown in agar-agar gel were observed to have the same morphology of a dipyramidal class with {001} and {111} habit faces, as that of grown in silica gel. Table 3 gives a detailed summary of the experiments and results on morphology and size of crystals grown in agar-agar gel. Fig. 3(a) shows single crystals of $Gd(C_4H_4O_6)_3 \cdot 3H_2O$ growing in agar-agar gel in a crystallizer. Fig. 3(b) is a photomicrograph, which

shows some single crystals of $Gd(C_4H_4O_6)_3 \cdot 3H_2O$. Fig. 3(c) is an optical micrograph showing a typical single crystal of $Gd(C_4H_4O_6)_3 \cdot 3H_2O$ grown in agar-agar gel and Fig. 3(d) illustrates an SEM micrograph of a typical single crystal of $Gd(C_4H_4O_6)_3 \cdot 3H_2O$.

3.2. Characterization

The percentage composition of carbon and hydrogen along with the normal gravimetric analysis suggests the empirical formula of the compound to be $GdC_3H_{15}O_{15}$. A literature survey of isomorphous compounds [20–22], suggests the chemical formula of gel grown gadolinium tartrate to be $[Gd^{3+}(C_4H_4O_6)^{2-}(C_4H_5O_6)^{-} \cdot 3H_2O]$. The coordination of three water molecules with gadolinium is further supported by the TG analysis, which shows weight loss (in the first two sub-stages of dehydration: 210–230 and 230–250 °C) corresponding to three water molecules. The fact that one of the tartrate ions is singly ionized is supported by the presence of absorption peaks at 1719.6 cm^{-1} in the FT-IR spectrum of gadolinium tartrate trihydrate. Table 4 shows the results of chemical analysis of gadolinium tartrate trihydrate single crystals grown in agar-agar gel, the theoretical values in the table are calculated on the basis of the suggested formula $Gd(C_4H_4O_6)_3 \cdot 3H_2O$. Chemical analysis was also performed on the single crystals grown in

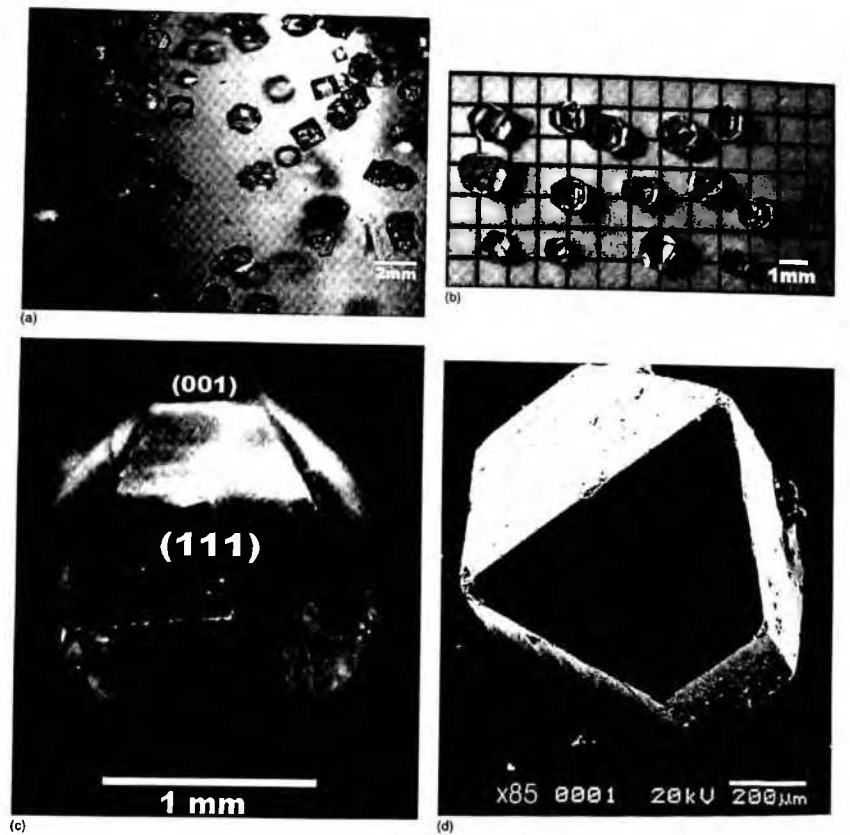


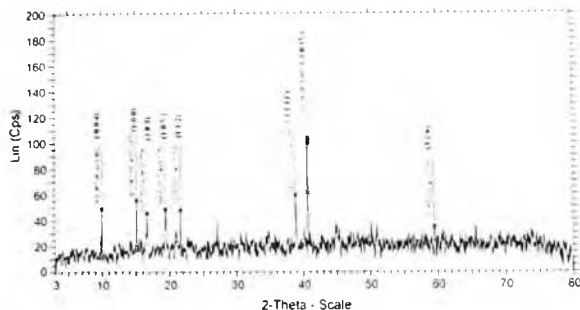
Fig. 3. (a) Photograph showing single crystals of $\text{Gd}(\text{C}_4\text{H}_4\text{O}_6)(\text{C}_4\text{H}_5\text{O}_6) \cdot 3\text{H}_2\text{O}$ growing in agar-agar gel; (b) photograph showing some single crystals of $\text{Gd}(\text{C}_4\text{H}_4\text{O}_6)(\text{C}_4\text{H}_5\text{O}_6) \cdot 3\text{H}_2\text{O}$ from agar-agar gel; (c) optical micrograph of a typical single crystal of $\text{Gd}(\text{C}_4\text{H}_4\text{O}_6)(\text{C}_4\text{H}_5\text{O}_6) \cdot 3\text{H}_2\text{O}$ from agar-agar gel at higher magnification; (d) SEM micrograph of a typical single crystal of $\text{Gd}(\text{C}_4\text{H}_4\text{O}_6)(\text{C}_4\text{H}_5\text{O}_6) \cdot 3\text{H}_2\text{O}$.

Table 4
Chemical composition of $\text{Gd}(\text{C}_4\text{H}_4\text{O}_6)(\text{C}_4\text{H}_5\text{O}_6) \cdot 3\text{H}_2\text{O}$ single crystals from agar-agar gel

Element	Experimental (%)	Theoretical (%)
C	18.82	18.86
H	2.97	2.97
O	46.7	47.13
Gd	30.2	31.03

Table 5
Chemical composition of $\text{Gd}(\text{C}_4\text{H}_4\text{O}_6)(\text{C}_4\text{H}_5\text{O}_6) \cdot 3\text{H}_2\text{O}$ single crystals from silica gel

Element	Experimental (%)	Theoretical (%)
C	18.26	18.86
H	3.15	2.97
O	47.3	47.13
Gd	30.7	31.03

Fig. 4. Powder X-ray diffractogram of $Gd(C_4H_4O_6)(C_4H_5O_6) \cdot 3H_2O$ crystals.Table 6
Powder X-ray diffraction data of $Gd(C_4H_4O_6)(C_4H_5O_6) \cdot 3H_2O$ crystals

<i>d</i> -Values (Å)	2 θ	Relative intensity	<i>hkl</i>	FWHM, β (2 θ)	Crystallite size, <i>L</i> (Å)
8.96194	9.862	45.8	0 0 4	0.195	409.12
5.90116	15.001	52.6	1 0 0	0.12	668.07
5.35069	16.554	42.2	1 0 3	0.23	349.21
4.60307	19.267	46.1	1 0 5	0.19	424.31
4.12377	21.532	44.7	1 1 2	0.14	577.90
2.31700	38.836	56.1	1 1 13	0.174	484.32
2.21799	40.644	100	1 0 15	0.193	439.14
1.55213	59.551	32.1	3 2 8	0.15	610.39

silica gel. The results are shown in Table 5. It is clear that the chemical composition of the single crystals grown from both agar-agar and silica gel is the same. The chemical composition of spherulites was also confirmed to be the same.

Through EDAX analysis, the presence of gadolinium in the $Gd(C_4H_4O_6)(C_4H_5O_6) \cdot 3H_2O$ crystals grown in the laboratory using agar-agar as well as silica gel was confirmed.

The powder XRD diffractogram of $Gd(C_4H_4O_6)(C_4H_5O_6) \cdot 3H_2O$ crystals is shown in Fig. 4. Table 6 provides the corresponding *d*-spacings of the observed lines together with their relative intensities and also FWHM data for each indexed line. The occurrence of highly resolved intense peaks at specific Bragg angles 2θ indicates the crystallinity of the grown mat-

rial. The data on crystallite sizes has been calculated according to Scherrer equation [42], $L = K/\beta \cos \theta$, where *K* is the shape factor and usually takes the value 0.9 [43], β is the full width at half maximum (FWHM). The data indicates the degree of crystallinity of the grown crystals. As given in Table 6, for instance, FWHM of 0.14 and 0.15 at 21.53 and 59.551 2θ , respectively, indicate the good degree of crystallinity. In order to identify the grown phase, the inorganic and organic database provided by International Centre for Diffraction Data (ICDD) in the electronic form (PDF-4) was searched. The search found three references of powder diffraction studies on gadolinium tartrate [13,19] as shown in Table 7. However, the powder X-ray data of the present investigation as given in Table 6 does not completely match the searched references. Moreover, the searched X-ray data is not indexed and bears a very low quality mark. Based on these findings the phase grown in the present investigation does not match completely with any one of the searched references. The authors did not even find any reference from the single crystal literature (CSD, ISCD and LPF). Therefore, it may be suggested that our material represents a new phase, the stoichiometric composition of which is $Gd(C_4H_4O_6)(C_4H_5O_6) \cdot 3H_2O$. The powder diffraction pattern of $Gd(C_4H_4O_6)(C_4H_5O_6) \cdot 3H_2O$ was indexed with the TREOR program [44], using the 15 most intense peaks. A tetragonal unit cell was found with cell parameters $a = 5.955 \text{ \AA}$, $c = 35.855 \text{ \AA}$, $\alpha = \beta = \gamma = 90^\circ$, $V = 1271.5 \text{ \AA}^3$. The observed *d*-values (based on Bragg's law) as provided by

Table 7
Powder diffraction data from ICDD searched references

S. no	<i>d</i> -Values of first three most intense lines	<i>D</i> 1 (Å)	<i>D</i> 2 (Å)	<i>D</i> 3 (Å)	PDF #	Quality mark
1	Gadolinium tartrate pentahydrate $C_{12}H_{12}Gd_2O_{16} \cdot 5H_2O$	4.4400	5.9100	3.1900	00-023 0119	0
2	Gadolinium hydrogen tartrate hydrate $GdH(CHOHCO_2)_2 \cdot 3H_2O$	4.2300	2.3100	5.9100	00-023 0990	0
3	Gadolinium tartrate hydrate $C_{12}H_{12}Gd_2O_{16} \cdot 2H_2O$	4.1907	13.392	2.5286	00-039 0579	0
4	Present investigation	2.21799	2.31700	5.90116		

Table 8
Observed and calculated d -values of $Gd(C_4H_4O_6)(C_4H_5O_6) \cdot 3H_2O$

Observed d -values	Calculated d -values	Difference Δd
8.962	8.962	0.000
5.901	5.955	-0.054
5.351	5.33	-0.021
4.603	4.581	-0.022
4.124	4.099	-0.025
2.317	2.307	-0.01
2.218	2.218	0.000
1.552	1.550	-0.002

Table 9
Assignment of some selected FT-IR wave numbers (cm^{-1}) of $Gd(C_4H_4O_6)(C_4H_5O_6) \cdot 3H_2O$ crystals

IR bands (cm^{-1})	Assignments of peaks/bands
3269.70	$\nu(OH)$ of water and acid
1719.60	$\nu(C=O)$, unionized COOH groups
1586.39	$\nu_{as}(COO^-)$
1409.02	$\nu_{sym}(COO^-)$
1138.98	$\nu(C-OH)$
1066.05	$\delta(C-H)$
839.50	$\delta(O-C=O)$

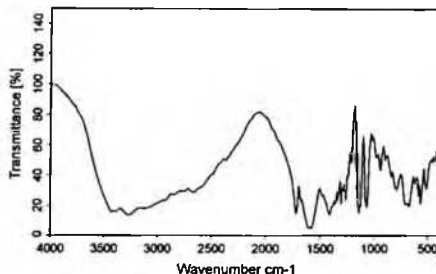


Fig. 5. FT-IR spectrum of $Gd(C_4H_4O_6)(C_4H_5O_6) \cdot 3H_2O$ crystals grown in silica gel.

the automated powder diffractometer (Bruker D8 advance) and the calculated d -values are shown in Table 8.

FT-IR spectrum of $Gd(C_4H_4O_6)(C_4H_5O_6) \cdot 3H_2O$ crystals grown in silica gel is shown in Fig. 5. The infrared spectrum in the range $400\text{--}4000\text{ cm}^{-1}$ shows a strong band centered at about 3269.7 cm^{-1} due to OH stretching vibration of water and OH of the acid group. The strong peak at 1719.6 cm^{-1} is

due to free carbonyl stretch $\nu(C=O)$, which shows that besides ionized COO^- groups there is also presence of unionized carboxyl groups (COOH) in the compound [45]. A band centered at approximately 1586 cm^{-1} is due to $C=O$ asymmetric stretch of coordinated carbonyl group. The absorption at 1409.4 cm^{-1} is attributed to $C=O$ symmetric vibration. FT-IR spectra of agar-agar gel grown $Gd(C_4H_4O_6)(C_4H_5O_6) \cdot 3H_2O$ crystals is identical to that of silica gel grown crystals. The assignment of some selected absorption band/peaks observed in the FT-IR spectrum of $Gd(C_4H_4O_6)(C_4H_5O_6) \cdot 3H_2O$ is shown in Table 9.

3.3. Thermal stability

Fig. 6 shows a thermogram of $Gd(C_4H_4O_6)(C_4H_5O_6) \cdot 3H_2O$ crystals grown in silica gel, recorded in the temperature range of $20\text{--}500\text{ }^\circ\text{C}$. From the TG curve, it is observed that the material remains stable up to a temperature of about $205\text{ }^\circ\text{C}$. It is clear from the DTG curve that the first stage of dehydration ($210\text{--}280\text{ }^\circ\text{C}$) actually consists of three sub-stages ($210\text{--}230$, $230\text{--}250$ and $250\text{--}276\text{ }^\circ\text{C}$). The first sub-stage ($210\text{--}230\text{ }^\circ\text{C}$) is due to loss of one H_2O molecule (observed loss: 3.33%; calculated: 3.52%). The second sub-stage ($230\text{--}250\text{ }^\circ\text{C}$) results in the elimination of two water molecules from the mate-

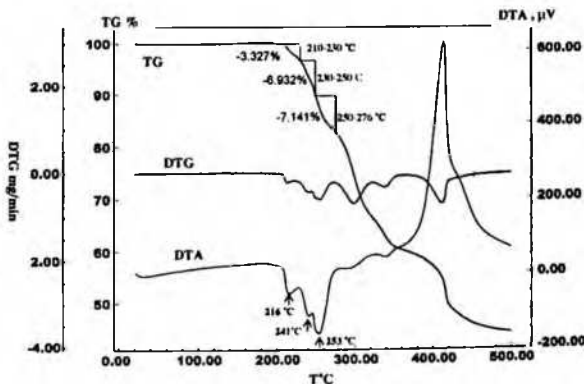


Fig. 6. TG, DTG and DTA curves for silica gel grown gadolinium tartrate trihydrate crystals.

nal (observed loss: 6.93%; calculated: 7%). In the third sub-stage (250–276 °C), there is loss of two (intramolecular) water molecules (observed loss: 7.14%; calculated: 7%). The total measured weight loss in the stage (210–280 °C) is about 17.65% (calculated loss: 17.7%), resulting in the elimination of five water molecules (two from intramolecular and three from coordinated water). Corresponding to these dehydration steps there are three endotherms in DTA, at 216, 241 and 253 °C, respectively. The thermal behavior of crystals grown in agar-agar gel is observed to be the same.

4. Conclusions

The use of gadolinium nitrate as upper reactant and L-tartaric acid as lower reactant results in the growth of $Gd(C_4H_4O_6)(C_4H_5O_6) \cdot 3H_2O$ crystals in silica and agar-agar gel. The pH of the gel medium has a profound effect on supersaturation and hence on the growth and morphology of crystals. Spherulites of $Gd(C_4H_4O_6)(C_4H_5O_6) \cdot 3H_2O$ are formed in the pH range of $4 \leq pH < 6$ whereas single crystals grow for $pH \leq 3.5$. Agar-agar gel leads to single crystal growth at much lower value of $pH = 2$. The morphology of single crystals in both media of growth is dipyramidal with the major habit faces as $\{111\}$ and $\{001\}$. CHN, gravimetric and thermogravimetric analyses suggest that the grown crystals bear the chemical formula $Gd^{3+}(C_4H_4O_6)^{2-}(C_4H_5O_6)^{1-} \cdot 3H_2O$. X-ray powder diffraction studies reveal the degree of crystallinity of the grown material. FT-IR spectrum shows the presence of tartrate ligands and establishes that one of the tartrate ions is singly ionized. Thermogravimetric analysis suggests that the material is thermally stable up to 205 °C.

Acknowledgements

One of the authors (BW) is thankful to the UGC, New Delhi and the Department of Higher Education, Government of J&K for providing the teacher fellowship. The corresponding author (PNK) is thankful to the All India Council of Technical Education, New Delhi for award of emeritus fellowship.

References

- [1] H.K. Henisch, *Crystal Growth in Gels*, Pennsylvania State University Press, University Park, PA, 1973.
- [2] H.K. Henisch, *Crystals in Gels and Liesegang Rings*, Cambridge University Press, Cambridge, 1988.
- [3] M.E. Torres, T. Lopes, J. Peraza, J. Stockel, A.C. Yanes, C. Gonzalez-Silgo, C. Ruiz-Perez, P.A. Lorenzo-Luis, *J. Appl. Phys.* 84 (1998) 5729.
- [4] M.H. Rahimkuty, K. Rajendra Babu, K. Shreedharan Pillai, M.R. Sudarshan Kumar, C.M.K. Narr, *Bull. Mater. Sci.* 24 (2001) 249.
- [5] M.E. Torres, A.C. Yanes, T. Lopez, J. Stockel, J.F. Peraza, *J. Cryst. Growth* 156 (1995) 421.
- [6] M.E. Torres, T. Lopez, J. Stockel, X. Solans, M. Garcia-Valle, E. Rodriguez-Castellon, C. Gonzalez-Silgo, *J. Solid State Chem.* 163 (2002) 491.
- [7] J. Foucek, L.E. Cross, K. Seely, *Ferroelectrics* 1 (1970) 61.
- [8] N.R. Ivanov, *Ferroelectr. Lett.* 27 (1984) 45.
- [9] S.K. Arora, V. Patel, B. Chudasama, Himesh Anni, *J. Cryst. Growth* 275 (2005) e671–e661.
- [10] K. Suryanarayana, S.M. Dharmaprasadh, *Mater. Lett.* 42 (2000) 92–96.
- [11] S.K. Arora, V. Patel, A. Kothari, B. Anni, *Cryst. Growth Des.* 4 (2004) 343–349.
- [12] P.N. Kotru, K.K. Raina, N.K. Gupta, *Cryst. Res. Technol.* 22 (1987) 177–182.
- [13] P.N. Kotru, N.K. Gupta, K.K. Raina, *Cryst. Res. Technol.* 21 (1986) 15–22.
- [14] P.N. Kotru, K.K. Raina, *J. Mater. Sci. Lett.* 5 (1986) 760–762.
- [15] P.N. Kotru, K.K. Raina, N.K. Gupta, *J. Mater. Sci.* 21 (1986) 90–96.
- [16] V. Mansotra, K.K. Raina, P.N. Kotru, *J. Mater. Sci.* 26 (1991) 3780–3786.
- [17] A. Jain, A.K. Razdan, P.N. Kotru, *Mater. Sci. Eng. B* 8 (1991) 129.
- [18] A. Jain, A.K. Razdan, P.N. Kotru, *Mater. Chem. Phys.* 45 (1996) 180.
- [19] R. Pastorek, *Monatsh. Chem.* 101 (1970) 693.
- [20] J.A. Mathew, G.B. Michael Drew, S. Morris, A.R. David, *Polishedron* 15 (1996) 3377–3383.
- [21] W. Chuan-De, Z. Xiao-Ping, L. Can-Zhong, Z. Hong-Hui, H. Jin-Shun, *Acta Crystallogr. E* 58 (2002) 228–230.
- [22] F.C. Hawthorne, I. Borys, R.B. Ferguson, *Acta Crystallogr. C* 39 (1983) 540.
- [23] P.J. Phillips, *Rep. Prog. Phys.* 53 (1990) 549.
- [24] P.J. Phillips, Spherulitic crystallization in macromolecules, in: D.I.J. Hurler (Ed.), *Handbook of Crystal Growth*, vol. 2, Elsevier, Amsterdam, 1993 (Chapter 18).
- [25] G. Ryschenkov, G. Faivre, *J. Cryst. Growth* 87 (1988) 221.
- [26] J. Bisault, G. Ryschenkov, G. Faivre, *J. Cryst. Growth* 110 (1991) 889.
- [27] S.C. Jain, S.A. Agnihotry, V.G. Bhude, *Mol. Cryst. Liq. Cryst.* 88 (1982) 281.
- [28] J.L. Hutter, J. Bechhoefer, *Physica A* 239 (1997) 103.
- [29] V. Hangloo, S. Pandita, K.K. Bamzai, P.N. Kotru, *J. Mater. Sci.* 39 (2004) 1743–1749.
- [30] V. Hangloo, S. Pandita, K.K. Bamzai, P.N. Kotru, N. Sahni, *Cryst. Growth Des.* 3 (2003) 753–759.
- [31] H.D. Keith, F.J. Padden, *J. Appl. Phys.* 34 (1963) 2409.
- [32] E.E. Bolotov, E.W. Muravev, in: D.E. Ovsienko (Ed.), *Growth and Imperfections of Metallic Crystals*, Consultants Bureau, New York, 1968, p. 76.
- [33] B. Felton, C.A. Griffiths, *J. Appl. Phys.* 39 (1968) 3663.
- [34] D.C. Bassett, A.S. Vaughan, *Macromolecules* 33 (2000) 8781.
- [35] J.H. Magill, *J. Mater. Sci.* 36 (2001) 3143.
- [36] V. Alexeyev, *Quantitative Analysis*, Mir Publishers, Moscow, 1969, p. 84.
- [37] H.K. Henisch, *Crystal Growth in Gels*, Pennsylvania State University Press, University Park, PA, 1973, p. 90.
- [38] W. Ostwald, *Z. Phys. Chem.* 23 (1897) 365.
- [39] J. Kawano, et al., *J. Cryst. Growth* 237–239 (2002) 419–423.
- [40] T. Jung, W.-S. Kim, C.K. Cho, *Mater. Sci. Eng. C* 24 (2004) 31–33.
- [41] R.A. Laudise, *The Growth of Single Crystals*, Prentice-Hall, Englewood Cliffs, NJ, 1970, p. 272.
- [42] P. Scherrer, *Nachr. Ges. Wiss. Göttingen, Math. Phys. Kl.* 2 (1918) 96–100.
- [43] H.P. Klug, L.E. Alexander, *X-ray Diffraction Procedures*, 2nd ed. Wiley-Interscience, New York, 1974, p. 856.
- [44] P.E. Werner, L. Eriksson, M. Westdahl, *J. Appl. Crystallogr.* 18 (1985) 367–370.
- [45] K. Nakamoto, *Infrared and Raman Spectra of Inorganic and Coordination Compounds*, 5th ed., John Wiley & Sons, 1997, p. 70 (Part B Chapter III).

Growth of ytterbium tartrate trihydrate crystals in silica and agar-agar gels and their characterization

B. Want^{1,2}, F. Ahmad¹, and P. N. Kotru^{*2}

¹ Department of Physics, University of Kashmir, Srinagar-190006, J & K, India

² Crystal Growth and Materials Research Laboratory, Department of Physics and Electronics, University of Jammu, Jammu-180006-India

Received 3 April 2006, accepted 16 May 2006

Published online 15 November 2006

Key words crystal growth, ytterbium tartrate trihydrate, XRD, FTIR, SEM, thermal stability.

PACS 81.10.Dn, 61.10.Nz, 67.80.Gb, 78.30.-j, 68.37.Hk

Single crystals of ytterbium tartrate trihydrate have been grown by gel method using silica and agar-agar gels as media of growth. The medium of growth influences the morphology of grown crystals, silica gel yielding single and polycrystalline in the form of spherulites whereas agar-agar gel leading to growth of single and twinned crystals. Materials grown as single crystals have been characterized by using optical and scanning electron microscopy (SEM), EDAX, XRD, FT-IR, CHN and thermogravimetric techniques. The stoichiometry of the grown single crystals is suggested to be $\text{Yb}(\text{C}_4\text{H}_4\text{O}_6) \cdot (\text{C}_4\text{H}_4\text{O}_6) \cdot 3\text{H}_2\text{O}$. The FT-IR spectrum shows the presence of singly as well as doubly ionized tartrate ligands. Results of thermal analysis indicate that the material is thermally stable up to a temperature of 200°C.

© 2006 WILEY-VCH Verlag GmbH & Co. KGaA, Weinheim

1 Introduction

Most tartrate compounds have interesting physical properties such as ferroelectricity, piezoelectricity and optical second harmonic generation [1–6]. Consequently, they are used in transducers and several linear and nonlinear mechanical devices [1,2,4]. Many investigators have grown and studied characteristics of single crystals of tartrate compounds by gel method using silica gel [7–9]. Rare earth tartrates bearing the general formula $\text{R}_2(\text{C}_4\text{H}_4\text{O}_6) \cdot x\text{H}_2\text{O}$ (R = Nd, Dy, Gd, La, Di, Pr, Sm and Y) have also been grown by gel method using silica gel as a medium of growth [10–16]. However, there is scanty information in the literature on the growth and characteristics of single crystals of ytterbium tartrate. Also, to the best of author's knowledge gels other than that of sodium metasilicate have hardly been tried for the growth of rare earth tartrates in general and ytterbium tartrate in particular. The authors used two different types of gels for the growth of ytterbium tartrate crystals and the present paper reports on the growth of these crystals by gel method using both silica (inorganic) and agar-agar (organic) gels as media of growth.

2 Experimental procedure

Ytterbium tartrate shows poor solubility in water; it decomposes before melting, and does not vaporize or sublime. Consequently, the only alternative to grow single crystals of this kind of material is by chemical reaction at a controlled rate using gel method. Therefore, crystallization of ytterbium tartrate was accomplished using the single gel diffusion technique [17, 18]. The crystals were grown in a crystallizer consisting of a single glass tube of length 20 cm and diameter 2.5 cm. Silica gel was prepared by adding a solution of sodium metasilicate (0.5 M–1.5 M) to L-tartaric acid (0.25 M–1 M), drop by drop with continuous stirring to avoid

* Corresponding author: e-mail: pn_kotru@yahoo.com

excessive local ion concentration, which may cause premature local gelling and make the final solution inhomogeneous. The pH of the gel medium was adjusted between a value of 2.5 and 6 (i.e., $2.5 \leq \text{pH} \leq 6$). The solution with the desired value of pH was then transferred to several glass tubes. Once gelled, an aqueous solution of ytterbium nitrate (0.5 M–2 M) was carefully poured with the help of a pipette over the set gel, in order to avoid any gel breakage. The Yb^{3+} ions diffuse slowly through the narrow pores of the gel to react with the tartrate ions, giving rise to the formation of ytterbium tartrate crystals.

Agar-agar gel was prepared by dissolving (0.8–1.6% w/v) of agar-agar in water that was preheated to a temperature of 60°C. The agar-agar solution was then mixed with L-tartaric acid (0.25–2 M) in various proportions by volume. The pH of the agar-agar medium was adjusted to a value of 2. The mixed solution was then transferred to several glass tubes. After the setting of gel, an aqueous solution of ytterbium nitrate (0.5 M–2 M) was carefully poured over it. After a period of about four weeks, very small single crystals of ytterbium tartrate start appearing below the gel/solution interface and after about two months, the whole gel column gets impregnated with well-shaped crystals. All the experiments were carried out at a temperature of 35°C.

The powder XRD pattern of grown crystals was obtained using a Bruker AXS D8 Advance X-ray diffractometer with Cu K α radiation, the C and H contents in the obtained crystals were determined by using Vario-EL III CHNS-analyzer. An energy dispersive spectrometer (OXFORD ISIS-300 system) attached to a scanning electron microscope JEOL JSM-5800 was used to identify the presence of ytterbium. The FT-IR spectra of the material in the wave number range of 400–4000 cm^{-1} were recorded on a Bruker Vector 22 spectrometer using KBr pellet technique. The thermal behavior (TGA, DTG and DTA) of the crystals was recorded on a Perkin-Elmer thermal analyzer in N_2 atmosphere at a heating rate of 10K/min. The morphology of grown crystals was examined using an optical microscope (Epignost of Carl Zeiss, Germany), a large incident light microscope (Neophot-2 of Carl Zeiss, Germany) and a scanning electron microscope (HITACHI S-3000H).

3 Results and discussion

Growth of crystals from silica gel Table 1 gives a detailed summary of the experiments and results on morphology, nucleation density and size of ytterbium tartrate crystals grown in silica gel. The results in table 1 show that single crystals of ytterbium tartrate grow at a gel pH of 2.5, 3 and 3.5; and for a gel pH > 3.5, the crystals attain spherulitic morphology. Here we shall describe results on single crystals of ytterbium tartrate which are found to have crystallized as trihydrates with the chemical formula $[\text{Yb}(\text{C}_4\text{H}_4\text{O}_6)(\text{C}_4\text{H}_7\text{O}_6)_3(\text{H}_2\text{O})]$. The results on spherulites of ytterbium tartrate are in the process of investigation and would be discussed elsewhere.

As soon as the upper reactant (ytterbium nitrate) is poured over the set gel containing tartrate ions, there is an instantaneous reaction between the ytterbium and tartrate ions resulting in the spontaneous formation of a precipitate. It is observed that the strength of precipitation depends profoundly on the gel pH, higher the pH stronger is the precipitation (other parameters of growth like upper and lower reactant concentrations, gel age and gel concentration remaining the same). For gel pH > 3.5, a strong precipitate is observed to form at the gel/solution interface. Due to this, the supersaturation available for three-dimensional surface nucleation and growth becomes very high which results in the formation of spherulites. However, at lower values of gel pH (2.5, 3 and 3.5), negligible precipitation occurs at the gel/solution interface upon pouring of upper reactant and after a period of about 10 days, very small single crystals of ytterbium tartrate trihydrate (YbTT) start appearing at different sites near the gel/solution interface. The formation of single crystals at pH values ≤ 3.5 may be explained as follows. Firstly, the concentration of the precipitant ions $\text{C}_4\text{H}_4\text{O}_6^{2-}$, which are anions of tartaric acid, depends on the H^+ ion concentration. The concentration of precipitant ions decreases with the decrease in pH [19]. Therefore, the degree of precipitation depends strongly on pH of the medium. Secondly, in a low pH medium the solubility of ytterbium tartrate gets raised with the result that the local concentration product $[\text{Yb}^{3+}][\text{C}_4\text{H}_4\text{O}_6^{2-}]$ becomes less than the solubility product K_{sp} [20]. Due to this, the value of supersaturation developed at different sites inside the gel changes and becomes as low as may be appropriate for the growth of single crystals. However, it was also observed that at low pH values the nucleation density became very high which puts a limit to the size of crystals.

It was further observed that even few single crystals grew near the bottom of some tubes, which were initially set at gel pH = 5 and were kept for about six months. It could be because of the fact that as the reaction proceeds for the formation of a stable product (ytterbium tartrate); there is release of HNO_3 as a by-product,

which further reduces the pH of the gel medium. This observation was confirmed by measuring the pH of the gel medium at the time of gelling and at the time of taking out the crystals from the gel. It was observed that after such a long period, the pH of the medium was reduced to a much lower value of 2. Figure 1a shows some single crystals of ytterbium tartrate trihydrate (YbTT) growing in a crystallizer containing gel of initial pH value 3.5. Optical micrograph of some typical single crystals is shown in figure 1b. Single crystals of YbTT have morphology of a dipyrnidal class and the crystals are bound by $\{111\}$ and $\{001\}$ habit faces, $\{001\}$ faces being more dominant than $\{111\}$. This shows that the faces $\{001\}$ grow at a relatively slower rate as compared to $\{111\}$.

Table 1 Detailed summary of experiments ¹ for the growth of ytterbium tartrate crystals in silica gel. [†] UR = upper reactant (ytterbium nitrate) [‡] LR = Lower reactant (L - tartaric acid). * The time interval between setting of gel and pouring of upper reactant.

Experiment	Constant parameters	Variable parameters	Results
1.	Gel Conc.: 0.5M	<i>Gel pH</i>	<i>Morphology:</i> (i) Single crystals with well developed faces at pH 2.5, 3 and 3.5 (ii) Normal and coalesced spherulites for gel pH > 3.5.
Variation of Gel pH	UR [†] Conc.: 1 M LR [‡] Conc.: 0.5M Gel age*: 72hrs.	2.5, 3, 3.5, 4, 5 and 6.	<i>Size:</i> (i) Maximum size of single crystals at gel pH 3.5 (~1 mm × 1 mm × 0.5 mm). (ii) Maximum size of spherulites at pH 4 (~6 mm diameter).
2.	Gel Conc.: 0.5M LR Conc.: 0.5M Gel pH: 3.5 Gel age: 72hrs.	<i>Upper reactant concentration:</i> 0.5 M, 0.75 M, 1 M, 2 M.	<i>Nucleation density:</i> Maximum at pH 2.5 and minimum at pH 6. <i>Morphology:</i> (i) Single crystals with well developed $\{001\}$ and $\{111\}$ faces and (ii) twinned crystals.
Variation of UR Conc.			<i>Size:</i> Maximum size of single crystals at UR Conc. of 1 M (~1mm × 1 mm × 0.5 mm). <i>Nucleation density:</i> Minimum at the UR Conc. of 0.5 M and maximum at 2M.
3.	Gel Conc.: 0.5M UR Conc.: 1 M Gel pH: 3.5 Gel age: 72hrs.	<i>Lower reactant concentration:</i> 0.25 M, 0.5 M, 0.75 M and 1 M,	<i>Morphology:</i> (i) Single crystals with well developed $\{001\}$ and $\{111\}$ faces and (ii) twinned crystals
Variation of LR Conc.			<i>Size:</i> Maximum size of crystals at LR Conc. of 0.5M (size ~1mm × 1 mm × 0.5 mm) <i>Nucleation density:</i> Minimum at 0.25 M and maximum at 1M.
4.	LR Conc.: 0.5M UR Conc.: 1M Gel pH: 3.5 Gel age: 72hrs.	<i>Gel concentration:</i> 0.5 M, 0.75 M, 1M and 1.5M	<i>Morphology:</i> (i) Single crystals with well developed $\{001\}$ and $\{111\}$ faces and (ii) twinned crystals
Variation of Gel Conc.			<i>Size:</i> Maximum size of single crystals at gel concentration of 0.5M (size ~ 1mm × 1 mm × 0.5 mm). <i>Nucleation density:</i> Minimum at 1 M and maximum at 0.5 M. Gel Conc. of 1.5 M not suitable for growth.
5.	Gel Conc.: 0.5M UR Conc.: 1 M LR Conc.: 0.5M Gel pH: 3.5	<i>Gel age:</i> 48hrs, 72hrs, 120 hrs, 144hrs.	<i>Morphology:</i> (i) Single crystals with well developed $\{001\}$ and $\{111\}$ faces (ii) twinned crystals
Variation of Gel age			<i>Size:</i> Maximum size of crystals at a gel age of 72 hrs (1mm × 1 mm × 0.5 mm) <i>Nucleation density:</i> Minimum at gel age of 144hrs and maximum at 48 hrs.

Fig. 1 a) Photograph showing single crystals of ytterbium tartrate trihydrate growing in a crystallizer in silica gel. b) Optical micrograph of some typical single crystals of YbTT.



Table 2 Detailed summary of experiments for the growth of ytterbium tartrate crystals in agar-agar gel. † Agar-agar gel concentration in % w/v. ‡ AA : TA = Ratio of agar-agar : tartaric acid solutions.

Experiment	Constant parameters	Variable parameters	Results
1 Variation of Gel Conc. †	LR Conc.: 1M UR Conc.: 2 M AA : TA ‡ = 4 : 1	Agar-agar gel concentration (% w/v) 0.8, 1, 1.2, 1.4 and 1.6	<i>Morphology:</i> (i) Single crystal of dipyrarnidal class with {111} and {001} as dominant faces in all cases and (ii) Twinned crystals. <i>Size:</i> Maximum size of single crystals at gel concentration of 1.2 % w/v (size ~ 1.5 mm × 1.5 mm × 2 mm). <i>Nucleation density:</i> Minimum at gel concentration 1.6 % w/v and maximum at 0.8 % w/v.
2 Variation of AA : TA ratio	LR Conc.: 1M UR Conc.: 2 M Gel Conc.: 1.2 %w/v	AA : TA ratio 1 : 1, 2 : 1, 3 : 1, 4 : 1, and 5 : 1	<i>Morphology:</i> (i) Single crystal of dipyrarnidal class with well developed faces in all cases and (ii) Twinned crystals. <i>Size:</i> Maximum size of single crystals at AA : TA ratio of 4 : 1 (size ~ 1.5 mm × 1.5 mm × 2 mm). <i>Nucleation density:</i> Minimum at 5 : 1 and maximum at 1 : 1.
3 Variation of LR Conc.	UR Conc.: 2 M AA : TA = 4 : 1 Gel Conc.: 1.2 %w/v	Lower reactant concentration 0.25 M, 0.5 M, 1 M, 2 M	<i>Morphology:</i> (i) Single crystal of dipyrarnidal class with well developed faces in all cases (ii) Twinned crystals and aggregation of single crystals. <i>Size:</i> Maximum size of single crystals at a lower reactant concentration of 1M (size ~ 1 mm × 1 mm × 2 mm) <i>Nucleation density:</i> Minimum at 0.5 M and max. at 2M.
4 Variation of UR Conc.	LR Conc.: 1M AA : TA = 4 : 1 Gel Conc.: 1.2 %w/v	Upper reactant concentration 0.5 M, 1 M, 1.5 M, 2 M	<i>Morphology:</i> (i) Single crystal of dipyrarnidal class with well developed faces in all cases. (ii) twinned crystals. <i>Size:</i> Maximum size of single crystals at an upper reactant concentration of 1.5 M (size ~ 1.5 mm × 1.5 mm × 2 mm). <i>Nucleation density:</i> Minimum at 0.5 M and max. at 2M.

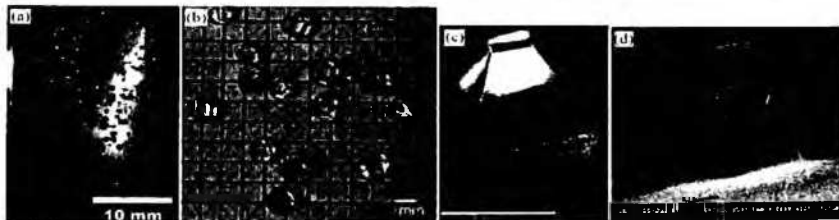


Fig. 2 a) Photograph showing single crystals of ytterbium tartrate growing in agar-agar gel. b) Optical photograph of some typical single crystals of ytterbium tartrate from agar-agar gel. c) An optical micrograph of a typical single crystal of YbTT. d) SEM micrograph of a typical single crystal of YbTT grown from agar-agar gel.

Growth of YbT crystals from agar-agar gel The growth of single crystals at pH values of 2.5, 3 and 3.5 in silica gel led us to carry out further experiments at much lower values of pH. However, experiments on gelatin of silica gel showed that at a pH of 1.5 the gel did not set at all, whereas at a pH of 2 the gel was so loosely set that it could not support the upper reactant. Therefore, to grow single crystals of ytterbium tartrate at low values of pH, agar-agar gel was used. Being a physical gel it can be made to set at much lower values of pH. In the present case, the pH of the agar-agar gel was adjusted to a value of 2 by adding few drops of nitric acid to the agar-agar-tartaric acid solution. At this condition of growth, no precipitation occurred at the gel/solution interface upon pouring of upper reactant and after a period of about two months, the whole gel column got full of single and twinned crystals of YbTT. Table 2 gives a detailed summary of the experiments and results on morphology, nucleation density and size of crystals grown in agar-agar gel. The results show that the use of agar-agar gel leads to only single and twinned crystals of YbTT under all conditions of growth. Figure 2a shows single crystals growing in agar-agar gel in a crystallizer. Figure 2b is a photograph, which shows some single crystals of YbTT. Figure 2c is an optical micrograph showing a single crystal of YbTT grown in agar-agar gel and figure 2d illustrates an SEM micrograph of a typical single crystal of ytterbium

tartrate trihydrate. It is clear from figure 2d that the single crystals have a well-developed morphology of dipyramidal class with {001} and {111} as habit faces. The morphology is same as that of single crystals grown in silica gel, except that {111} faces are more dominant than {001}. This could be attributed to differences in the rate of growth of faces in two different gels. Moreover, the agar-agar gel grown crystals are, in general, found to be more perfect than those grown in silica gel. The surface of the former are smoother and crystals have less inclusions incorporated in them.

4 Characterization

Elemental analysis The percentage composition of carbon and hydrogen along with the normal gravimetric analysis suggests the empirical formula of the compound to be $\text{YbC}_3\text{H}_4\text{O}_7$. A literature survey of isomorphous compounds [21-23], suggests the chemical formula of gel grown ytterbium tartrate trihydrate to be $[\text{Yb}(\text{C}_4\text{H}_4\text{O}_6)(\text{C}_2\text{H}_2\text{O}_2)_3 \cdot 3(\text{H}_2\text{O})]$. The coordination of three water molecules with ytterbium is further supported by the TG analysis, which shows weight loss in the first dehydration step corresponding to five water molecules (three coordinated and two intramolecular water molecules). The fact that one of the tartrate ions is singly ionized is supported by the presence of absorption peaks at 1718 cm^{-1} in the FT-IR spectrum of YbTT. Table 3 shows the results of chemical analysis of single crystals of YbTT grown in agar-agar gel. Chemical analysis was also performed on the single crystals grown in silica gel. The results are shown in table 4. It is clear that the chemical composition of the two crystals is same.

Table 3 Chemical composition of YbTT single crystals from agar-agar gel.

Element	Experimental (%)	Theoretical (%)
C	18.39	18.33
H	3.15	2.88
O	45.4	45.78
Yb	30.2	33

Table 4 Chemical composition of YbTT single crystals from silica gel.

Element	Experimental (%)	Theoretical (%)
C	18.43	18.33
H	2.69	2.88
O	45.3	45.78
Yb	31.2	33

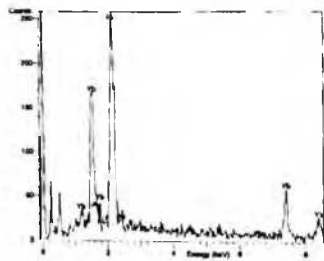


Fig. 3 EDAX spectrum of ytterbium tartrate trihydrate showing ytterbium peaks.

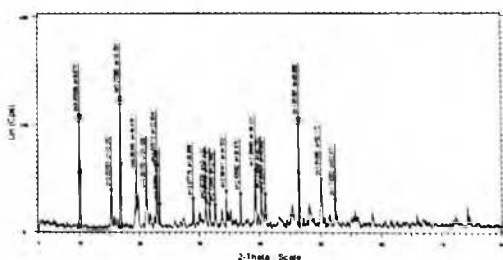


Fig. 4 Powder X-ray diffractogram of YbTT.

EDAX results The EDAX spectrum of YbTT from agar-agar gel is shown in figure 3. The presence of ytterbium is clearly seen in the EDAX trace. The Au peaks shown in the spectrum are due to gold coating of the sample. It is confirmed that the EDAX analysis of crystals grown from silica gel also shows the presence of ytterbium.

Powder X-ray diffraction results The powder XRD diffractogram of YbTT crystals is shown in figure 4. Table 5 provides the corresponding d-spacings of the observed lines together with their relative intensities. The occurrence of intense peaks at specific Bragg angles 2θ indicates the crystallinity of the grown material. In order to identify the grown phase, inorganic and organic database provided by International Centre for Diffraction Data (ICDD) in the electronic form (PDF-4) was searched. The search did not find any references from the powder diffraction data. Based on these findings it may be suggested that our material represents a new phase, the stoichiometric composition of which is $\text{Yb}(\text{C}_4\text{H}_4\text{O}_6)(\text{C}_4\text{H}_5\text{O}_6) \cdot 3(\text{H}_2\text{O})$.

Table 5 Powder X-ray diffraction data of YbTT crystals.

d-values (Å)	Relative Intensity	d-values(Å)	Relative Intensity
8.95398	86.2	2.73965	17.6
5.80781	29.5	2.59747	28.3
5.27585	100	2.43592	26.7
4.55366	43.2	2.28893	44.4
4.20172	28.3	2.23648	28.5
3.87973	47.8	2.20151	26.3
3.80559	19	1.95265	84.2
3.07776	22.8	1.81685	37.9
2.8723	20.2	1.74252	22.6
2.81986	18.7		

FT-IR results Figure 5 shows FT-IR spectrum of YbTT crystals grown in agar-agar gel. The infrared spectrum in the range $400\text{--}4000\text{cm}^{-1}$ shows a strong band centered at about 3265 cm^{-1} due to OH stretching vibration of water and OH of the acid group. The strong peak at 1718 cm^{-1} is due to free carbonyl stretch $\nu(\text{C}=\text{O})$, which shows that besides ionized COO^- groups there is also presence of unionized carboxyl groups (COOH) in the compound [24]. A band centered at approximately 1587 cm^{-1} is due to $\text{C}=\text{O}$ asymmetric stretch of coordinated carbonyl group. The absorption at 1410 cm^{-1} is attributed to $\text{C}=\text{O}$ symmetric vibration. FT-IR spectrum of silica gel grown ytterbium tartrate crystals is found to be identical to that of agar-agar gel grown crystals. The assignment of some selected absorption band/peaks observed in the FT-IR spectrum of YbTT is shown in table 6.

Table 6 Assignment of some selected IR wave numbers (cm^{-1}) of YbTT crystals.

IR bands / cm^{-1}	Assignments of peaks/bands
3265.54	$\nu(\text{OH})$ of water and acid
1718.65	$\nu(\text{C}=\text{O})$, unionized COOH groups
1587.40	$\nu_{\text{asy}}(\text{COO})$
1410.86	$\nu_{\text{sy}}(\text{COO})$
1140.84	$\nu(\text{C}-\text{O}-\text{H})$
1067.21	$\delta(\text{C}-\text{H})$
840.45	$\delta(\text{O}-\text{C}=\text{O})$

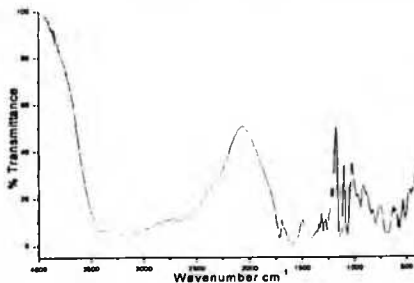


Fig. 5 FT-IR spectrum of YbTT grown in agar-agar gel.

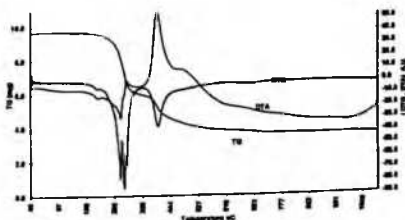


Fig. 6 TGA, DTG, DTA curves for ytterbium tartrate trihydrate crystals grown in agar-agar gel.

Thermal stability results Figure 6 shows a thermogram of YbTT grown in agar-agar gel, recorded in the temperature ranging from 40 to 1100°C. From the TG curve, it is observed that the material remains stable up to a temperature of about 200°C. It is clear from the DTG curve that the first stage of decomposition actually consists of two sub stages (200–285°C and 285–354°C). The first sub stage (200–285°C) is due to dehydration resulting in the elimination of water molecules from the material. The measured weight loss in this stage is about 17.4% (calculated loss, 17.15%), resulting in the elimination of five water molecules (two from intramolecular and three from coordinated water). Corresponding to this dehydration step there is an endotherm in DTA, at 283°C. The trihydration of the ytterbium tartrate is further supported by the fact that after an observed mass loss of 62.26%, ytterbium oxide is formed, which is clear from the saturation of TG curve from 700°C onwards. The calculated mass loss for the formation of ytterbium oxide from the starting composition $\text{Yb}(\text{C}_4\text{H}_6\text{O}_6)_3 \cdot 3(\text{H}_2\text{O})$ is 62.29%. This result clearly indicates that there are three water molecules of hydration associated with the grown material. The thermal behavior of crystals grown in silica gel is observed to be the same.

5 Conclusions

The use of ytterbium nitrate as upper reactant and L-tartaric acid as lower reactant results in the growth of ytterbium tartrate single crystals in silica gel at gel pH = 2.5, 3, 3.5 and in agar-agar at gel pH = 2. Spherulites of ytterbium tartrate are also formed in silica gel for gel pH > 3.5. The single crystals of ytterbium tartrate are found to have crystallized as trihydrates both in silica and agar-agar gels. The morphological form of single crystals is dipyratidial with the major habit faces as {111} and {001}. EDAX confirms the presence of ytterbium. FTIR spectrum shows the presence of tartrate ligands and establishes that one of the tartrate ions is singly ionized. CHN analysis combined with thermogravimetric analysis suggests that the grown crystals of ytterbium tartrate bear the formula $\text{Yb}(\text{C}_4\text{H}_4\text{O}_6)(\text{C}_4\text{H}_6\text{O}_6) \cdot 3(\text{H}_2\text{O})$. Thermogravimetric analysis reveals that the material is thermally stable up to 200°C.

Acknowledgements One of the authors (Basharat Wani) is thankful to the UGC, New Delhi and the Department of Higher Education, Government of J & K for providing the teacher fellowship. The corresponding author (PNK) is thankful to the All India Council of Technical Education (AICTE), New Delhi for the award of Eminent Fellowship.

References

- [1] M. E. Torres, T. Lopez, J. Peraza, J. Stockel, A. C. Yanes, C. Gonzalez-Silgo, C. Ruiz-Perez, and P. A. Lorenzo-Luis, *J. Appl. Phys.* **84**, 5729 (1998).
- [2] M. H. Rahimkuty, K. Rajendra Babu, K. Shreedharan Pillai, M. R. Sudarshanakumar, and C. M. K. Nair, *Bull. Mater. Sci.* **24**, 249 (2001).
- [3] M. E. Torres, A. C. Yanes, T. Lopez, J. Stockel, and J. F. Peraza, *J. Cryst. Growth* **156**, 421 (1995).
- [4] M. E. Torres, T. Lopez, J. Stockel, X. Solans, M. Garcia-Valles, E. Rodriguez-Castellon, and C. Gonzalez-Silgo, *J. Solid State Chem.* **163**, 491 (2002).
- [5] J. Fousek, L. E. Cross, and K. Seely, *Ferroelectrics* **1**, 63 (1970).
- [6] N. R. Ivanov, *Ferroelec. Lett.* **27**, 45 (1984).
- [7] S. K. Arora, Vipul Patel, Bhupendra Chudasama, and Brijesh Amin, *J. Cryst. Growth* **275**, e657 (2005).
- [8] K. Suryanarayana and S. M. Dharmaprakash, *Mater. Lett.* **42**, 92 (2000).
- [9] S. K. Arora, Vipul Patel, Anjana Kothari, and Brijesh Amin, *Cryst. Growth Des.* **4**, 343 (2004).
- [10] P. N. Kotru, K. K. Raina, and N. K. Gupta, *Cryst. Res. Technol.* **22**, 177 (1987).
- [11] P. N. Kotru, N. K. Gupta, and K. K. Raina, *Cryst. Res. Technol.* **21**, 15 (1986).
- [12] P. N. Kotru and K. K. Raina, *J. Mater. Sci. Lett.* **5**, 760 (1986).
- [13] P. N. Kotru, K. K. Raina, and N. K. Gupta, *J. Mater. Sci.* **21**, 90 (1986).
- [14] V. Mansotra, K. K. Raina, and P. N. Kotru, *J. Mater. Sci.* **26**, 3780 (1991).
- [15] A. Jain, A. K. Razdan, and P. N. Kotru, *Mater. Sci. Eng. B* **8**, 129 (1991).
- [16] A. Jain, A. K. Razdan, and P. N. Kotru, *Mater. Chem. Phys.* **45**, 180 (1996).
- [17] H. K. Henisch, *Crystal Growth in Gels*, Pennsylvania State University Press, University Park, PA, 1973.
- [18] H. K. Henisch, *Crystals in Gels and Liesegang Rings*, Cambridge University Press, Cambridge, 1988.
- [19] V. Alexeyev, *Quantitative Analysis*, Mir Publishers, Moscow, 1969, page 84.
- [20] R. A. Laudise, *The Growth of Single Crystals*, Prentice-Hall, Inc. Englewood Cliffs, New Jersey, page 272.
- [21] J. A. Mathew, G. B. Michael, D. S. Morris, and A. R. David, *Polyhedron* **15**, 3377 (1996).
- [22] W. Chuan-De, Z. Xiao-Ping, L. Can-Zhong, Z. Hong-Hui, and H. Jin-Shun, *Acta Cryst. E* **58**, 228 (2002).
- [23] F. C. Hawthorne, I. Borys, and R. B. Ferguson, *Acta Cryst. C* **39**, 540 (1983).
- [24] K. Nakamoto, *Infra Red and Raman Spectra of Inorganic and Coordination Compounds*, 5th Ed., John Wiley & Sons, 1997, Part B, Chapter 3, page 70.



Dielectric characterization of gadolinium tartrate trihydrate crystals

Basharat Wani^{a,1}, Farooq Ahmad^a, P.N. Kotru^{b,*}

^a Department of Physics, University of Kashmir, Srinagar 190006, Jammu and Kashmir, India

^b Department of Physics and Electronics, University of Jammu, Jammu 180006, Jammu and Kashmir, India

Received 29 June 2006; received in revised form 11 August 2006; accepted 10 September 2006

Abstract

Single crystals of gadolinium tartrate trihydrate have been grown by gel diffusion technique. Single crystal X-ray diffraction analysis shows the crystals belong to the tetragonal system with non-centrosymmetric space group. The dielectric constant, dielectric loss and ac conductivity have been measured as a function of frequency in the range 1 kHz–5 MHz and temperature range 20–300 °C. The dielectric constant increases with temperature, attains a peak around 240 °C and then decreases as the temperature exceeds 240 °C. The dielectric anomaly at 240 °C is suggested to be due to phase transition brought about in the material, which is further supported by the thermal studies. The variation of ac conductivity with temperature has been measured and the material is suggested to show protonic conductivity.

© 2006 Published by Elsevier B.V.

Keywords: Gadolinium tartrate trihydrate crystals; Phase transition; Ferroelectricity; Protonic conduction

Introduction

The salts of tartaric acid are found to exhibit a range of interesting physical properties such as ferroelectricity, piezoelectricity and optical second harmonic generation (SHG) [1–7]. Consequently, they are used in transducers and several linear and non-linear mechanical devices [1,2,4]. The unusual dielectric properties of Rochelle salt ($\text{NaKC}_4\text{H}_4\text{O}_6 \cdot 4\text{H}_2\text{O}$) first led to the notion of ferroelectricity in the double salt of tartaric acid. Subsequently, dielectric studies were carried out on isomorphous lithium tantalum tartrates [9] and lithium ammonium tartrate [10] to search for ferroelectricity in these compounds. Many investigators have examined the dielectric properties of tartaric acid salts with monovalent cations such as lithium thallium tartrate [11], rubidium hydrogen tartrate [12], ammonium tartrate [13] and sodium tartrate [14]. The dielectric properties of tartaric acid salts with divalent cations such as calcium [15], cadmium [1], manganese [16], zinc [17] and strontium tartrate [18] have also been investigated. Some of them have been shown to exhibit ferroelectric property [1,8–11,15] while others are non-

ferroelectric [13,14]. Literature survey reveals that the dielectric behaviour of trivalent metal tartrates (particularly rare earth tartrates) has hardly been investigated. In this paper, we describe the investigations based on measurements of the dependence of dielectric constant, dielectric loss as well as ac conductivity on applied frequencies and temperature of gadolinium tartrate trihydrate $\text{Gd}(\text{C}_4\text{H}_4\text{O}_6)(\text{C}_4\text{H}_5\text{O}_6) \cdot 3\text{H}_2\text{O}$ crystals, which is a trivalent tartrate salt. Single crystal X-ray diffraction analysis (the details of which would be published elsewhere) has shown that $\text{Gd}(\text{C}_4\text{H}_4\text{O}_6)(\text{C}_4\text{H}_5\text{O}_6) \cdot 3\text{H}_2\text{O}$ belongs to tetragonal system with cell parameters $a = 6.021 \text{ \AA}$, $c = 36.37 \text{ \AA}$, $V = 1318.5 \text{ \AA}^3$ and bearing the non-centrosymmetric space group. The powder diffraction data of gadolinium tartrate trihydrate has also yielded almost the same cell parameters [19]. Therefore, we may expect it to exhibit various polar effects such as piezoelectricity, pyroelectricity and ferroelectricity. In this paper, we report only the dielectric characteristics of the material. The results obtained on dielectric studies have been correlated with thermal studies viz., differential thermal analysis (DTA) and thermogravimetric analysis (TGA) of the crystals.

2. Experimental procedure

Single crystals of gadolinium tartrate trihydrate were grown by single gel diffusion method [20,21] using two types of gels – an inorganic (silica) gel and an organic (agar-agar) gel. The details

* Corresponding author. Tel.: +91 191 2450939; fax: +91 191 2453079.

E-mail address: pn.kotru@yahoo.com (P.N. Kotru).

Presently working at Crystal Growth and Materials Research Laboratory, Department of Physics and Electronics, University of Jammu, Jammu 180006.

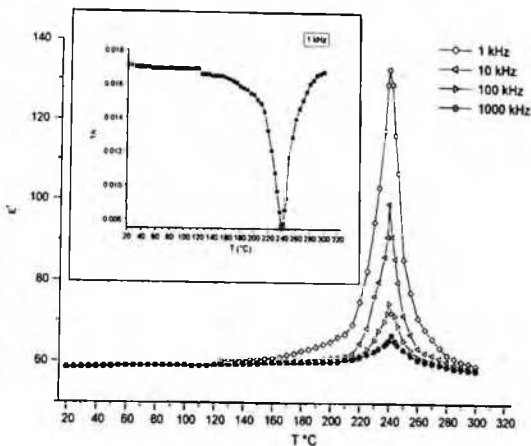


Fig. 1. Variation of dielectric constant with temperature at different frequencies. The inset of figure shows the variation of inverse real dielectric constant with temperature at 1 kHz.

of various experiments on the growth of these crystals have been published elsewhere [19]. The crystals obtained from all experiments were of small size and thus it was not possible to carry out direct measurement of dielectric properties on a single crystal. Therefore, the dielectric measurements were carried out on powdered samples in the form of pellets. To obtain the pellet samples, the single crystals were finely ground and the resulting powder was compressed into a die 13 mm in diameter and 0.8–1.2 mm in thickness under a pressure of 5 tonnes/cm² using a hand operated hydraulic press. The samples were silver electroded by using a fine paintbrush to coat both faces of the pellets with a thin layer of silver paint. The samples were then placed in a dry atmosphere for about 24 h to ensure maximum conductivity and adhesion of the silver paste. The dielectric measurements were carried out in the frequency range 1 kHz–5 MHz and over the temperature range 20–300 °C using a Hewlett-Packard impedance analyzer LF 4192A and further automated by using a computer for data recording, storage and analysis. A microprocessor based furnace fitted with a temperature controller and a specially designed two-terminal sample holder was used to heat the sample at a heating rate of 2 °C/min. The impedance analyzer directly provides the values of capacitance (C) and dielectric loss ($\tan \delta$). Other parameters such as dielectric constant (ϵ') and conductivity (σ_{ac}) were computed using the relations;

$$\epsilon' = \frac{Ct}{\epsilon_0 A} \quad \text{and} \quad \sigma_{ac} = 2\pi f \epsilon_0 \epsilon' \tan \delta;$$

where C is the capacitance (F), t the thickness (m), A the area (m²), $\epsilon_0 = 8.854 \times 10^{-12}$ F m⁻¹ and f is the frequency (Hz) of the applied electric field.

Single crystal X-ray diffraction analysis of Gd(C₄H₄O₆)(C₄H₅O₆)·3H₂O was carried out using Enraf-Nonius CAD4

diffractometer using Cu K α radiation. Thermal behaviour (thermogravimetric analysis and differential thermal analysis) of this material was investigated using a Shimadzu DTG 60 thermal analyzer.

3. Results and discussion

The dependence of dielectric constant (ϵ'), dielectric loss ($\tan \delta$) and ac conductivity (σ_{ac}) on temperature and frequency of the applied ac field is studied in the temperature range of 20–300 °C and frequency range of 1 kHz–5 MHz. The results are described as follows.

Fig. 1 shows the variation of real dielectric constant (ϵ') with temperature at four frequencies (1, 10, 100 and 1000 kHz) of applied ac field. The inset of Fig. 1 shows the variation of inverse dielectric constant with temperature at 1 kHz. It is clear from Fig. 1 that in the temperature range 20 < T < 160 °C, the dielectric constant of gadolinium tartrate trihydrate is practically temperature independent. Other tartrate salts [1,14,15] also show this type of behaviour. Beyond 160 °C, the dielectric constant increases almost exponentially with temperature, attains a peak around 240 °C and then decreases as the temperature exceeds 240 °C. This peak may suggest a phase transition in the material. To account for this behaviour, we have two possibilities. The first possibility is that on heating the sample up to 250 °C, there is a loss of three water molecules that are associated with gadolinium tartrate trihydrate and because of dehydration, a transition occurs at about 240 °C. This possibility is ruled out by the result of thermal behaviour. Fig. 2 shows thermogravimetric and differential thermal analytic curves of gadolinium tartrate trihydrate. The material loses one water molecule in the temperature range 210–230 °C (observed loss: 3.33%, calculated loss: 3.52%

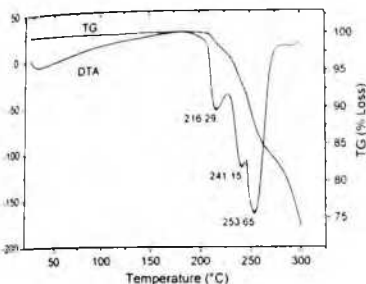


Fig. 2. Simultaneous TG and DTA curves of gadolinium tartrate trihydrate.

two H_2O molecules in the temperature range 230–250 °C (observed loss: 6.93%, calculated loss: 7%). Thus, dehydration water occurs in two stages; first from 210 to 230 °C and second from 230 to 250 °C. Therefore, it may appear that there should be two transitions; first in the temperature range 210–230 °C and second in the temperature range 230–250 °C. Torres et al. have observed two phase transitions in the cadmium tartrate crystals; one due to structural changes and the other due to loss of water. However, in the present case the only transition that has been observed is around 240 °C. Therefore, the possibility of the material showing the dielectric anomaly exclusively due to loss of water molecules may be ruled out in the present case. A second possibility is that the material is ferroelectric similar to calcium or cadmium tartrate [15,11]. A close look at the DTA curve of Fig. 2 shows an endothermic peak near about 241.15 °C, which is very close to the transition temperature observed around 240 °C in the dielectric versus temperature curve (Fig. 1). Thus, it is suggested that a crystallographic change due to polymorphic phase transition may have occurred in the material (including the loss of coordinated water molecules) which led to the dielectric anomaly near 240 °C. Keeping these results in view it can be suggested that the material under investigation shows a dielectric behaviour in the temperature range $20 < T < 240$ °C. The phase transition in gadolinium tartrate trihydrate is observed to be of diffused type and does not follow Curie–Weiss law, but obeys the following type of temperature dependence:

$$\frac{1}{\epsilon'_{\max}} = A(T - T_c)^\gamma$$

where ϵ'_{\max} is the peak value of the dielectric constant and γ is a critical exponent which lies in the range $1 < \gamma \leq 2$. For $\gamma = 1$ represents an ideal Curie–Weiss behaviour while a value between 1 and 2 indicates a diffuse behaviour. Fig. 3 shows the variation of $\ln((1/\epsilon') - (1/\epsilon'_{\max}))$ with $\ln(T - T_c)$ at 1 kHz. The graph shows almost linear behaviour as the temperature changes. The value of exponent γ , was calculated from the slope of the curve which comes out to be equal to 1.3 at a frequency of 1 kHz, which implies a diffused phase transition. This suggests a microscopic inhomogeneity in the material under study, with different local Curie points. Such a type

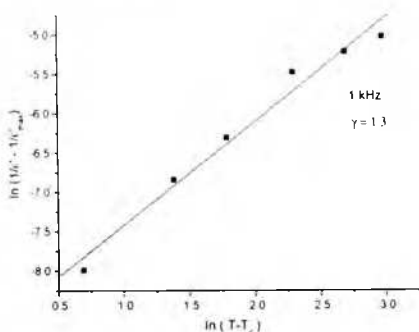


Fig. 3. $\ln((1/\epsilon') - (1/\epsilon'_{\max}))$ vs. $\ln(T - T_c)$ curve at a frequency of 1 kHz of applied ac.

of behaviour has also been found in many ceramic materials [22,23]. The variation in the value of diffusivity parameter γ with frequency has not been studied in the present investigation.

Fig. 4 shows the variation of dielectric loss versus temperature at three frequencies (1, 10 and 100 kHz). The dielectric loss curves also show a peak around 240 °C. It is clear from the graph that dielectric loss peak is frequency independent. The behaviour of dielectric loss with temperature shown in Fig. 4 is typical of polar dielectrics, where apart from dipole losses, losses due to electrical conduction also occur [24].

The variation of ac conductivity with temperature at four frequencies (1, 10, 100 and 1000 kHz) is shown in Fig. 5. It is clear from the figure that in the temperature range $20 < T < 200$ °C, the ac conductivity of gadolinium tartrate trihydrate is practically almost temperature independent. Above 200 °C ac conductivity approaches a maximum value at about 240 °C and decreases above this temperature. The large increase in conductivity in the

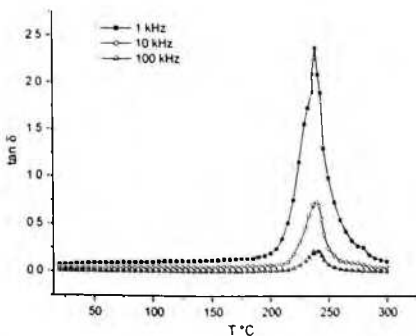


Fig. 4. Variation of dielectric loss with temperature at frequencies 1, 10 and 100 kHz.

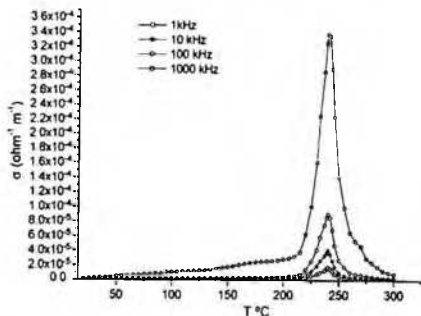


Fig. 5. Variation of ac conductivity with temperature at frequencies 1, 10, 100 and 1000 kHz.

temperature range $200 < T < 240$ °C can be understood as due to a large increase in the concentration of mobile charge carriers in the material. The material under investigation contains tartrate ligands (a dicarboxylic acid), besides three water molecules, coordinated to gadolinium. Therefore, the large increase in the conductivity may be due the dissociation of water molecules into H^+ and OH^- ions [25]. The activation energy (E_a) was calculated before and after the transition temperature by using the Arrhenius equation $\sigma = \sigma_0 \exp(E_a/kT)$. Fig. 6 shows the plot of $\ln \sigma_{ac}$ versus $1000/T$ at 1 kHz. In the inset of Fig. 6 is shown the graphical plot of $\ln \sigma_{ac}$ versus $1000/T$ at 1 kHz just before the

transition. The variation of $\ln \sigma_{ac}$ with reciprocal of temperature shows the change in slope exactly at the transition temperature of the material. Such type of anomaly has been observed in ferroelectric materials [26]. This is due to the difference in activation energy in the paraelectric and ferroelectric phases. The difference in the activation energy between the paraelectric and ferroelectric phases may be due to the grain boundary effect. The activation energy in ferroelectric (E_f) and paraelectric (E_p) phase at a frequency of 1 kHz has been estimated to be 1.71 and 1.74 eV respectively. The activation energy of this order has also been reported in the imidazolium salts of dicarboxylic acids, when electrical conductivity has been explained as due to proton transfer through hydrogen bonds [27]. It is worth noting in the present case that E_p ($=1.74$ eV) is higher than E_f ($=1.71$ eV). This could be attributed to the ordered state in the ferroelectric phase and the disordered state in the paraelectric region, where the charge carrier needs more activation energy to jump between adjacent sites. The electrical conductivity in gadolinium tartrate trihydrate may be explained as mainly due to proton transfer through hydrogen bonds. Many hydrogen bonded solids show conductivity via proton transfer through H-bonds [27–31]. The characteristic feature of rare earth tartrate salts is that in all these crystal structures rare earth cations and hydrogen bonds of O–H...O type involving water ligands, hydroxyl O and the carboxylate O atoms link the tartrate anions into layers parallel to (001); these layers are linked together by hydrogen bonding between adjacent tartrate molecule [32–34]. In these hydrogen bonded system the positively charged rare earth cations and negatively charged carboxylate anions may serve as channels for proton transport. This renders the gadolinium tartrate trihydrate as a protonic conductor.

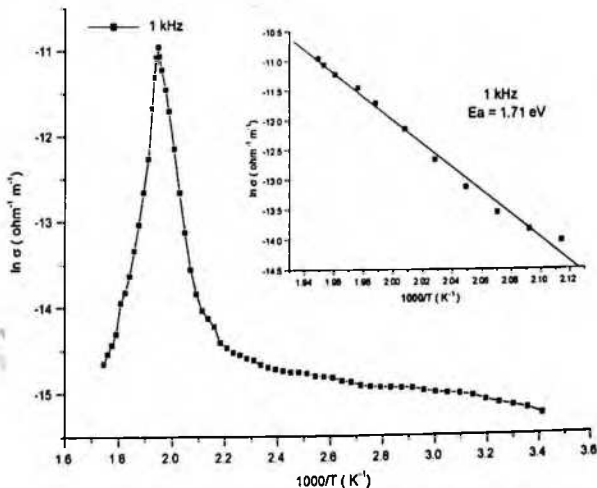


Fig. 6. Plot of $\ln \sigma_{ac}$ vs. $1000/T$ at 1 kHz. The inset of figure shows plot of $\ln \sigma_{ac}$ vs. $1000/T$ in the temperature $200 < T < 240$ °C used for calculating the activation energy.

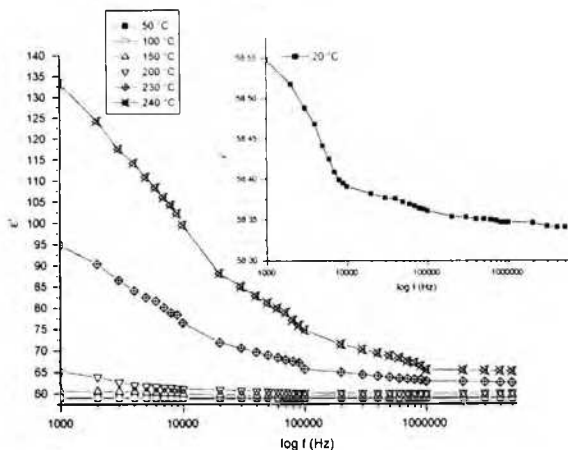


Fig. 7. Variation of dielectric constant with frequency. The inset of figure shows variation of dielectric constant with frequency at a temperature of 20 °C.

The variation of dielectric constant and dielectric loss as a function of frequency is shown in Figs. 7 and 8, respectively. The inset of Fig. 7 shows the variation of dielectric constant with frequency at 20 °C. It is clear from Figs. 7 and 8 that the dielectric constant and dielectric loss of gadolinium tartrate hydrate decreases gradually with increasing frequency. The increase of dielectric constant with increase of frequency is a

normal dielectric behaviour and can be explained on the basis of polarization mechanism. There are four primary mechanisms of polarization in materials, i.e., electronic, ionic or atomic, dipolar or orientational and space charge or interfacial polarization. At low frequencies, all the mechanisms of polarization contribute to the dielectric constant and with the increase in frequency, the contributions from different polarizations start decreasing.

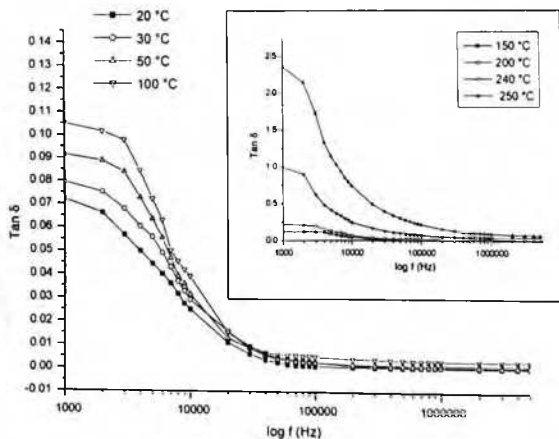


Fig. 8. Variation of dielectric loss with frequency at different temperatures. The inset of figure shows variation of dielectric loss with frequency around the transition temperature.

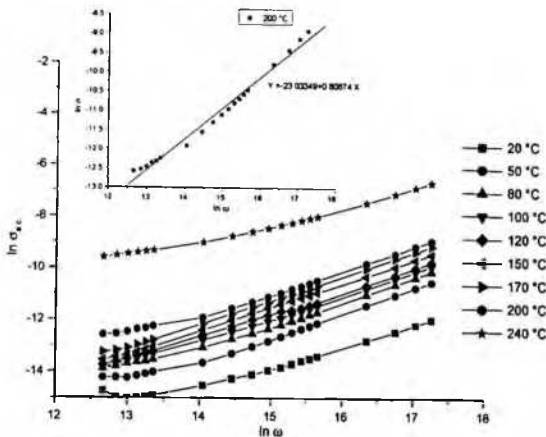


Fig. 9. Variation of $\ln \sigma_{ac}$ with $\ln \omega$ at different temperatures. The inset of the figure shows a representative curve of $\ln \sigma_{ac}$ vs. $\ln \omega$ at 200 °C used to calculate the exponent s in the equation $\sigma(\omega) = A \times \omega^s$.

For example, at very high frequencies (10^{15} Hz), only electronic polarization contributes to the dielectric constant, while ionic polarization takes place at IR frequencies ($\sim 10^{13}$ Hz). The high rise of dielectric constant at lower frequencies may be attributed to space charge polarization due to crystal lattice defects. The gradual decrease in dielectric constant and dielectric loss with frequency suggests that gadolinium tartrate trihydrate crystals have domains of different sizes and hence varying relaxation times.

The variation of ac conductivity with frequency at different temperatures is shown in Fig. 9. It is clear from the figure that conductivity increases with frequency and can be expressed as: $\sigma(\omega) = A \times \omega^s$, where $\omega = 2\pi f$. The value of exponent 's' is found by calculating the slope of the plot of $\ln \sigma_{ac}$ versus $\ln \omega$. A representative sample curve corresponding to temperature of 200 °C is shown in the inset of Fig. 9, where $s = 0.8$. It is observed that at a given temperature, the magnitude of conductivity is high at higher frequencies, thereby supporting the small polaron hopping model [35]. There occurs proton–phonon interaction such that when a proton tries to move, it has a strain field (a cloud of virtual thermal phonons) forming a quasi-particle like polaron. At higher frequencies of applied ac field, this quasi-particle disperses. When the cloud of phonons disperses, protons move and contribute to conductivity.

4. Conclusions

The study of the dielectric behaviour of gadolinium tartrate trihydrate crystals shows the strong dependence of dielectric constant on both temperature and frequency of the applied field. The dielectric constant (ϵ') varies with the temperature and attains a peak value around 240 °C after which it decreases,

thus, establishing this temperature as the transition temperature of the material. The decrease in dielectric constant and dielectric loss with frequency at different temperatures indicates that gadolinium tartrate trihydrate crystals may have domains of different sizes and of varying relaxation times. The anomalous behaviour of the dielectric constant near the transition temperature suggests the possibility of this material as being ferroelectric. The conductivity of the material is suggested to be due to protons transferring through hydrogen bonds, thus rendering the material as a protonic conductor.

Acknowledgements

One of the authors (B. Want) is thankful to the UGC, New Delhi, and Department of Higher Education, Government of Jammu and Kashmir for providing the teacher fellowship. The corresponding author is thankful to the All India Council of Technical Education, New Delhi, for award of Emeritus fellowship. We are thankful to the Head, Department of Physics and Electronics, University of Jammu for providing the necessary facilities.

References

- [1] M.E. Torres, T. Lo'pez, J. Peraza, J. Stockel, A.C. Yanes, C. González-silgo, C. Ruiz-perez, P.A. Lorenzo-luis, *J. Appl. Phys.* 84 (1998) 5729.
- [2] M.H. Rahimkuty, K. Rajendra Babu, K. Shreedharan Pillai, M.R. Sudashana Kumar, C.M.K. Nair, *Bull. Mater. Sci.* 24 (2001) 249.
- [3] M.E. Torres, A.C. Yanes, T. Lo'pez, J. Stockel, J.F. Peraza, *J. Cryst. Growth* 156 (1995) 421.
- [4] M.E. Torres, T. Lo'pez, J. Stockel, X. Solans, M. Garcia-valleés, Rodríguez-Castellón, C. González-silgo, *J. Solid State Chem.* 163 (2000) 491.
- [5] J. Fousek, L.E. Cross, K. Seely, *Ferroelectrics* 1 (1970) 63.

- [6] N.R. Ivanov, *Ferroelectr. Lett.* 27 (1984) 45.
- [7] F. Jona, G. Shirane, *Ferroelectr. Cryst.*, Dover Publications, Inc., New York, 1993 (Chapter VII).
- [8] J. Valasek, *Phys. Rev.* 19 (1921) 478.
- [9] W.J. Merz, *Phys. Rev.* 75 (1949) 687.
- [10] B. Matthias, J.K. Hulm, *Phys. Rev.* 82 (1951) 108.
- [11] S. Kambay, Z. G. Schaack, Z. J. Peitzely, B. Breznas, *J. Phys. Condens. Matter* 8 (1996) 4631.
- [12] C.C. Desai, A.H. Patel, M.S.V. Ramana, *Ferroelectrics* 23 (1990) 102.
- [13] M.M. Abdel-Kader, F. El-Kabbany, S. Taha, A. Abosehly, K.K. Tahoon, A. El-Sharkawy, *J. Phys. Chem. Solids* 52 (1991) 655.
- [14] M.M. Abdel-Kader, F. El-Kabbany, S. Taha, *J. Mater. Sci. Mater. Electron.* 1 (1991) 201.
- [15] H.B. Gon, *J. Cryst. Growth* 102 (1990) 501.
- [16] A.C. Yanes, T. Lopez, J.F. Peraza, M.E. Torres, *J. Mater. Sci.* 31 (1996) 2683.
- [17] T. Lopez, J. Stockel, J.F. Peraza, M.E. Torres, *Cryst. Res. Technol.* 30 (1995) 677.
- [18] S.K. Arora, V. Patel, R.G. Patel, B. Amin, A. Kothari, *J. Phys. Chem. Solids* 65 (2004) 965.
- [19] B. Wani, F. Ahmad, P.N. Kotru, *Mater. Sci. Eng. A* 431 (2006) 237.
- [20] H.K. Henisch, *Crystal Growth in Gels*, Pennsylvania State University Press, University Park, PA, 1973.
- [21] H.K. Henisch, *Crystals in Gels and Liesegang Rings*, Cambridge University Press, Cambridge, 1988.
- [22] S. Sharma, R. Sati, R.N.P. Choudhary, T.P. Sinha, *Mater. Lett.* 16 (1993) 281.
- [23] S. Bera, R.N.P. Choudhary, *Mater. Lett.* 22 (1995) 197.
- [24] B. Tareev, *Physics of Dielectric Materials*, Mir Publishers, Moscow, 1975, p. 155.
- [25] M. Nagai, T. Nishino, T. Kamizawa, *J. Mater. Sci. Lett.* 7 (1988) 720.
- [26] R.N.P. Choudhary, S.R. Shannigrahi, A.K. Singh, *Bull. Mater. Sci.* 22 (1999) 975.
- [27] K. Pogorzelec, Glaser, J. Garbarczyk, C.Z. Pawlaczyk, E. Markiewicz, *Mater. Sci.-Poland* 24 (2006) 245.
- [28] Y. Shihai, B.U. Yuxiang, Li Ping, *J. Chem. Phys.* 122 (2005) 054311.
- [29] A. Kawada, A.R. McGhie, M.M. Labes, *J. Phys. Chem.* 52 (1970) 3121.
- [30] H. Chojnacki, J.L. Bredas, M.P. Poskin, *J. Phys. Chem.* 88 (1984) 5882.
- [31] G.A. Jeffrey, *Cryst. Res. Technol.* 9 (2003) 135.
- [32] J.A. Matthew, G.B. Michael, D.S. Morris, A.R. David, *Polyhedron* 15 (1996) 3377.
- [33] W. Chuan, De, Z. Xiao-Ping, L. Can-Zhong, Z. Hong-Hui, H. Jin-Shun, *Acta Cryst. E* 58 (2002) 228.
- [34] F.C. Hawthorne, J. Borys, R.B. Ferguson, *Acta Cryst. C* 39 (1983) 540.
- [35] I.G. Austin, N.F. Mott, *Adv. Phys.* 18 (1969) 41.



Letter

Magnetic moment measurements of gadolinium, holmium, and ytterbium tartrate trihydrate crystals

Basharat Want^a, Farooq Ahmad^a, P.N. Kotru^{b,*}

^a Department of Physics, University of Kashmir, Srinagar 190006, India

^b Department of Physics and Electronics, University of Jammu, Jammu 180006, India

Received 18 December 2006; accepted 7 January 2007

Abstract

Magnetic moment and susceptibility of single crystals of rare earth tartrates of the type $R(C_4H_4O_6)(C_4H_5O_6) \cdot 3H_2O$ (where $R = Gd, Ho, \text{ and } Yb$), using a vibration sample magnetometer are reported. The experimental values of molar susceptibilities for $Gd(C_4H_4O_6)(C_4H_5O_6) \cdot 3H_2O$, $Ho(C_4H_4O_6)(C_4H_5O_6) \cdot 3H_2O$, and $Yb(C_4H_4O_6)(C_4H_5O_6) \cdot 3H_2O$ are 2.58×10^{-6} , 4.66×10^{-6} , and 8.03×10^{-6} (in cgs em units), respectively. The calculated effective magnetic moments are in good agreement with the theoretical predictions on rare earth ions.

© 2007 Published by Elsevier B.V.

Keywords: Rare earth compounds; Magnetic measurements

The magnetic properties of solids are very important, and attempts to understand them have led to a deep insight into the fundamental structure of many solids, both metallic and non-metallic. Rare earth compounds are interesting because of their magnetic properties. There is a vast amount of literature that reports the magnetic behavior of metallic compounds of rare earth elements [1–5]. Non-metallic compounds such as the rare earth nitrides, phosphides, arsenides, and selenides have also been studied for their magnetic behavior by several authors [6–7]. The magnetic susceptibilities of neodymium, samarium, and gadolinium ultra phosphates as a function of temperature are also reported in the literature. All these compounds exhibit a paramagnetic response following Curie's law [8]. In general most compounds of tartaric acid have shown to exhibit interesting physical properties such as, ferroelectricity, piezoelectricity, and optical second harmonic generation [9–14]. Consequently, some of them are used in transducers, and several linear and nonlinear mechanical devices [9–10,12]. Rare earth tartrates show poor solubility in water. They decompose before melting, and do not vaporize or sublime. Consequently, the only alternative to grow single crystals of these materials is by chemical reaction at a controlled rate using gel diffusion method.

Therefore, crystallization of gadolinium, holmium, and ytterbium tartrate trihydrate was accomplished using the gel diffusion technique. The details of various experiments on the growth and characterization of these crystals are reported elsewhere [15–17]. The stoichiometry of these crystals is established as $Gd(C_4H_4O_6)(C_4H_5O_6) \cdot 3H_2O$, $Ho(C_4H_4O_6)(C_4H_5O_6) \cdot 3H_2O$, and $Yb(C_4H_4O_6)(C_4H_5O_6) \cdot 3H_2O$. This letter reports the results of magnetic susceptibility and magnetic moment measurements carried out on these crystals.

The magnetic moments were measured by using a vibration sample magnetometer in a magnetic field of 5kOe at a temperature of 24 °C. Magnetic susceptibilities were corrected for diamagnetism of rare earth and tartrate ions, and water by using the value as -20×10^{-6} [18], -63.5×10^{-6} , and -0.722×10^{-6} [19], respectively. The molar susceptibility was calculated by using the equation

$$\chi_M = \frac{\chi_g M}{n}$$

where M is the molecular weight of the sample, n is the number of rare earth ions per molecule, and χ_g is the gram susceptibility. The effective magnetic moment in Bohr magnetons of rare earth ions is calculated by using the relation

$$\mu_{\text{eff}} = 2.828(\chi_M^{\text{corr}} T)^{1/2} \text{ B.M.}$$

* Corresponding author

E-mail address: pn.kotru@yahoo.com (P.N. Kotru).

Table 1
Magnetic susceptibility and magnetic moment measurements of some rare earth tartrates of the type $R(C_4H_4O_6)(C_4H_5O_6) \cdot 3H_2O$ (where R = Gd, Ho, and Yb)

Rare earth compound	Experimental molar susceptibility, χ_M (in cgs em units)	Corrected (for diamagnetism of constituent atoms) molar susceptibility, χ_M^{corr}	Observed magnetic moment, μ_{eff} (B.M.)	Theoretical effective magnetic moment of rare earth ions, $\mu_{eff} = [J(J+1)]^{1/2} \mu_B$ (B.M.)
Gd(C ₄ H ₄ O ₆)(C ₄ H ₅ O ₆)·3H ₂ O	2.58×10^{-2}	2.60×10^{-2}	7.89	7.94
Ho(C ₄ H ₄ O ₆)(C ₄ H ₅ O ₆)·3H ₂ O	4.66×10^{-2}	4.68×10^{-2}	10.59	10.61
Yb(C ₄ H ₄ O ₆)(C ₄ H ₅ O ₆)·3H ₂ O	8.03×10^{-3}	8.19×10^{-3}	4.43	4.54

where $\chi_M^{corr} = \chi_M + \chi^{dia}$ (total diamagnetic correction), T is the temperature (K) at which the measurements are made. Table 1 gives the observed values of molar susceptibilities, and effective magnetic moments of the rare earth tartrates. The observed values of the effective magnetic moments are compared with the theoretical values for respective rare earth ions. The results obtained reveal a good agreement between the observed, and the theoretical values of effective magnetic moments of free rare earth tripositive ions.

Acknowledgements

One of the authors (BW) is thankful to the UGC, New Delhi, and Department of Higher Education, Government of J & K for extending the tenure of the teacher fellowship. The corresponding author (PNK) is thankful to the All India Council of Technical Education, New Delhi for the award of Emeritus fellowship.

References

[1] J. Kanamori, *J. Alloys. Compd.* 408–412 (2006) 2–8.
 [2] A.L. Lima, *J. Magn. Magn. Mater.* 310 (2007) 51–56.
 [3] E. Talik, M. Klimeczak, R. Troc, J. Kusz, W. Hofmeister, A. Damm, *J. Alloys Compd.* 427 (2007) 30–36.

[4] Y.O. Tokaychuk, O.I. Bodak, Y.K. Gorenko, K. Yvon, *J. Alloys Compd.* 415 (2006) 8–11.
 [5] X.C. Kou, R. Grossinger, G. Wiesinger, *Phys. Rev. B: Condens. Matter* 51 (1995) 8254.
 [6] D. Garcia, M. Faucher, *Handbook on the Physics and Chemistry of Rare Earths*, vol. 21, 1995, pp. 263–304.
 [7] M.K. Wilkinson, E.O. Wollen, W.C. Kocher, *Phys. Rev.* 131 (1963) 922.
 [8] M. Cole, M.R. Lees, J.A.K. Howard, R.J. Newport, G.A. Saunders, E. Schonherr, *J. Solid State Chem.* 150 (2000) 377.
 [9] M.E. Torres, T. Lopes, J. Peraza, J. Stockel, A.C. Yanes, C. Gonzalez-Silgo, C. Ruiz-Perez, P.A. Lorenzo-Luis, *J. Appl. Phys.* 84 (1998) 5729.
 [10] M.H. Rahimkuty, K. Rajendra Babu, K. Shreedharan Pillai, M.R. Sudarshanakumar, C.M.K. Nair, *Bull. Mater. Sci.* 24 (2001) 249.
 [11] M.E. Torres, A.C. Yanes, T. Lopez, J. Stockel, J.F. Peraza, *J. Cryst. Growth* 156 (1995) 421.
 [12] M.E. Torres, T. Lopez, J. Stockel, X. Solans, M. Garcia-Valleis, E. Rodriguez-Castellon, C. Gonzai Lez-Silgo, *J. Solid State Chem.* 163 (2002) 491.
 [13] J. Fousek, L.E. Cross, K. Seely, *Ferroelectrics* 1 (1970) 63.
 [14] N.R. Ivanov, *Ferroelectr. Lett.* 27 (1984) 45.
 [15] B. Want, F. Ahmad, P.N. Kotru, *Mater. Sci. Eng. A* 431 (2006) 237.
 [16] B. Want, F. Ahmad, P.N. Kotru, *J. Cryst. Growth*, in press.
 [17] B. Want, F. Ahmad, P.N. Kotru, *Cryst. Res. Technol.* 41 (2006) 1167–1173.
 [18] P.W. Selwood, *Magneto Chemistry*, 2nd ed., Wiley-Interscience, New York, 1956.
 [19] P.W. Selwood, *Magneto Chemistry*, 2nd ed., Wiley-Interscience, New York, 1956, p. 435.



Single crystal growth and characterization of holmium tartrate trihydrate

Basharat Wani^{a,1}, Farooq Ahmad^a, P.N. Kotru^{b,*}

^aDepartment of Physics, University of Kashmir, Srinagar 190006, J. and K. India

^bDepartment of Physics and Electronics, University of Jammu, Jammu 180006, J. and K. India

Received 15 May 2006; received in revised form 17 November 2006; accepted 17 November 2006

Communicated by H. Katochi

Available online 26 January 2007

Abstract

The growth of holmium tartrate trihydrate (HTT) single crystals is achieved in organic (agar-agar) as well as in inorganic (silica) gels by single gel diffusion method. Results of the study on nucleation kinetics of crystals grown in silica gel are described. The crystals exhibit the morphological form of a tetragonal dipyramidal class with {001} and {111} as dominant faces. Elemental and thermogravimetric analysis (TGA) supplemented by energy dispersive analysis of X-rays (EDAX) support the suggested chemical formula of the grown crystals to be $[\text{Ho}(\text{C}_4\text{H}_4\text{O}_6)(\text{C}_2\text{H}_2\text{O}_4)_3 \cdot 3\text{H}_2\text{O}]$. Single crystal X-ray diffraction (XRD) studies indicate that the crystals belong to tetragonal system with the cell parameters $a = 5.97 \text{ \AA}$, $c = 36.09 \text{ \AA}$ bearing the space group $P4_1$. Fourier transform infrared (FT-IR) spectroscopic study indicates the presence of tartrate ligands and suggests that one of the tartrate ions is singly ionized. TGA suggests that the material is thermally stable up to 220 °C.

© 2007 Elsevier B.V. All rights reserved.

PII: S0022-0248(06)01122-5

Keywords: A1. Crystal growth; A1. FTIR; A1. SEM; A1. Thermal stability; A1. XRD; B1. Holmium tartrate trihydrate

1. Introduction

The salts of tartaric acid are found to exhibit a range of interesting physical properties such as ferroelectricity, piezoelectricity and optical second harmonic generation (SHG) [1–7]. Consequently, they are used in transducers and several linear and nonlinear mechanical devices [1,2,4]. This has led many investigators to grow single crystals of tartrate compounds and study their characteristics [8–11]. Many investigators have grown rare earth tartrates bearing the general formula $R_2(\text{C}_4\text{H}_4\text{O}_6)_3 \cdot \text{H}_2\text{O}$ ($R = \text{Nd, Dy, Gd, La, Di, Pr, Sm}$ and Y) by gel method [12–18]. However, there is no information in the literature on the growth and

study of nucleation kinetics of rare earth tartrates in general and holmium tartrate trihydrate crystals in particular. In this paper, the authors describe the growth of single crystals of holmium tartrate trihydrate (HTT) in silica and agar-agar gels. The results obtained by single and powder X-ray diffraction (XRD) studies, energy dispersive analysis of X-rays (EDAX), Fourier transform infra-red spectroscopy (FT-IR), carbon and hydrogen analysis (CHN), and thermogravimetric analysis (TGA and DTA) of HTT crystals are described.

2. Experimental procedure

The crystallization of HTT was accomplished using single gel diffusion technique [19,20]. The crystals were grown in a single glass tube of length 200 mm and diameter 25 mm. Silica gel was prepared by adding a solution of sodium metasilicate of molarity (0.3–1.5 M) to tartaric acid of a particular molarity (0.2–2.5 M) drop by drop with

*Corresponding author. Tel.: +91 0191 2450939.

fax: +91 0191 2453079.

E-mail address: pn_kotru@yahoo.com (P.N. Kotru).

¹Presently working at Crystal Growth and Materials Research Laboratories, Department of Physics and Electronics, University of Jammu, Jammu 180006, India.

continuous stirring. The solution with the desired value of pH (3–6) was then transferred to several glass tubes. Once gelled, an aqueous solution of holmium nitrate (upper reactant) of desired molarity (0.25–2 M) was carefully poured with the help of a pipette along the walls of the tubes over the set gel.

Experiments were also carried out to grow single crystals of HTT in organic agar–agar medium. Agar–agar gel was prepared by dissolving desired concentration (% w/v) of agar–agar in water. The agar–agar solution was then mixed with desired concentration of *t*-tartaric acid in various proportions by volume. The mixed solution was transferred to several glass tubes. After setting of the gel, an aqueous solution of holmium nitrate of desired concentration was carefully poured over it. All the experiments in silica as well as agar–agar gels were carried out at an ambient temperature of 36 °C.

The carbon and hydrogen contents in the obtained crystals were determined by using Elementar Vario-EL III CHNS analyzer. An energy dispersive spectrometer (OXFORD ISIS-300 system) attached to a scanning electron microscope JEOL JSM-5800 was used to determine the atomic as well as weight percentage of Ho and O in the compound. Single crystal XRD analysis of HTT was carried out using Enraf-Nonius CAD4 diffractometer with Cu K α radiation. The powder XRD patterns of the grown crystals were obtained using a Bruker AXS D8 advance XRD with Cu K α radiation ($\lambda = 1.5406 \text{ \AA}$). The FT-IR spectrum of the material in the wave number range of 400–4000 cm^{-1} was recorded on a Bruker Vector 22 spectrometer using KBr pellet technique. The thermal behavior (TGA and DTA) of the HTT crystals was recorded on a Shimadzu DTG 60 thermal analyzer in N $_2$ atmosphere at a heating rate of 10 °C/min.

3. Results and discussion

3.1. Growth from silica gel

In silica gel, a gel pH of 3, 3.5, and 3.75 yields single crystals of HTT and for a pH ≥ 4 , two distinct types of spherulites, one just below the gel/solution interface and the other in the lower half of the gel column were formed. The spherulites grown just below the gel/solution interface were recognized as holmium nitro-tartrate hydrate, while those in the lower half as HTT. For gel pH ≥ 4 , a strong precipitation was observed to occur at the gel/solution interface just after pouring of upper reactant. This initial precipitation results due to instantaneous reaction between the holmium and tartrate ions. Due to this, the local supersaturation available for three-dimensional nucleation and growth becomes very high which results in the formation of spherulites. However, our study here refers to only single crystals of HTT, which form at gel pH ≤ 3.75 . The single crystals formation at pH values ≤ 3.75 may be explained as follows. Firstly, in the silica gel (containing tartaric acid) of a particular pH, the concentration of the

precipitant ions $\text{C}_4\text{H}_4\text{O}_6^{2-}$, which are anions of tartaric acid, depends on the H^+ ion concentration. The concentration of precipitant ions decreases with the decrease in pH [21]. Secondly, in a low pH medium the solubility of holmium tartrate gets raised with the result that the local concentration product $[\text{Ho}^{3+}][\text{C}_4\text{H}_4\text{O}_6^{2-}]$ decreases and becomes less than the solubility product K_{sp} . Otherwise, if local concentration product is greater than K_{sp} , a strong precipitation occurs at the interface [22], which often leads to the formation of spherulites as well as amorphous precipitates. Thus, in a low pH medium, the value of local supersaturation with respect to HTT developed at different sites inside the gel changes and becomes as low as may be appropriate for the growth of single crystals. Fig. 1(a) shows some single crystals of HTT growing in a crystallizer. Fig. 1(b) shows an optical micrograph of a typical single crystal of HTT. It is clear from Fig. 1(b) that single

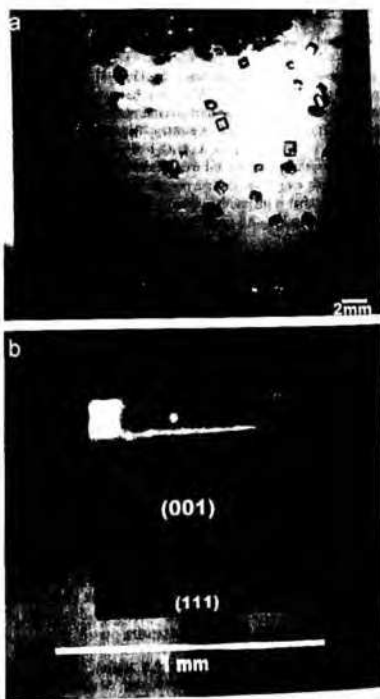


Fig. 1. (a) Photograph showing single crystals of HTT growing at isolated sites in silica gel in a crystallizer. (b) An optical micrograph of a typical single crystal of HTT grown from silica gel revealing its morphological development.

crystals of HTT exhibit the morphology of a dipyramidal class. The crystals are bounded by $\{111\}$ and $\{001\}$ habit faces, $\{001\}$ faces being more dominant than $\{111\}$.

3.2 Nucleation kinetics

The effect of various growth parameters such as concentration of upper reactant, gel concentration, gel age and gel pH on the nucleation density, as measured by the total number of crystals that appear in the gel column were investigated by conducting the experiments at an ambient temperature of 36 °C.

- (1) *Effect of upper reactant concentration* Gels of pH 3.5 were prepared with 0.5M sodium metasilicate and 0.5M L-tartaric acid and allowed to set in a number of test tubes. After a gel age of 72h, 20mL of holmium nitrate of different concentration from 0.25 to 2M was poured over the set gel and the crystal count was recorded. It was observed that the crystal count increased with the concentration of upper reactant as shown in Fig. 2, as has been reported in the literature for $KClO_4$ crystals [23]. By increasing upper reactant concentration beyond 2M, spherulites were formed.
- (2) *Effect of gel concentration* Gels of different concentrations were prepared by mixing sodium metasilicate of molarity varying from 0.5 to 1.5M with 0.5M L-tartaric acid. The pH of the gel medium was maintained at 3.5 by varying the amount of L-tartaric acid. After a gel age of 72h, 20mL of upper reactant of molarity 0.5M was poured over the set gel. It was observed that the high concentration gels take lesser time for setting and are mechanically stronger; however, they contaminate the growing crystals with silica. The variation of crystal count with gel concentration is shown in Fig. 3.
- (3) *Effect of gel aging* Gels of fixed pH 3.5 were prepared with 0.5M sodium metasilicate and 0.5M L-tartaric

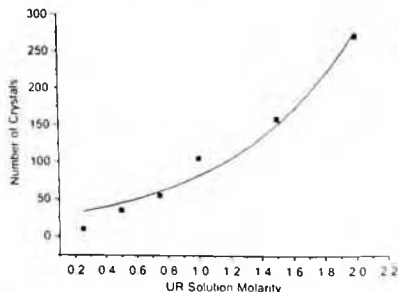


Fig. 2. Variation of crystal count with molarity of upper reactant in silica gel medium.

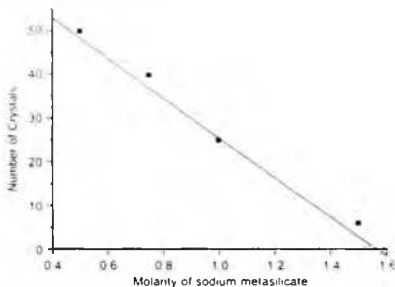


Fig. 3. Variation of crystal count with molarity of sodium metasilicate solution.

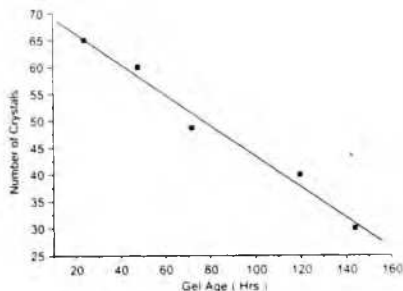


Fig. 4. Variation of crystal count with silica gel age.

- acid and allowed to set in a number of test tubes. The gels were allowed to age for different periods (24–144 hrs) before pouring a fixed amount (20 mL) of upper reactant of molarity 0.5M. The variation of crystal count with gel age is shown graphically in Fig. 4.
- (4) *Effect of gel pH* In order to study the pH dependence on the crystal count, gels with different pH values varying from 3 to 6 were prepared by adjusting the amount of 0.5M L-tartaric acid incorporated in the gel. All other parameters e.g. gel concentration (0.5M), gel age (72 h) concentration of upper reactant (0.5M) were kept constant. The observed change in the crystal count with gel pH is graphically illustrated in Fig. 5.

The experimental results as described above reveal that the number of crystals increases exponentially in some cases (Fig. 2), whereas it decreases linearly or exponentially in some other cases (Figs. 3 & 4). Arora et al. [10] also

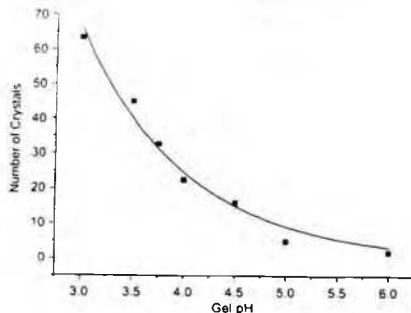


Fig. 5. Variation of crystal count with silica gel pH.

observed such types of trends on the dependence of number of crystals on various growth parameters. According to them, the trends are consequences of (i) three-dimensional nucleation rate, (ii) diffusion rate in the gel due to variation in the gel structure which may include pore size, cross linkage of cell boundaries, etc. and (iii) diffusion rate in the gel due to changes in the hydrostatic pressure resulting from the height of upper reactant solution. According to these authors, the equation giving the variation of nucleation rate J with supersaturation S is found to be applicable for explanation of the observed trends i.e. $J = J_0 \exp[-\frac{16\pi\Omega^2}{3kT} k^{-3} (\ln S)^2]$, where δ is a shape factor, γ is the nucleus solution interfacial tension, Ω is the volume of one growth unit in the nucleus, k is Boltzmann constant, T is the temperature in Kelvin and $S = C/C_0$ is the supersaturation ratio (C_0 is the equilibrium solution concentration which is related to solubility product, while C is actual solution concentration). The equation is reported to be applicable to a non-electrolyte [24,25]. According to nucleation theory, the amount of work which must be done to form a spherical critical nucleus is given by $W^* = 16\pi\Omega^2 \gamma^3 / 3(kT \ln S)^2$ [20]. The nucleation probability P is proportional to the Boltzmann factor $\exp(-W^*/kT)$, so that $P \propto \exp[-16\pi\Omega^2 \gamma^3 / 3kT^3 (\ln S)^2]$. Since the growth occurs in the same medium, it may be supposed that the interfacial tension γ has a negligible influence on the probability of nucleation. Thus, under isothermal conditions, the probability of nucleus formation depends sharply on supersaturation S , i.e. $P = \exp[-h/(\ln S)^2]$, where h is a constant [20]. Now the supersaturation in gel growth is determined by concentration of reactants as well as by the diffusion rate of reactants in the gel column. The factor that affects the diffusion processes is the gel structure of the medium. Therefore, it may be argued that the nucleation probability under isothermal conditions of growth is mainly determined by the concentration of reactants and gel structure (which is affected by gel pH, gel concentration

and gel age). By increasing the molarity of upper reactant (other parameters remaining constant), the probability of Ho^{3+} ions to react with tartrate ions in the gel increases. Consequently, the supersaturation increases which leads to an increase in the probability of nucleus formation. It is expected that the number of crystals will increase with the increase in the probability of nucleation. Therefore, the number of crystals in the gel column increases as shown in Fig. 2. Increase in supersaturation leading to an increased number of crystals has also been reported by Judge et al. [26] in case of tetragonal lysozyme crystals. The increase in the gel concentration and the gel age both have the effect of decreasing the average pore size of the silica gel [27]. Due to this the supersaturation and hence nucleation probability decreases as many nuclei find themselves in cells of too small a size to support growth to visible crystal sizes. Therefore, crystal count decreases as shown in Figs. 3 and 4. By increasing the pH, the gel structure lacks the property of cross linkage and becomes more and more hard leading to retardation of free motion of the ions, which is essential for the nucleation. Therefore, the crystal count decreases as the pH of the gel is increased as shown in Fig. 5.

3.3. Growth from agar-agar gel

Experiments were also carried out to grow single crystals of holmium tartrate in agar-agar gel. Being a physical gel it can be made to set at much lower values of pH. In the present case, the pH of the agar-agar medium was set at equal to 2. At this condition of growth, no precipitation occurred at the gel/solution interface upon pouring of upper reactant and after a period of 4 weeks, the whole gel column became impregnated with single and twinned crystals of HTT. In the case of agar-agar gel, only single and twinned crystals of holmium tartrate are observed under all conditions of growth. The single crystals have a well-developed morphology of dipyrarnidal class with $\{001\}$ and $\{111\}$ as habit faces. The morphology is same as that of single crystals grown in silica gel, except that $\{111\}$ faces are more dominant than $\{001\}$. This could be attributed to differences in the rate of growth of faces in two different gels. The agar-agar gel grown crystals are, in general, more transparent and perfect than those grown in silica gel. The surface of the former are smoother and crystals have lesser inclusions incorporated in them. Fig. 6(a) shows single crystals of HTT growing in agar-agar gel in a crystallizer. Fig. 6(b) is a photomicrograph of a typical single crystal of HTT, showing the dipyrarnidal morphology.

Twinned crystals of HTT were also observed to grow in agar-agar gel. Fig. 7(a) illustrates penetration twinning in the crystals. The plane parallel to a face of the unit dipyrarnid $\{111\}$, appears to act as the twinning plane. This type of penetration twinning is commonly observed in dipyrarnidal crystals of tetragonal system. A region of Fig. 7(a) at a higher magnification is shown in Fig. 7(b), revealing the habit faces of the twinned crystals.

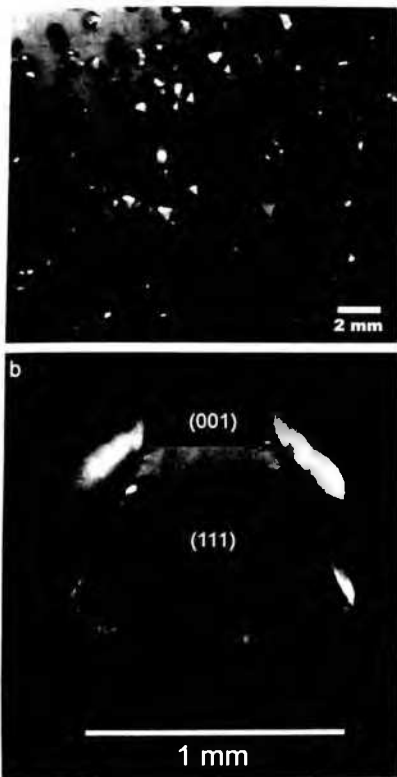


Fig. 6. (a) Photograph showing single crystals of HTT growing in agar-agar gel in a crystallizer. (b) An optical micrograph of a typical single crystal of HTT grown from agar-agar gel.

4. Characterization

4.1. Elemental analysis

Table 1 shows the results of carbon and hydrogen analysis carried on single crystals of HTT grown from both agar-agar and silica gel. The atomic and weight percentage of O and Ho as obtained by EDAX of the compound are shown in Table 2. The theoretical values in Table 1 are calculated according to the suggested empirical formula

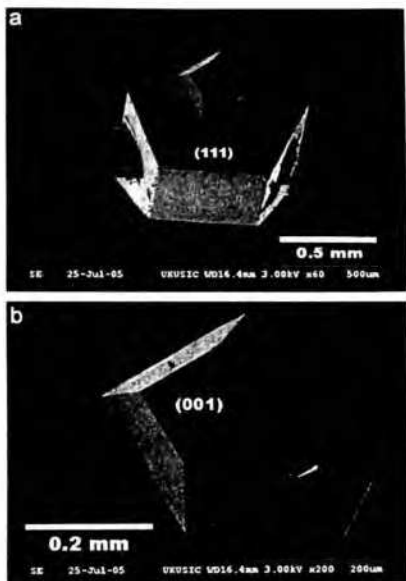


Fig. 7. (a) An SEM micrograph illustrating penetration twinning in HTT crystals grown from agar-agar gel. (b) A region of (a) at a higher magnification, showing the habit faces of the twinned crystal.

Table 1
Percentage composition of C and H as obtained by CHN analysis.

Element	Experimental (%)		Theoretical (%)
	Agar-agar gel grown crystals	Silica gel grown crystals	
C	18.61	18.63	18.62
H	2.94	2.92	2.93

$\text{HoC}_6\text{H}_{11}\text{O}_8$. The percentage composition of C, H, O and Ho as revealed by CHN and EDAX analyses compare well with those calculated from the proposed formula. The experimental and theoretically determined values are in agreement within the acceptable limits. A literature survey of the isomorphous compounds [28–31], suggests the chemical formula of gel grown HTT to be $[\text{Ho}(\text{C}_4\text{H}_6\text{O}_6)_3(\text{H}_2\text{O})_3]$ ($\text{C}_4\text{H}_6\text{O}_6$) $_3(\text{H}_2\text{O})_3$. The formula shows that one tartrate

Table 2
Atomic and weight percentage of O and Ho as obtained by EDAX analysis

Element	Experimental				Theoretical	
	Agar-agar gel grown crystals		Silica gel grown crystals		Weight (%)	Atomic (%)
	Weight (%)	Atomic (%)	Weight (%)	Atomic (%)		
O	61.35	92.92	60.95	92.24	59.27	93.75
Ho	38.65	7.08	39.05	7.76	40.73	6.25

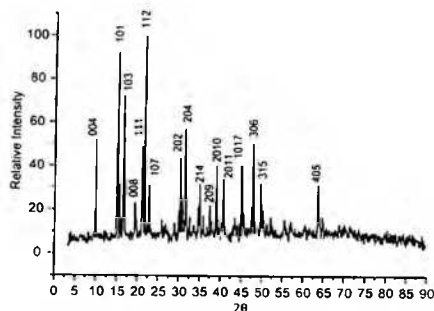


Fig. 8. Powder X-ray diffractogram of HTT

ion is singly ionized and the other doubly ionized. The fact that one of the tartrate ions is singly ionized is supported by the presence of absorption peak at 1719.07 cm^{-1} in the FT-IR spectrum of HTT. These results suggest that there are three water molecules bonded to holmium and the tartrate is disordered between a singly and a doubly ionized species.

3.4.2. XRD results

The powder XRD of HTT crystals is shown in Fig. 8. Table 3 provides the data for observed and calculated d -spacings as well as the corresponding planes. The experimental values were found to correspond with the calculated d -values of unit cell dimensions determined from single crystal XRD analysis: $a = 5.97\text{ \AA}$, $c = 36.09\text{ \AA}$, $\alpha = \beta = \gamma = 90^\circ$, $V = 1287.12\text{ \AA}^3$. Single crystal XRD results also confirm that the material grown in the present investigation is isomorphous with erbium ditartrate trihydrate [30], yttrium tartrate hydrate [31] and samarium tartrate trihydrate as reported in Ref. [32]. Table 4 gives a comparison of some crystallographic parameters of HTT with those of reported rare earth tartrates.

3.4.3. FT-IR spectroscopy results

Fig. 9 shows the FT-IR spectrum of HTT crystals grown in agar agar gel. The infrared spectrum in the range

Table 3
Powder XRD data for HTT

2θ	Observed d -values (\AA)	Calculated d -values (\AA)	hkl
9.939	8.89199	9.023	004
15.221	5.81633	5.89	101, 011
15.790	5.60787	5.668	012, 102
16.696	5.30578	5.348	013, 103
19.657	4.51258	4.511	008
21.164	4.19664	4.193	111
21.747	4.08335	4.110	112
22.804	3.89649	3.902	107
30.333	2.94429	2.945	202
31.608	2.82834	2.834	204
35.065	2.55704	2.560	214
37.465	2.39854	2.394	209
39.129	2.30034	2.300	2010
40.826	2.20854	2.208	2011
45.243	2.00264	2.000	1017
48.032	1.89265	1.889	306
49.835	1.82834	1.826	315
63.721	1.45932	1.462	405

$400\text{--}4000\text{ cm}^{-1}$ show a strong broad band centered at 3267.18 cm^{-1} due to OH stretching vibration of water and carboxylic acid group. Due to very strong interlinked H-bonding, the peak assignment for carboxylic acid group (OH), C-H vibrations and that of (OH) of water gets overlapped. The strong peak at 1719.07 cm^{-1} is attributed to stretching vibration of (C=O) bonds, which shows the presence of unionized carboxyl groups in the compound [32]. A band centered at approximately 1585.43 cm^{-1} is due to the C=O asymmetric stretch of coordinated carbonyl group. The absorption at 1410.82 cm^{-1} is attributed to C=O symmetric vibration. The value $\Delta\nu = 174\text{ cm}^{-1}$, the difference between two wavenumbers $\nu_{\text{as}}(\text{COO}^-)$ and $\nu_{\text{s}}(\text{COO}^-)$, indicates the bridging mode of the carboxylate group [33]. The absorption bands around 1066.91 cm^{-1} have been assigned to $\nu(\text{C-OH})$ stretching vibration. FT-IR spectrum of silica gel grown HTT crystals is observed to be the same as that of agar-agar gel grown crystals. The assignment of some selected absorption band peaks observed in the FT-IR spectrum of HTT grown in both media is given in Table 5. It is thus clear that the FT-IR spectroscopic results of HTT crystals confirm the

Table 4
Comparison of crystallographic parameters of different rare earth tartrates.

Compound	Crystal system	Space group	<i>a</i> (Å)	<i>c</i> (Å)	Volume (Å ³)
Y(C ₂ H ₂ O ₆)(C ₂ H ₂ O ₆) · 2.5 H ₂ O [24]	Tetragonal	P4 ₂ ,2 ₁ ,2	6.010	36.421	1315.5
Sm(C ₂ H ₂ O ₆)(C ₂ H ₂ O ₆) (H ₂ O) ₂ [25]	Tetragonal	P4 ₂ ,2 ₁ ,2	6.103	36.826	1371.6
Er · 2 C ₂ H ₂ O ₆ · 3 H ₂ O [26]	Tetragonal	P4 ₂ ,2 ₁ ,2	5.995	36.433	1309.4
Ho(C ₂ H ₂ O ₆)(C ₂ H ₂ O ₆) · 3H ₂ O (present investigation)	Tetragonal	P4 ₂	5.97	36.09	1287.12

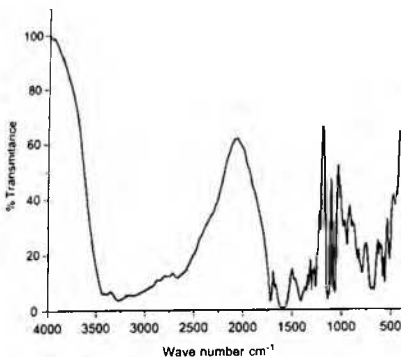


Fig. 9. FT-IR spectrum of HTT crystals grown from agar-agar gel.

Table 5
Assignment of some selected FT-IR wave numbers (cm⁻¹) of HTT

IR bands/cm ⁻¹		Assignments of peaks/bands
Silica gel grown crystals	Agar-agar gel grown crystals	
2600–3500	2600–3434	ν_s (OH) + ν_{as} (OH) of water and OH of carboxylic acid
1721.11	1719.07	ν (C=O); unionized COOH groups
1614.31	1585.43	ν_{as} (COO ⁻)
1415.74	1410.82	ν_s (COO ⁻)
1208.94	1209.15	ν_{as} C–C
1067.09, 1140.23	1066.91, 1140.03	ν (C–OH) + δ (C–H) + π (C–H)
942.39	943.02	ν_s C–C
840.45	840.45	δ (C O O)

presence of tartrate ligands and establish that one of the tartrate ions is singly ionized.

3.4.4. Thermal stability results

Fig. 10 shows the TGA and DTA curves of HTT crystals grown in agar-agar gel, in the temperature range from 26

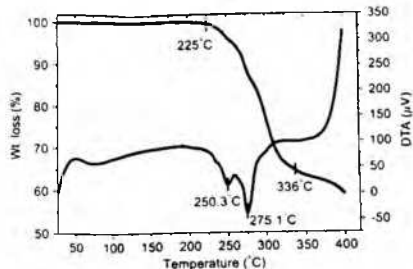


Fig. 10. TG and DTA curves of HTT crystals grown from agar-agar gel

to 400 °C. From the TG curve, it is observed that the material remains stable up to a temperature of about 220 °C. In the temperature range 225–336 °C, the material loses five water molecules and two CO₂ molecules, leading to the formation of holmium acrylate [34] (calculated weight loss: 34.5%, observed: 35%). The loss of five water molecules includes three coordinated and two intramolecular water molecules. The loss of two intramolecular water molecules results into the dehydration of the tartrate, thus leading to formation of holmium fumarate complex. Probably this complex can undergo radical induced ketonol tautomerism, accounting for the relatively weak absorption maximum at 936.19 cm⁻¹ (belonging to C=C band) in the FT-IR spectrum of the intermediate obtained at 280 °C. With subsequent loss of two CO₂ molecules, the fumarate complex decomposes to holmium acrylate. The formation of acrylate complex was confirmed by carrying out CHN analysis of the intermediate obtained at 340 °C (calculated; C = 21.3%, H = 1.5%; observed: C = 20.96%, H = 1.55%). The thermal analysis of silica gel grown crystals was observed to be the same.

4. Conclusions

The silica and agar-agar gel growth system involving the use of holmium nitrate as upper reactant and L-tartaric acid as lower reactant results in the crystallization of HTT. Silica gel system leading to single-crystal growth for gel pH ≤ 3.75 whereas for gel pH ≥ 4 the crystals assume

spherulitic morphology. Use of agar-agar gel yields single and twinned crystals. The morphological form of single crystals is dipyramidal with the major habit faces as $\{111\}$ and $\{001\}$. The morphological development of the crystals grown in silica and agar-agar gels indicates differential rate of growth along certain directions. The experimental results obtained for the crystal count on the variation of growth parameters suggest that the crystals grown in silica gel follow classical laws of three-dimensional nucleation. Single crystal XRD results show that the crystals belong to tetragonal system with cell parameters $a = 5.97$, $c = 36.09$ and $V = 1287.12 \text{ \AA}^3$, bearing a non-centrosymmetric space group $P4_1$. Infra red spectrum shows the presence of tartrate ligands and establishes that one of the tartrate ions is singly ionized. The stoichiometric composition of the crystals is established to be $[\text{Ho}(\text{C}_4\text{H}_4\text{O}_6)](\text{C}_2\text{H}_3\text{O}_6) \cdot 3(\text{H}_2\text{O})$. TGA reveals that the material is thermally stable up to 220 °C.

Acknowledgments

One of the authors (B. Wanti) is thankful to the UGC, New Delhi and Department of Higher Education, Government of J and K for providing the teacher fellowship. The authors are grateful to Prof. T.P. Singh, Head, Department of Biophysics, All India Institute of Medical Sciences, New Delhi for providing the single crystal X-ray diffraction facility. The corresponding author is thankful to the All India Council of Technical Education, New Delhi for award of Emeritus fellowship.

References

[1] M.E. Torres, T. Lo'pez, J. Peraza, J. Stockel, A.C. Yanes, C. Gonzalez-Silgo, C. Ruiz-Perez, P.A. Lorenzo-Luis, *J. Appl. Phys.* **84** (1998) 5729.
 [2] M.H. Rahimkutti, K. Rajendra Babu, K. Shreedharan Pillai, M.R. Sudarshanakumar, C.M.K. Nair, *Bull. Mater. Sci.* **24** (2001) 249.
 [3] M.E. Torres, A.C. Yanes, T. Lo'pez, J. Stockel, J.F. Peraza, *J. Crystal Growth* **156** (1995) 421.
 [4] M.E. Torres, T. Lo'pez, J. Stockel, X. Solans, M. Garcia-Valle S, E. Rodriguez-Castello N. C. Gonzalez-Lopez-Silgo, *J. Solid State Chem.* **163** (2002) 491.
 [5] J. Foucek, L.E. Cross, K. Seely, *Ferroelectrics* **1** (1970) 63.
 [6] N.R. Ivanov, *Ferroelectrics Lett.* **27** (1984) 45.

[7] J. Jona-Gh. Shirane, *Ferroelectric Crystals*, Dover Publications, Inc., New York, 1993 Chapter VII.
 [8] S.K. Arora, V. Patel, B. Chudasama, B. Amin, *J. Crystal Growth* **275** (2005) e657.
 [9] K. Suryanarayana, S.M. Dharmaprakash, *Mater. Lett.* **42** (2000) 92.
 [10] S.K. Arora, V. Patel, A. Kothari, B. Amin, *Cryst. Growth Des.* **4** (2004) 343.
 [11] K. Suryanarayana, S.M. Dharmaprakash, *Mater. Chem. Phys.* **77** (2002) 179.
 [12] P.N. Kotru, K.K. Raina, N.K. Gupta, *Cryst. Res. Technol.* **22** (1987) 177.
 [13] P.N. Kotru, N.K. Gupta, K.K. Raina, *Cryst. Res. Tech.* **21** (1986) 15.
 [14] P.N. Kotru, K.K. Raina, *J. Mater. Sci. Lett.* **5** (1986) 760.
 [15] P.N. Kotru, K.K. Raina, N.K. Gupta, *J. Mater. Sci.* **21** (1986) 90.
 [16] V. Mansotra, K.K. Raina, P.N. Kotru, *J. Mater. Sci.* **26** (1991) 3780.
 [17] A. Jain, A.K. Razdan, P.N. Kotru, *Mater. Sci. Eng. B* **8** (1991) 12.
 [18] A. Jain, A.K. Razdan, P.N. Kotru, *Mater. Chem. Phys.* **45** (1999) 180.
 [19] H.K. Henisch, *Crystal Growth in Gels*, Pennsylvania State University Press, University Park, PA, 1973.
 [20] H.K. Henisch, *Crystals in Gels and Liesegang Rings*, Cambridge University Press, Cambridge, 1988, pp. 93, 153.
 [21] V. Alexeyev, *Quantitative Analysis*, Mir Publishers, Moscow, 1984, p. 84.
 [22] R.A. Laudise, *The Growth of Single Crystals*, Prentice-Hall, 1 Englewood Cliffs, NJ, 1970, p. 272.
 [23] A.R. Patel, A. Venkateshwara Rao, *J. Crystal Growth* **43** (1978) 24.
 [24] K. Sangwal (Ed.), *Elementary Crystal Growth*, Saar Pabst Lublin, Poland, 1994.
 [25] W. Mullin, *Crystallization*, fourth ed., Butterworth-Heinemann Oxford, UK, 2001, p. 182.
 [26] R.A. Judge, R.S. Jacobs, T. Frazier, E.H. Snell, M.L. Pusey, *Bio. J.* **77** (1999) 1585.
 [27] H.K. Henisch, *Crystal Growth in Gels*, Pennsylvania State University Press, University Park, PA, 1973, p. 93.
 [28] F.C. Hawthorne, I. Borys, R.B. Ferguson, *Acta Crystallogr.* (1983) 540.
 [29] J.A. Mathew, G.B. Michael, D.S. Morris, A.R. David, *Polyhedron* (1996) 3377.
 [30] W. Chuan-De, Z. Xiao-Ping, L. Can-Zhong, Z. Hong-Hui, I. Shun, *Acta Crystallogr.* **E 58** (2002) 228.
 [31] S. Mondal, M. Mukherjee, S. Chakaborty, A. Mukherjee, *Growth Des.* **6** (2006) 940.
 [32] K. Nakamoto, *Infra red and Raman Spectra of Inorganic Coordination Compounds*, part B, Fifth ed., Wiley, New York, p. 70 (Chapter III).
 [33] K. Nakamoto, *Infra red and Raman Spectra of Inorganic Coordination Compounds*, part B, fifth ed., Wiley, New York, p. 60 (Chapter III).
 [34] R.C. Mackenzie (Ed.), *Differential Thermal Analysis*, Academic Press, London, 1972, p. 500 Chapter 44.

Dielectric and thermal behaviour of holmium tartrate trihydrate crystals

B. Want¹, F. Ahmad¹, and P. N. Kotru^{*2}

¹ Department of Physics, University of Kashmir, Srinagar-190006 J & K, India

² Department of Physics and Electronics, University of Jammu, Jammu-180006, India

Received 1 February 2007, revised 26 March 2007, accepted 3 April 2007

Published online 10 July 2007

Key words holmium tartrate trihydrate, phase transition, thermal stability, non-isothermal kinetics

PACS 77.22.-d, 77.80.Bh, 65.40.-b

Measurements on dielectric constant of holmium tartrate trihydrate crystals at frequencies of the applied a.c. in the range 1 kHz to 1 MHz and at temperature in the range 30°C to 330°C are reported. The dielectric constant ϵ' increases with temperature at all frequencies, attains a peak near 250°C, and then decreases as the temperature goes beyond 250°C. The anomalous dielectric behaviour at near about 250°C is attributed to be as a result of crystallographic/polymorphic phase transition brought about in the material. The results on the dielectric behaviour of the material are supplemented by results of thermal analysis viz., TG and DTA. Thermogravimetric and differential thermal analytic techniques have been used to study thermal behaviour of the material. It is shown that the material is thermally stable up to 220°C beyond which it decomposes through three stages till the formation of holmium oxide at 1200°C. The non-isothermal kinetic parameters e.g., activation energy and the frequency factor have been evaluated for first two stages of thermal decomposition by using the integral method of Coats and Redfern.

© 2007 WILEY-VCH Verlag GmbH & Co. KGaA, Weinheim

1 Introduction

The salts of tartaric acid belong to an important class of materials because of their interesting physical properties such as ferroelectricity, piezoelectricity and non-linear optical properties (Second Harmonic Generation) [1–7]. The Ferroelectricity was first discovered in 1921 in the double salt of tartaric acid i.e., Na K C₄H₄O₆ · 4 H₂O [8]. Subsequently, other types of double salts of tartaric acid were investigated for their dielectric behavior [9, 10]. Dielectric and thermal properties of many tartrate salts with monovalent cations; such as rubidium hydrogen tartrate [11], sodium tartrate [12] and ammonium tartrate [13] and divalent cations; such as calcium tartrate [14], cadmium tartrate [1], manganese tartrate [15], zinc tartrate [16] and strontium tartrate [17, 18] have been investigated. Some of these materials have shown to be ferroelectric [1, 8–10, 14] while others are non-ferroelectric [12, 13]. The rare earth tartrates bearing the formula R₂ (C₄H₄O₆)_x · xH₂O (where R = Y, Sm) are shown to be thermally unstable and start decomposing at a temperature of about 50°C [19]. Studies on thermal decomposition of lanthanum-titanium tartrate complex have been reported, which shows the material to be stable up to 50–60°C [20]. Deb [21] has reported thermal decomposition of lanthanum tartrate decahydrate compound, which starts dehydrating even at room temperature. In this paper we describe the dielectric and thermal behaviour of holmium tartrate trihydrate: Ho(C₄H₄O₆)(C₄H₃O₆) · 3 H₂O, which is a trivalent tartrate salt. The single crystals of holmium tartrate trihydrate are shown to be thermally stable up to a temperature of about 220°C as compared to most divalent tartrate salts that decompose at much lower temperatures [14–17]. The results obtained on dielectric studies are correlated with the thermal studies viz., thermogravimetric analysis (TGA), differential thermal analysis (DTA) of the crystals. The material under

* Corresponding author: e-mail: pn_kotru@yahoo.com

spherulitic morphology. Use of agar-agar gel yields single and twinned crystals. The morphological form of single crystals is dipyrmidal with the major habit faces as $\{111\}$ and $\{001\}$. The morphological development of the crystals grown in silica and agar-agar gels indicates differential rate of growth along certain directions. The experimental results obtained for the crystal count on the variation of growth parameters suggest that the crystals grown in silica gel follow classical laws of three-dimensional nucleation. Single crystal XRD results show that the crystals belong to tetragonal system with cell parameters $a = 5.97$, $c = 36.09$ and $V = 1287.12 \text{ \AA}^3$, bearing a non-centrosymmetric space group $P4_1$. Infra red spectrum shows the presence of tartrate ligands and establishes that one of the tartrate ions is singly ionized. The stoichiometric composition of the crystals is established to be $[\text{Ho}(\text{C}_4\text{H}_7\text{O}_6)_2(\text{C}_2\text{H}_3\text{O}_6)_3 \cdot 3(\text{H}_2\text{O})]$. TGA reveals that the material is thermally stable up to 220 °C.

Acknowledgments

One of the authors (B. Wanta) is thankful to the UGC, New Delhi and Department of Higher Education, Government of J and K for providing the teacher fellowship. The authors are grateful to Prof. T.P. Singh, Head, Department of Biophysics, All India Institute of Medical Sciences, New Delhi for providing the single crystal X-ray diffraction facility. The corresponding author is thankful to the All India Council of Technical Education, New Delhi for award of Emeritus fellowship.

References

- [1] M.E. Torres, T. Lo'pez, J. Peraza, J. Stockel, A.C. Yanes, C. Gonzalez-Silgo, C. Ruiz-Perez, P.A. Lorenzo-Luis, *J. Appl. Phys.* **84** (1998) 5729.
- [2] M.H. Rahimkutti, K. Rajendra Babu, K. Shreedharan Pillai, M.R. Sudarshanakumar, C.M.K. Nair, *Bull. Mater. Sci.* **24** (2001) 249.
- [3] M.E. Torres, A.C. Yanes, T. Lo'pez, J. Stockel, J.F. Peraza, *J. Crystal Growth* **156** (1995) 421.
- [4] M.E. Torres, T. Lo'pez, J. Stockel, X. Solans, M. Garcia-Valle-S. E. Rodriguez-Castello, N. C. Gonzalez' Lez-Silgo, *J. Solid State Chem.* **163** (2002) 491.
- [5] J. Fousek, L.E. Cross, K. Seely, *Ferroelectrics* **1** (1970) 63.
- [6] N.R. Ivanov, *Ferroelectrics Lett.* **27** (1984) 45.
- [7] I. Jona, G. Shirane, *Ferroelectric Crystals*, Dover Publications, Inc., New York, 1993 Chapter VII.
- [8] S.K. Arora, V. Patel, B. Chudasama, B. Amin, *J. Crystal Growth* **275** (2005) e657.
- [9] K. Suryanarayana, S.M. Dharmaprakash, *Mater. Lett.* **42** (2000) 92.
- [10] S.K. Arora, V. Patel, A. Kothari, B. Amin, *Cryst. Growth Des.* **4** (2004) 343.
- [11] K. Suryanarayana, S.M. Dharmaprakash, *Mater. Chem. Phys.* **77** (2002) 179.
- [12] P.N. Kotru, K.K. Raina, N.K. Gupta, *Cryst. Res. Technol.* **22** (1987) 177.
- [13] P.N. Kotru, N.K. Gupta, K.K. Raina, *Cryst. Res. Tech.* **21** (1986) 15.
- [14] P.N. Kotru, K.K. Raina, *J. Mater. Sci. Lett.* **5** (1986) 760.
- [15] P.N. Kotru, K.K. Raina, N.K. Gupta, *J. Mater. Sci.* **21** (1986) 90.
- [16] V. Mansotra, K.K. Raina, P.N. Kotru, *J. Mater. Sci.* **26** (1991) 3780.
- [17] A. Jain, A.K. Razdan, P.N. Kotru, *Mater. Sci. Eng. B* **8** (1991) 129.
- [18] A. Jain, A.K. Razdan, P.N. Kotru, *Mater. Chem. Phys.* **45** (1996) 180.
- [19] H.K. Henisch, *Crystal Growth in Gels*, Pennsylvania State University Press, University Park, PA, 1973.
- [20] H.K. Henisch, *Crystals in Gels and Liesegang Rings*, Cambridge University Press, Cambridge, 1988, pp. 93, 153.
- [21] V. Alexeyev, *Quantitative Analysis*, Mir Publishers, Moscow, 1969 p. 84.
- [22] R.A. Laudise, *The Growth of Single Crystals*, Prentice-Hall, Inc., Englewood Cliffs, NJ, 1970, p. 272.
- [23] A.R. Patel, A. Venkateswara Rao, *J. Crystal Growth* **43** (1978) 351.
- [24] K. Sangwal (Ed.), *Elementary Crystal Growth*, Saan Publishers, Lublin, Poland, 1994.
- [25] W. Mullin, *Crystallization*, fourth ed., Butterworth Heinemann, Oxford, UK, 2001, p. 182.
- [26] R.A. Judge, R.S. Jacobs, T. Frazier, E.H. Snell, M.L. Pusey, *Biophys. J.* **77** (1999) 1585.
- [27] H.K. Henisch, *Crystal Growth in Gels*, Pennsylvania State University Press, University Park, PA, 1973, p. 93.
- [28] F.C. Hawthorne, I. Borys, R.B. Ferguson, *Acta Crystallogr. C* **39** (1983) 540.
- [29] J.A. Mathew, G.B. Michael, D.S. Morris, A.R. David, *Polyhedron* **15** (1996) 3377.
- [30] W. Chuan-De, Z. Xiao-Ping, L. Can-Zhong, Z. Hong-Hui, H. Jin-Shun, *Acta Crystallogr. E* **58** (2002) 228.
- [31] S. Mondal, M. Mukherjee, S. Chakraborty, A. Mukherjee, *Cryst. Growth Des.* **6** (2006) 940.
- [32] K. Nakamoto, *Infra red and Raman Spectra of Inorganic and Coordination Compounds, part B, Fifth ed.*, Wiley, New York, 1997, p. 70 (Chapter III).
- [33] K. Nakamoto, *Infra red and Raman Spectra of Inorganic and Coordination Compounds, part B, fifth ed.*, Wiley, New York, 1997, p. 60 (Chapter III).
- [34] R.C. Mackenzie (Ed.), *Differential Thermal Analysis*, vol. 2, Academic Press, London, 1972, p. 500 Chapter 44.



Dielectric and thermal behaviour of holmium tartrate trihydrate crystals

B. Want¹, F. Ahmad¹, and P. N. Kotru^{*2}

¹ Department of Physics, University of Kashmir, Srinagar-190006 J & K, India

² Department of Physics and Electronics, University of Jammu, Jammu-180006, India

Received 1 February 2007; revised 26 March 2007; accepted 3 April 2007

Published online 10 July 2007

Key words holmium tartrate trihydrate, phase transition, thermal stability, non-isothermal kinetics

PACS 77.22.-d, 77.80.Bh, 65.40.-b

Measurements on dielectric constant of holmium tartrate trihydrate crystals at frequencies of the applied a.c. in the range 1 kHz to 1 MHz and at temperature in the range 30°C to 330°C are reported. The dielectric constant ϵ' increases with temperature at all frequencies, attains a peak near 250°C, and then decreases as the temperature goes beyond 250°C. The anomalous dielectric behaviour at near about 250°C is attributed to be as a result of crystallographic/polymorphic phase transition brought about in the material. The results on the dielectric behaviour of the material are supplemented by results of thermal analysis viz., TG and DTA. Thermogravimetric and differential thermal analytic techniques have been used to study thermal behaviour of the material. It is shown that the material is thermally stable up to 220°C beyond which it decomposes through three stages till the formation of holmium oxide at 1200°C. The non-isothermal kinetic parameters e.g., activation energy and the frequency factor have been evaluated for first two stages of thermal decomposition by using the integral method of Coats and Redfern.

© 2007 WILEY-VCH Verlag GmbH & Co. KGaA, Weinheim

1 Introduction

The salts of tartaric acid belong to an important class of materials because of their interesting physical properties such as ferroelectricity, piezoelectricity and non-linear optical properties (Second Harmonic Generation) [1-7]. The Ferroelectricity was first discovered in 1921 in the double salt of tartaric acid i.e., Na K $C_4H_4O_6 \cdot 4 H_2O$ [8]. Subsequently, other types of double salts of tartaric acid were investigated for their dielectric behavior [9, 10]. Dielectric and thermal properties of many tartrate salts with monovalent cations; such as rubidium hydrogen tartrate [11], sodium tartrate [12] and ammonium tartrate [13] and divalent cations; such as calcium tartrate [14], cadmium tartrate [1], manganese tartrate [15], zinc tartrate [16] and strontium tartrate [17, 18] have been investigated. Some of these materials have shown to be ferroelectric [1, 8-10, 14] while others are non-ferroelectric [12, 13]. The rare earth tartrates bearing the formula $R_2 (C_4H_4O_6)_x \cdot xH_2O$ (where R = Y, Sm) are shown to be thermally unstable and start decomposing at a temperature of about 50°C [19]. Studies on thermal decomposition of lanthanum-titanium tartrate complex have been reported, which shows the material to be stable up to 50-60°C [20]. Deb [21] has reported thermal decomposition of lanthanum tartrate decahydrate compound, which starts dehydrating even at room temperature. In this paper we describe the dielectric and thermal behaviour of holmium tartrate trihydrate: $Ho(C_4H_4O_6)(C_4H_4O_6) \cdot 3 H_2O$, which is a trivalent tartrate salt. The single crystals of holmium tartrate trihydrate are shown to be thermally stable up to a temperature of about 220°C as compared to most divalent tartrate salts that decompose at much lower temperatures [14-17]. The results obtained on dielectric studies are correlated with the thermal studies viz., thermogravimetric analysis (TGA), differential thermal analysis (DTA) of the crystals. The material under

* Corresponding author: e-mail: pn_kotru@yahoo.com

study is proposed to show the ferroelectric behaviour. Thermal behaviour of the material has been studied using thermogravimetric and differential thermal analytic techniques.

2 Experimental

Single crystals of holmium tartrate trihydrate were grown by single gel diffusion method [22, 23]. The details of various experiments on the growth of these crystals have been published elsewhere [24]. The crystals obtained from all experiments were of small size and thus it was not practically possible to carry out direct measurement of dielectric constant on a single crystal. Therefore, the dielectric measurements were carried out on powdered samples in the form of pellets. To obtain the pellet samples, the single crystals were finely ground and the resulting powder was compressed into a die 13 mm in diameter and 1.2–1.5 mm in thickness under a pressure of about 3.9×10^4 N/cm² using a hand operated hydraulic press. The samples were silver electroded by using a fine paint brush to coat both faces of the pellets with a thin layer of silver paint. The dielectric measurements were carried out in the frequency range 1 kHz – 1 MHz and over the temperature range 30 – 330°C using a Hewlett-Packard impedance analyzer LF 4192A. A microprocessor based furnace fitted with a temperature controller and a specially designed two-terminal sample holder was used to heat the sample. The impedance analyzer directly provides the values of capacitance (C) and as such the dielectric constant (ϵ') is computed using the relation

$$\epsilon' = C t / \epsilon_0 A$$

where C is the capacitance (in farad), t is the thickness (in metre), A the area (in m²), $\epsilon_0 = 8.854 \times 10^{-12}$ F m⁻¹ and f is the frequency (in Hz) of the applied electric field.

Single crystal X-ray diffraction analysis of holmium tartrate trihydrate was carried out using Enraf-Nonius CAD4 diffractometer with Cu K α radiation. The FT-IR spectra of the material in the wave number range of 400–4000 cm⁻¹ were recorded on a Bruker Vector 22 spectrometer using KBr pellet technique. Thermal behaviour (thermogravimetric analysis and differential thermal analysis) of this material was investigated using a Perkin-Elmer thermal analyser in N₂ atmosphere at a heating rate of 10 K/min.

3 Results and discussion

3.1 Dielectric characteristics

The dependence of real dielectric constant (ϵ') on temperature at various frequencies of the applied a.c. field was studied in the temperature range of 30–330°C and frequency range of 1 kHz – 1 MHz. The results are described as follows.

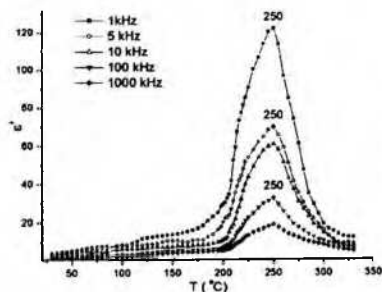


Fig. 1 Variation of dielectric constant with temperature at frequencies 1, 5, 10, 100 and 1000 kHz.

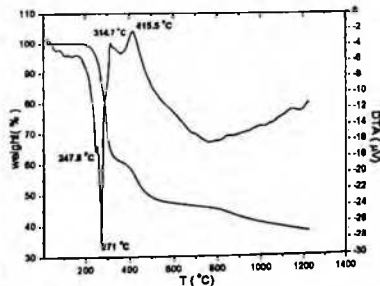


Fig. 2 TG and DTA curves of holmium tartrate trihydrate.

Figure 1 shows the variation of real dielectric constant (ϵ') with temperature at five frequencies (1, 5, 10, 100 and 1000 kHz) of the applied a.c. field. It is clear from figure 1 that in the temperature range $30 < T < 160^\circ\text{C}$, the dielectric constant of holmium tartrate trihydrate is practically temperature independent. Other tartrate salts also have been reported to show this type of behaviour [1, 14]. Beyond 160°C , the dielectric constant increases rapidly with temperature, attains a peak around 250°C , and then decreases as the temperature exceeds 250°C . The occurrence of this peak may suggest a phase transition in the material near 250°C . To account for this behaviour, we have carried out thermal analysis viz., TG and DTA on the material. Figure 2 shows the TG and DTA curves of holmium tartrate trihydrate. The DTA curve of figure 2 shows an endothermic peak near 247.8°C , thereby, suggesting a phase transition in the material. This temperature is close to the transition temperature (250°C) observed in the dielectric constant versus temperature curve (Fig. 1). Therefore, it may be suggested that the material shows a ferroelectric behaviour in the temperature range $30 < T < 250^\circ\text{C}$. The phase transition could be due to structural changes as well as due to dehydration of the compound. The phase transition due to loss of water molecules as well as due to structural changes has been reported by Torres et al. [1] in the case of cadmium tartrate crystals. However, in the present case the possibility of phase transition exclusively due to loss of water molecules is ruled out in the light of the results of thermal behaviour of the material. Fig. 3 shows thermogravimetric (TG) and DTG curves of holmium tartrate trihydrate in the temperature range $225 - 336^\circ\text{C}$. Up to a temperature of about 250°C , there occurs a loss of one H_2O molecule from the compound (Cal. wt. loss : 3.49 %; Obs. wt. loss : 3.35 %). Corresponding to this loss there is an endothermic peak at about 247.8°C as shown in the DTA curve of figure 2.

A further loss of 4 water molecules occurs in the temperature range of $250-280^\circ\text{C}$ (observed loss: 13.7%; calculated loss: 13.91%). Therefore, it may appear that there should be at least two transitions; first in the temperature range $225-250^\circ\text{C}$ (corresponding to DTA peak at 247.8°C) and second in the temperature range $250-280^\circ\text{C}$ (corresponding DTA peak at 271°C). However, in the present case the only transition that has been observed in the dielectric constant versus temperature curve (Fig. 1) is around 250°C . Therefore, the possibility of the material showing the phase transition near 250°C exclusively due to dehydration may be ruled out. The second possibility is that dielectric anomaly near 250°C is due to a crystallographic change/polymorphic phase transition brought about in the material (including due to loss of one H_2O molecule). The DTA curve of figure 2 shows an endothermic peak near 247.8°C , thereby, suggesting a phase transition in the material. This temperature is close to the transition temperature (250°C) observed in the dielectric constant versus temperature curve (Fig. 1). Therefore, it may be suggested that the material shows a ferroelectric behaviour up to the temperature of 250°C . The ferroelectricity in tartrate salts is believed to be due to the hydroxyl groups of the tartrate molecules. It is believed that the hydroxyl groups in the tartrate ions make the major contribution to the spontaneous polarization in salts of tartaric acid. The spontaneous polarization results from the two possible positions for hydrogen atoms which are believed to lie in intrinsically asymmetric double minimum potential well [25].

3.2 Thermal characteristics

TG/DTA curves of holmium tartrate trihydrate in the temperature range of $30 - 1200^\circ\text{C}$ are shown in figure 2 whereas figure 3 shows TG/DTG curves in the temperature range $225 - 336^\circ\text{C}$ only to illustrate the specific details of the first stage of decomposition. It is clear from the TG curve of figure 2 that the material remains stable up to a temperature of about 220°C . In the temperature range $225 - 336^\circ\text{C}$, the material loses five water molecules and two CO_2 molecules, leading to the formation of salt of holmium acrylate [26] (calculated wt loss: 34.5 %, observed wt. loss: 35 %). A close look at the DTG curve of figure 3 reveals that the first stage of decomposition ($225 - 336^\circ\text{C}$) actually consists of three sub stages ($225-250^\circ\text{C}$, $250-280^\circ\text{C}$ and $280-336^\circ\text{C}$). The first sub stage ($225-250^\circ\text{C}$) is due to dehydration resulting in the elimination of one water molecule from the material (Cal. loss : 3.49 %; Obs. loss : 3.35 %). The next sub-stage ($250-280^\circ\text{C}$) corresponds to the loss of four water molecules (Cal. loss : 13.91 %; Obs. loss : 13.7 %). The total loss of five water molecules in the temperature range $225-280^\circ\text{C}$ includes three coordinated and two intramolecular water molecules. Corresponding to these sub-stages there are two endothermic peaks in the DTA curve at about 247.8 and 271°C respectively (see Fig. 2). The dehydration temperature range ($225-280^\circ\text{C}$) which is quite high, suggests the presence of coordinated water in the compound [27]. The loss of two intramolecular water molecules results into the dehydration of the tartrate molecule, thus leading to the formation of holmium-fumarate complex. In the third sub-stage ($280-336^\circ\text{C}$) there occurs a loss of two CO_2 molecules (Cal. loss: 17 %; Obs. loss 16.95) and the holmium-fumarate complex decomposes to holmium acrylate. Corresponding to this sub-stage ($280-$

336°C), there is an exothermic peak in DTA, at about 314.7°C. The formation of holmium acrylate complex was confirmed by carrying out CHN analysis of the intermediate obtained at 340°C (Calculated; C = 21.3 %, H = 1.5 %, Observed; C = 20.96 %, H = 1.55 %). To further support the above arguments, we have carried out the FT-IR spectra of holmium tartrate trihydrate (at room temperature) and the intermediate products obtained at 285°C, and 340°C as shown in figure 4.

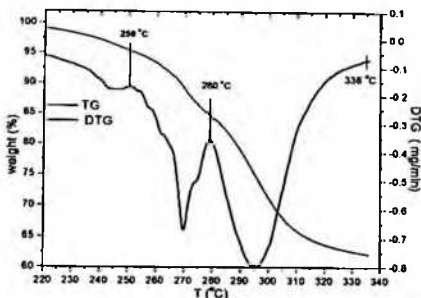


Fig. 3 TG and DTG curves of holmium tartrate trihydrate.

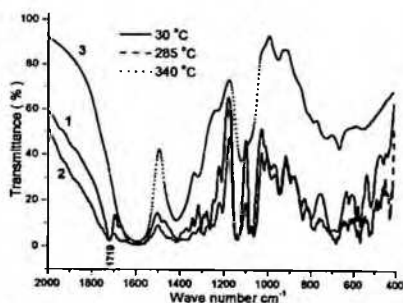


Fig. 4 FT-IR spectra of holmium tartrate trihydrate (curve-1) and the intermediate products obtained at 285°C (curve-2) and 340°C (curve-3).

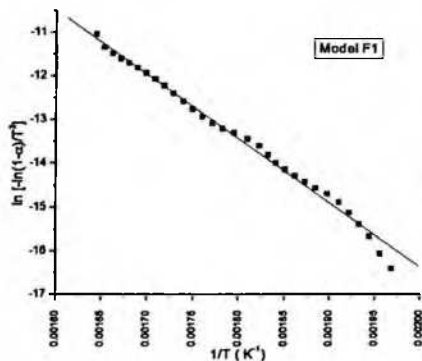


Fig. 5 Arrhenius plot of the best fitting function $g(\alpha)$ for stage-1 (225-336°C).

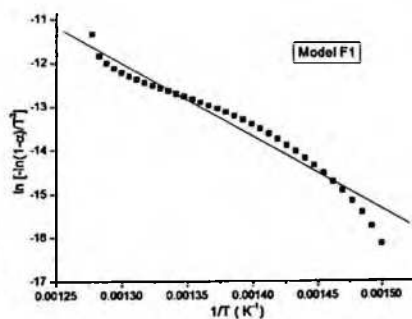
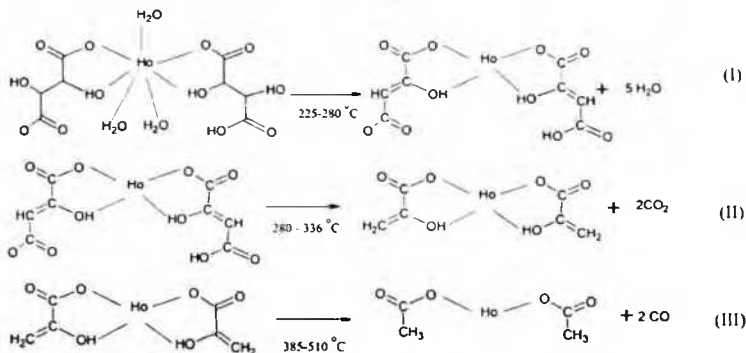


Fig. 6 Arrhenius plot of the best fitting function $g(\alpha)$ for stage 2 (385-510°C).

The strong peak at 1719 cm^{-1} , as shown in curve-1, is due to carboxylate unbounded group [28]. The absorption bands at approximately 1585 cm^{-1} and 1410 cm^{-1} are assigned to asymmetric and symmetric vibrations of carboxylate group. The band at 1066.9 cm^{-1} may be assigned to bond hydroxyl group $\nu(\text{OH})$. The FT-IR spectrum of intermediate (holmium fumarate, curve-2) obtained at 285°C shows presence of all functional groups in a tartrate molecule, thus confirming that the organic skeleton is in tact up to temperature of about 285°C . In the FT-IR spectrum of intermediate (holmium acrylate, curve-3) obtained at 340°C an absorption band at 1594.60 cm^{-1} and 1416.7 cm^{-1} corresponding to symmetric and asymmetric stretch $\nu(\text{C}=\text{O})$, suggesting the presence of carboxylate groups. The absorption peak at 1117 cm^{-1} is attributed to the stretching vibration of $\nu(\text{C}-\text{H})$ and a peak at 947 cm^{-1} to the stretching vibration $\nu(\text{C}-\text{C})$. Thus the FT-IR spectrum obtained at 360°C is in conformity with the proposed product i.e. holmium acrylate. In the second

stage between the temperature interval 385–510 °C, the acrylate of holmium decomposes and gets reduced to holmium acetate. The second stage of decomposition corresponds to the elimination of two CO molecules from the material. The observed weight loss in this stage is about 11.1% (calculated wt loss 10.85%). Corresponding to this stage there is an exothermic peak at about 415.5 °C. After 510 °C the residual material suffers a continuous weight loss until at about 1200 °C holmium oxide is formed. A total observed weight loss of about 62.4% from 30 °C to 1200 °C corresponds to the formation of holmium oxide (calculated loss: 63.4%). The formation of oxides of other rare earth compounds from their coordination complexes has also been reported in the literature [29].

Single crystal X-ray diffraction studies indicate that the crystals of holmium tartrate trihydrate belong to tetragonal system with the cell parameters $a = 5.97 \text{ \AA}$, $c = 36.09 \text{ \AA}$, bearing the space group $P4_1$ [24]. These results show that the material grown under present investigation is isomorphous with those reported in the literature [30–32]. Based on these findings we expect the structure of holmium tartrate trihydrate to be similar to those of reported structures of rare earth tartrates [30–32]. Therefore, we suggest the molecular structure of the compound under investigation to be the one shown on the LHS of reaction I (see below). The thermal decomposition of holmium tartrate trihydrate that occurs through the reactions is given below.



The non-isothermal kinetic parameters have been worked out for the complete stage-1 (225–336 °C) and stage-2 (385–510 °C) using the integral method by applying the Coats – Redfern approximation [33]:

$$\ln \left[\frac{g(\alpha)}{T^2} \right] = \ln \left(\frac{AR}{E\beta} \left(1 - \frac{2RT}{E} \right) \right) - \frac{E}{RT} \quad (\text{I})$$

where α is the fraction of reactant used, $g(\alpha)$ is the conversion function dependent on the mechanism of the reaction, R the gas constant ($= 8.314 \text{ J K}^{-1} \text{ mol}^{-1}$), E is the activation energy (kJ mol^{-1}), T the absolute temperature (K), β the linear heating rate (K s^{-1}) and A is the frequency factor (s^{-1}). This equation is most often

used to describe the kinetics of thermal decomposition of solids in general. A plot of $\ln \left[\frac{g(\alpha)}{T^2} \right]$ versus $1/T$ gives a straight line for the correct model.

The statistical parameters; correlation coefficient r and Snedecor's variable F were calculated to aid the selection of the $g(\alpha)$ function best describing the experimental results [34]. The values of the kinetic and statistical parameters for all analysed models are listed in table 1.

The Arrhenius plot for the best-fitting curve for the stage 1 and stage 2 is shown in figure 5 and figure 6 respectively. It is clear from table 1 that the best fitting expression for the stages 1 and 2 is that of random nucleation model F1 with activation energies 121.95 kJ/mol and 137.35 kJ/mol respectively. The corresponding frequency factors are $1.05 \times 10^6 \text{ (s}^{-1}\text{)}$ and $3.56 \times 10^4 \text{ (s}^{-1}\text{)}$ respectively.

Table 1 Kinetic and statistical parameter values from the TG experiment.

Stage	Model	E (kJ/mol)	A s ⁻¹	r	F
1	D1	178.56	5.93×10 ¹⁰	0.96774	8853
	D2	196.5	2.05×10 ¹²	0.97894	13798
	D3	48.73	2.22×10 ¹	0.98739	23338
	D4	204.9	3.23×10 ¹²	0.98351	17739
	F1	121.95	1.05×10 ⁶	0.9961	76402
	F2	185.83	3.19×10 ¹²	0.97554	11814
	A2	56.35	2.61	99534	63932
	A3	34.48	1.60×10 ²	0.99436	52760
	R2	100.23	3.06×10 ¹	0.98439	18774
	R3	106.7	9.52×10 ¹	0.98969	28650
2	D1	179.68	1.42×10 ⁷	0.91537	3509
	D2	205.1	7.47×10 ⁸	0.93765	4941
	D3	51.65	2.16×10 ²	0.95003	6288
	D4	217.14	1.48×10 ⁸	0.94743	5953
	F1	137.35	3.56×10 ⁴	0.97909	15729
	F2	230.5	7.28×10 ¹¹	0.97838	15192
	A2	62.66	2.18×10 ¹	0.97469	12907
	A3	37.77	7.97×10 ²	0.96886	10397
	R2	106.04	5.52×10 ¹	0.94726	5933
	R3	115.33	2.07×10 ²	0.95983	7945

4 Conclusions

The study of the dielectric behaviour of holmium tartrate trihydrate crystals shows the strong dependence of dielectric constant on temperature. The dielectric constant (ϵ') varies with the temperature and attains a peak value around 250°C after which it decreases, thus establishing this temperature as the transition temperature of the material. Thermogravimetric analysis shows that the material is thermally stable up to a temperature of about 220°C. Decomposition of holmium tartrate trihydrate occurs in three complete stages ultimately leading to the formation of holmium oxide. The reactions corresponding to stages 1 and 2 are both governed by random nucleation model F1 with activation energies 121.95 kJ/mol and 137.35 kJ/mol respectively.

Acknowledgements One of the authors (B.Want) is thankful to the UGC, New Delhi and Department of Higher Education, Government of J & K for extending the tenure of the teacher fellowship. The corresponding author (PNK) is thankful to the All India Council of Technical Education, New Delhi for award of Emeritus fellowship.

References

- [1] M. E. Torres, T. Lo'pez, J. Peraza, J. Stockel, A. C. Yanes, C. Gonza' Lez-Silgo, C. Ruiz-Perez, and P. A. Lorenzo-Luis, *J. Appl. Phys.* **84**, 5729 (1998).
- [2] M. H. Rahimkuty, K. Rajendra Babu, K. Shreedharan Pillai, M. R. Sudarshana Kumar, and C. M. K. Nair, *Bull. Mater. Sci.* **24**, 249 (2001).
- [3] M. E. Torres, A. C. Yanes, T. Lo'pez, J. Stockel, and J. F. Peraza, *J. Cryst. Growth* **156**, 421 (1995).
- [4] M. E. Torres, T. Lo'pez, J. Stockel, X. Solans, M. Garcia-Valle's, E. Rodriguez-Castello'n, and C. Gonza'lez-Silgo, *J. Solid State Chem.* **163**, 491 (2002).
- [5] J. Fousek, L. E. Cross, and K. Seely, *Ferroelectrics* **1**, 63 (1970).
- [6] N. R. Ivanov, *Ferroelectrics Lett.* **27**, 45 (1984).
- [7] F. Jona and G. Shirane, "Ferroelectric Crystals", ch. VII, Dover Publications, Inc., New York (1993).
- [8] J. Valasek, *Phys. Rev.* **19**, 478 (1921).
- [9] W. J. Merz, *Phys. Rev.* **75**, 687 (1949).
- [10] B. Matthias and J. K. Hulm, *Phys. Rev.* **82**, 108 (1951).

- [11] C. C. Desai, A. H. Patel, and M. S. V. Ramana, *Ferroelectrics* **23**, 102 (1990)
- [12] M. M. Abdel-Kader, F. El-Kabbany, and S. Taha, *J. Mater. Sci. Mater. Elect.* **1**, 201 (1991)
- [13] M. M. Abdel-Kader, F. El-Kabbany, S. Taha, A. Abosehly, K. K. Tahooun, and A. El-Sharkawy, *J. Phys. Chem. Solids* **52**, 655 (1991)
- [14] H. B. Gon, *J. Cryst. Growth* **102**, 501 (1990)
- [15] A. C. Yanes, T. Lopez, J. Stockel, J. F. Peraza, and M. E. Torres, *J. Mater. Sci.* **31**, 2683 (1996)
- [16] T. Lopez, J. Stockel, J. E. Peraza, and M. E. Torres, *Cryst. Res. Technol.* **30**, 677 (1995)
- [17] S. K. Arora, V. Patel, R. G. Patel, B. Amin, and Anjana Kothari, *J. Phys. Chem. Solids* **65**, 965 (2004)
- [18] S. K. Arora, V. Patel, and A. Kothari, *Mater. Chem. Phys.* **84**, 323 (2004)
- [19] A. Jain, S. Bhat, S. Pandita, M. L. Kaul, and P. N. Kotru, *Bull. Mater. Sci.* **20**, 1089 (1997)
- [20] D. S. Todorovsky, M. M. Getsova, and M. M. Milanova, *Synth. React. Inorg. Metal-Organic Chem.* **33**, 223 (2003)
- [21] N. Deb, *J. Therm. Anal.* **78**, 227 (2004)
- [22] H. K. Henisch, in "Crystal Growth In Gels" (Pennsylvania State University Press, University Park, Pa 1973)
- [23] H. K. Henisch, in "Crystals in Gels and Liesegang Rings" Cambridge University Press, Cambridge (1988)
- [24] B. Want, F. Ahmad, and P. N. Kotru, *J. Cryst. Growth* **299**, 336 (2007)
- [25] P. Schuster, in "The Hydrogen Bond - Recent Developments In Theory and Experiments", North-Holland Publ. Co., Amsterdam, p. 1142 (1976)
- [26] R. C. Mackenzie (Ed.), "Differential Thermal Analysis", Academic Press London, Vol. 2, Chap. 44, p. 500 (1972)
- [27] S. C. Manna, E. Zangrando, J. Ribas, and N. R. Chaudhuri, *Polyhedron* **25**, 1779 (2006)
- [28] K. Nakamoto, "Infrared and Raman Spectra Of Inorganic and Coordination Compounds", 5th Edition, John Wiley & Sons, Part B, Chap. III, p. 70 (1997)
- [29] T. V. Albu, S. Plostinaru, L. Patron, and E. Segal, *J. Therm. Anal.* **50**, 425 (1997)
- [30] F. C. Hawthorne, I. Borys, and R. B. Ferguson, *Acta Cryst. C* **39**, 540 (1983)
- [31] J. A. Mathew, G. B. Michael, D. S. Morris, and A. R. David, *Polyhedron* **15**, 3377 (1996)
- [32] W. Chuan-De, Z. Xiao-Ping, L. Can-Zhong, Z. Hong-Hui, and H. Jin-Shun, *Acta Cryst. E* **58**, 228 (2002)
- [33] A. W. Coats and J. P. Redfern, *Nature* **201**, 68 (1964)
- [34] J. Straszko, M. Olszak-Humienik, and J. Mozejko, *J. Therm. Anal.* **39**, 935 (2000)

Dielectric and thermal characteristics of gel grown single crystals of ytterbium tartrate trihydrate

Basharat Wani · Farooq Ahmad · P. N. Kotru

Received: 30 November 2006 / Accepted: 31 May 2007 / Published online: 2007
© Springer Science+Business Media, LLC 2007

Abstract Dielectric and thermal characteristics of gel grown single crystals of ytterbium tartrate trihydrate have been carried out. The dielectric constant has been measured as a function of frequency in the range 2 kHz–1 MHz and temperature range 30–300 °C. The dielectric constant increases with temperature, attains a peak near 215 °C, and then decreases as the temperature exceeds 215 °C. The dielectric anomaly at 215 °C is suggested to be due to phase transition brought about in the material. The dielectric behaviour of the material is correlated with the results on thermal analysis. Thermogravimetric and differential thermal analysis have been used to study the thermal characteristics of the material. The experimental results show that the material is thermally stable up to 200 °C. The decomposition process occurs in two stages until ytterbium oxide is formed at 700 °C. The non-isothermal kinetic parameters e.g., activation energy and the frequency factor have been evaluated for each stage of thermal decomposition by using the integral method, applying the Coats–Redfern approximation.

Introduction

The salts of tartaric acid belong to an important class of materials because of their interesting physical properties

such as Ferroelectricity, Piezoelectricity and non-linear optical properties (Second Harmonic Generation) [1–7]. The Ferroelectricity was first discovered in 1921 in the double salt of tartaric acid i.e., $\text{NaKC}_4\text{H}_4\text{O}_6 \cdot 4\text{H}_2\text{O}$ [8]. Subsequently, other types of double salts of tartaric acid were investigated for their dielectric behaviour [9, 10]. Dielectric and thermal properties of many tartrate salts with monovalent cations; such as rubidium hydrogen tartrate [11], sodium tartrate [12] and ammonium tartrate [13] and divalent cations; such as calcium tartrate [14], cadmium tartrate [1] manganese tartrate [15], zinc tartrate [16] and strontium tartrate [17, 18] have been investigated. Some of these materials have shown to be ferroelectric [1, 8–10, 14] while others are non-ferroelectric [12, 13]. The spherulitic polycrystals of rare earth tartrates bearing the formula $\text{R}_2(\text{C}_4\text{H}_4\text{O}_6)_3 \cdot \text{H}_2\text{O}$ (where $\text{R} = \text{Y}, \text{Sm}$) were shown to be thermally unstable and start decomposing at a temperature of about 50 °C [19]. Studies on thermal decomposition of lanthanum tartrate decahydrate have been reported, which shows the material to be unstable even at room temperature [20]. In this paper we describe the dielectric and thermal behaviour of single crystals of ytterbium tartrate trihydrate: $\text{Yb}(\text{C}_4\text{H}_4\text{O}_6)(\text{C}_4\text{H}_4\text{O}_6) \cdot 3\text{H}_2\text{O}$, which is a trivalent tartrate salt. The single crystals of ytterbium tartrate trihydrate are thermally stable up to a temperature of about 200 °C as compared to most divalent tartrate salts that decompose at much lower temperatures [14–17]. The results obtained on dielectric studies are correlated with the thermal studies viz., thermogravimetric analysis (TGA) and differential thermal analysis (DTA) of the crystals. The material under study is proposed to show the ferroelectric behaviour. Thermal characteristics of the material have been studied using thermogravimetry and differential thermal analytic techniques.

B. Wani · F. Ahmad

Department of Physics, University of Kashmir, Srinagar, Jammu & Kashmir 190006, India

P. N. Kotru (✉)

Department of Physics and Electronics, University of Jammu, Jammu 180006, India
e-mail: pn_kotru@yahoo.com



Journal 10853
Article No. 1907
ISSN Code 1907

Dispatch 25-6-2007 Page: 7
 HTML
 PDF
 EPUB
 DISK

Experimental

Single crystals of ytterbium tartrate trihydrate (YbTT) were grown by single gel diffusion method [21, 22] using two types of gels: an inorganic (silica) gel and an organic (agar-agar) gel. The details of various experiments on the growth of these crystals have been published elsewhere [23]. The crystals obtained from all experiments were of small size and thus it was not possible to carry out direct measurement of dielectric properties on a single crystal. Therefore, the dielectric measurements were carried out on powdered samples in the form of pellets. To obtain the pellet samples, the single crystals were finely ground and the resulting powder was compressed into a die 13 mm in diameter and 1–1.3 mm in thickness under a pressure of 5 tons/cm² using a hand operated hydraulic press. The samples were silver electroded by using a fine paintbrush to coat both faces of the pellets with a thin layer of silver paint. The dielectric measurements were carried out in the frequency range 2 kHz–1 MHz and over the temperature range 30–300 °C using a Hewlett-Packard impedance analyzer LF 4192A and further automated by using a computer for data recording, storage and analysis. A microprocessor-based furnace fitted with a temperature controller and a specially designed two-terminal sample holder was used to heat the sample. The impedance analyzer directly provides the values of capacitance (C) and, so the dielectric constant (ϵ') is computed using the relation:

$$\epsilon' = C / \epsilon_0 A$$

where C is the capacitance (in farad), t is the thickness (in m), A the area (in m²), $\epsilon_0 = 8.854 \times 10^{-12}$ F m⁻¹ and f is the frequency (in Hz) of the applied electric field.

X-ray powder diffraction analysis of ytterbium tartrate trihydrate was carried out using Bruker D8 Advance X-ray diffractometer with Cu K α radiation ($\lambda = 1.5406$ Å). The FT-IR spectra of the material in the wave number range of 400–4,000 cm⁻¹ were recorded on a Bruker Vector 22 spectrometer using KBr pellet technique. Thermal behaviour (thermogravimetric analysis and differential thermal analysis) of the material was investigated using a Perkin-Elmer thermal analyser in N₂ atmosphere at a heating rate of 10 °C/min.

Results and discussion

Powder X-ray diffraction results

The powder X-ray diffractogram of YbTT crystals is shown in Fig. 1. The occurrence of intense peaks at specific Bragg angles 2θ indicates the crystallinity of the

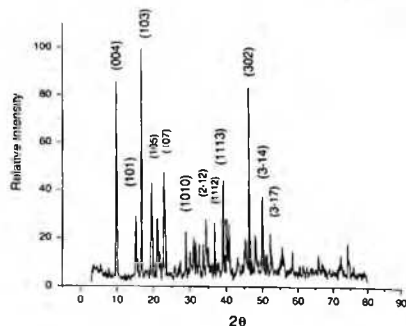


Fig. 1 Powder X-ray diffractogram of ytterbium tartrate trihydrate crystals

grown material. The powder diffraction pattern of YbTT was indexed with the TREOR program [24], using the 20 most intense peaks. A tetragonal unit cell was found with cell parameters $a = 5.885(4)$ Å, $c = 35.801(1)$ Å, $\alpha = \beta = \gamma = 90^\circ$, $V = 1239.9(5)$ Å³, where the numbers in the parentheses are standard deviations in the last significant digits. The calculated cell parameters are consistent with those of reported isomorphous materials [25–27].

Dielectric characteristics

The dependence of real dielectric constant (ϵ') on temperature at various frequencies of the applied a.c. field is studied in the temperature range of 30–300 °C and frequency range of 2 kHz–1 MHz. The results are described as follows.

Figure 2 shows the variation of real dielectric constant (ϵ') with temperature at four frequencies (2, 10, 100 and 1,000 kHz) of the applied a.c. field. It is clear from Fig. 2 that in the temperature range $30 < T < 180$ °C, the dielectric constant of ytterbium tartrate trihydrate is practically temperature independent in the higher frequency range 100–1,000 kHz whereas it shows slight dependence at the lower frequencies of 2 and 10 kHz. Other tartrate salts also have been reported to show this type of behaviour [1, 14]. Beyond 180 °C, the dielectric constant increases almost suddenly with temperature, attains a peak around 215 °C, and then decreases as the temperature exceeds 215 °C. The occurrence of this peak may suggest a phase transition in the material near 215 °C. To account for this behaviour, we have two possibilities. The first possibility is that on heating the sample up to 225 °C, there is loss of some water molecules and because of this dehydration a

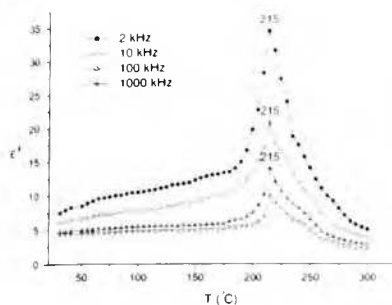


Fig. 2 Variation of dielectric constant with temperature at frequencies 2, 10, 100 and 1,000 kHz

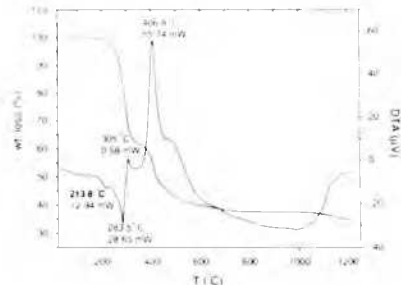


Fig. 4 TG and DTA curves of ytterbium tartrate trihydrate

transition appears to have occurred at about 215 °C. The phase transition due to loss of water molecules as well as due to structural changes has been reported by Torres et al. [1] in the case of cadmium tartrate crystals. However, the possibility of phase transition exclusively due to loss of water molecules is ruled out in the light of the results of thermal behaviour of the material under consideration. Figure 3 shows thermogravimetric (TG) and DTG curves of ytterbium tartrate trihydrate. The material loses about five water molecules (three from coordinated water and two from intramolecular, observed weight loss: 17.4%, calculated weight loss: 17.15%) in the temperature range of 20–285 °C. Up to a temperature of about 225 °C, there occurs a loss of about 0.5 H₂O (observed loss: 1.8%; calculated loss: 1.72%). Corresponding to this loss there is an endothermic peak at about 213.8 °C as shown by the DTA curve of Fig. 4. A further loss of 4.5 water molecules occurs in the temperature range of 225–285 °C (observed loss: 15.6%; calculated loss: 15.43%). Therefore, it may

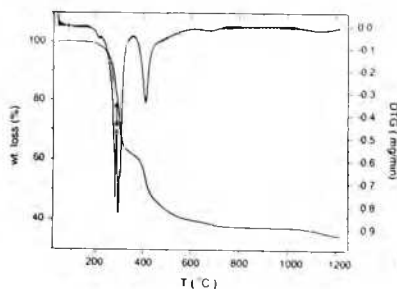
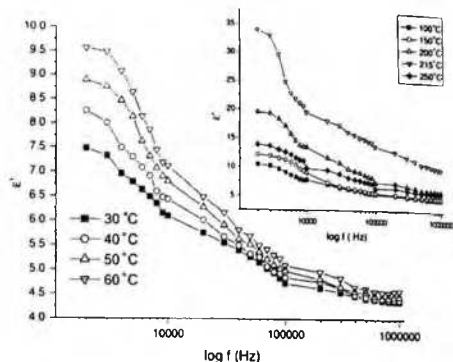


Fig. 3 TG and DTG curves of ytterbium tartrate trihydrate

appear that there should be at least two transitions: first in the temperature range 200–225 °C (corresponding to DTA peak 213.8 °C) and second in the temperature range 225–285 °C (corresponding to DTA peak 283.5 °C). However, in the present case the only transition that has been observed in the dielectric constant versus temperature curve (Fig. 2) is around 215 °C. Therefore, the possibility of the material showing the phase transition near 215 °C exclusively due to loss of water molecules may be ruled out. The second possibility is that dielectric anomaly near 215 °C is due to a crystallographic change/polymorphic phase transition brought about in the material (including due to loss of 0.5 H₂O molecules). The DTA curve of Fig. 4 shows an endothermic peak near 213.8 °C, thereby, suggesting a phase transition in the material. This temperature is close to the transition temperature (215 °C) observed in the dielectric constant versus temperature curve (Fig. 2). Therefore, it may be suggested that the material shows a ferroelectric behaviour up to the temperature of 215 °C. The characteristic feature of rare earth tartrate salts is that in all these crystal structures, rare earth cations and hydrogen bonds of O–H...O type involving water ligands, hydroxyl O and the carboxylate O atoms, link the tartrate anions into layers parallel to (001); these layers are linked together by hydrogen bonding between adjacent tartrate molecule [25–27]. It is believed that the hydroxyl groups in the tartrate ions make the major contribution to the spontaneous polarization in salts of tartaric acid. The spontaneous polarization results from the two possible positions for hydrogen atoms, which are believed to lie in intrinsically asymmetric double minimum well potential [28].

The variation of dielectric constant as a function of frequency is shown in Fig. 5. The inset of Fig. 5 shows the variation of dielectric constant with frequency at high temperatures. It is clear from Fig. 5 that dielectric constant

Fig. 5 Variation of dielectric constant with frequency. The inset of the figure shows variation of dielectric constant with frequency at temperatures of 100, 150, 200, 215 and 250 °C



of ytterbium tartrate trihydrate decreases gradually with increasing frequency. The decrease of dielectric constant with increase of frequency is a normal dielectric behaviour and can be explained on the basis of various polarization mechanisms. There are four primary mechanisms of polarization in materials i.e., electronic, ionic or atomic, dipolar or orientational and space charge or interfacial polarization. At low frequencies, all the mechanisms of polarization contribute to the dielectric constant and with the increase in frequency, the contributions from different polarizations start decreasing. For example, at very high frequencies (10^{15} Hz), only electronic polarization contributes to the dielectric constant, while ionic polarization takes place at IR frequencies ($\sim 10^{13}$ Hz). In the material under present investigation the high rise of dielectric constant at lower frequencies may be attributed to space charge polarization due to crystal lattice defects. The gradual decrease in dielectric constant with frequency suggests that ytterbium tartrate trihydrate has domains of different sizes and hence varying relaxation times.

220 Thermal characteristics

Simultaneous recording of TG and DTA was made in the temperature range 40–1,200 °C. The results thus obtained are shown in Figs. 3 and 4. Figure 3 shows the TGA/DTG curves of ytterbium tartrate trihydrate crystals. From the TG curve, it is observed that the material remains stable up to a temperature of about 200 °C. In the temperature range 200–354 °C, the material loses five water molecules and two CO_2 molecules, leading to the formation of ytterbium acrylate [29] (calculated weight loss: 34%, observed weight loss: 35.4%). A close look at the DTG curve reveals that the first stage of decomposition (200–354 °C) actually consists of

two sub stages (225–285 °C and 285–354 °C). The first sub stage (200–285 °C) is due to dehydration resulting in the elimination of five water molecules from the material. This includes three coordinated and two intramolecular water molecules. The dehydration temperature range (200–285 °C), which seems to be high, suggests the presence of coordinated water in the compound [30]. The measured weight loss in the first sub-stage is about 17.4% (calculated loss, 17.15%). Corresponding to this dehydration step there are two endothermic peaks in the DTA curve at about 213.8 and 283 °C, respectively (see Fig. 4). The loss of two intramolecular water molecules results into the dehydration of the tartrate, thus leading to the formation of ytterbium-fumarate complex. In the second sub-stage (285–354 °C), there occurs a loss of two CO_2 molecules and the ytterbium-fumarate complex decomposes to ytterbium acrylate. Corresponding to this sub-stage (285–354 °C), there is an exothermic peak in DTA, at about 305 °C. The formation of acrylate complex was confirmed by carrying out CHN analysis of the intermediate obtained at 360 °C (Calculated; C = 20.82%, H = 1.45%, Observed; C = 19.96%, H = 1.5%). The FT-IR spectrum of ytterbium tartrate trihydrate (curve 1) and the intermediate product (curve 2) obtained at 360 °C is shown in Fig. 6. The strong peak at $1,718 \text{ cm}^{-1}$, as shown in curve 1, is due to free carbonyl stretch $\nu(\text{C}=\text{O})$, which shows that besides ionized COO^- group there is also presence of unionized carboxyl groups (COOH) in the compound [31]. A band centred at approximately $1,587 \text{ cm}^{-1}$ is due to C=O asymmetric stretch of carbonyl group. The absorption at $1,410 \text{ cm}^{-1}$ is attributed to C=O symmetric vibration. In the FT-IR spectrum of intermediate (ytterbium acrylate, curve 2) an absorption peaks at $1,595.20 \text{ cm}^{-1}$ and $1,418 \text{ cm}^{-1}$ corresponds to symmetric and anti symmetric stretch of C=O and the absorption peak at



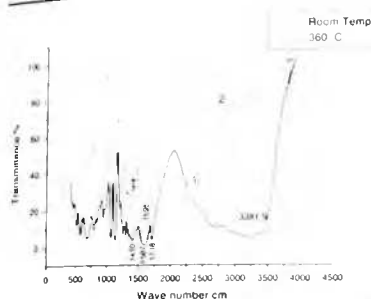
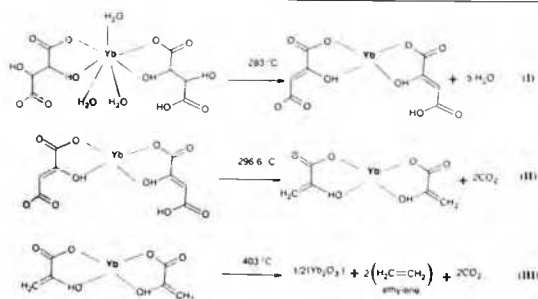


Fig. 6 FT-IR spectrum of ytterbium tartrate trihydrate crystals obtained at room temperature (curve 1) and at 360 °C (curve 2)

3381.9 cm^{-1} is attributed to the stretching vibration of hydroxyl group. Thus the FT-IR spectrum obtained at 360 °C is in conformity with the proposed product i.e. ytterbium acrylate. In the second stage between temperature 385 and 700 °C, the acrylate of ytterbium decomposes and gets reduced to ytterbium oxide, which is clear from the saturation of TG curve from 700 °C onwards. The second stage of decomposition corresponds to the elimination of two CO_2 and two $\text{CH}_2=\text{CH}_2$ molecules from the material. The observed weight loss in this stage is about 26.86% (calculated weight loss: 28.29%). Corresponding to this stage there is an exothermic peak at about 406.8 °C. The thermal decomposition of ytterbium tartrate trihydrate that occurs through the reactions I, II, and III are given below. Based on the reported isomorphous materials [25–27], we suggest the molecular structure of the compound under investigation to be the one shown on the L.H.S of reaction (I)



The temperature written above the arrow corresponds to the maximum decomposition rate as shown by DTG curve. It may be emphasized here that the proposed molecular structure agrees well with the decomposition steps of ytterbium tartrate trihydrate as shown above.

The non-isothermal kinetic parameters have been worked out for the complete stage 1 (200–354 °C) and stage 2 (385–700) using the integral method by applying the Coats–Redfern approximation [32].

$$\ln \left[\frac{g(x)}{T^2} \right] = \ln \left(\frac{AR}{E\beta} \left(1 - \frac{2RT}{E} \right) \right) - \frac{E}{RT} \quad (1)$$

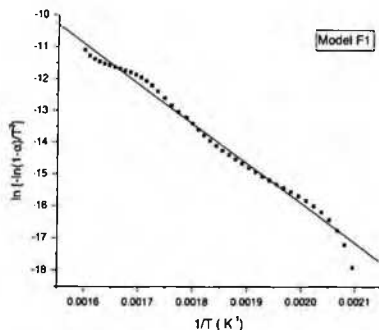
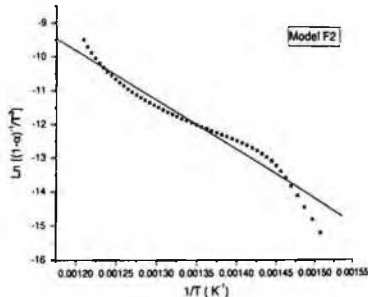
where x is the fraction of reactant used, $g(x)$ is the conversion function dependent on the mechanism of the reaction, R is the gas constant ($=8.314 \text{ J K}^{-1} \text{ mol}^{-1}$), E is the activation energy (kJ mol^{-1}), T the absolute temperature (K), β the linear heating rate (K s^{-1}) and A is the frequency factor (s^{-1}). This equation is most often used to describe the kinetics of thermal decomposition of solids in general. A plot of $\ln \left[\frac{g(x)}{T^2} \right]$ versus $1/T$ gives a straight line for the correct model.

The statistical parameter, correlation coefficient r and Snedecor's variable F were calculated to aid the selection of the $g(x)$ function best describing the experimental results [33]. The values of the kinetic and statistical parameters for all analysed models are listed in Table 1. The Arrhenius plot for the best-fitting curve for the stage 1 and stage 2 is shown in Fig. 7 and 8, respectively. It is clear from the Table 1 that the best fitting expression for the stage 1 is that of random nucleation model F1 with activation energy of 103.6 kJ/mol whereas for stage 2 the second order reaction model F2 fits best to the experimental results with activation energy 136.33 kJ/mol.



Table 1 Kinetic and statistical parameter values for stages 1 and 2

Stage	Model	E (kJ/mol)	A (s ⁻¹)	lnI	F	
1	D1	159.58	7.27E × 10 ¹¹	0.97435	15,917	
	D2	172.75	9.07 × 10 ¹²	0.98192	22,838	
	D3	41.325	9.53 × 10 ⁴	0.98702	32,067	
	D4	179.06	9.27 × 10 ¹²	0.98529	28,225	
	F1	103.6	1.73 × 10 ⁷	0.9954	91,735	
	F2	155.23	4.82 × 10 ¹²	0.97629	17,272	
	A2	47.26	1.55 × 10 ⁴	0.99439	75,049	
	A3	44.42	7.50 × 10 ⁵	0.99302	60,161	
	R2	86.825	1.38 × 10 ⁵	0.98555	28,744	
	R3	91.745	3.11 × 10 ⁵	0.98977	40,847	
	2	D1	69.30	4.4E × 10 ⁷	0.8378	2,532
		D2	72.52	2.0 × 10 ⁷	0.84078	2,592
		D3	15.43	2.4 × 10 ⁷	0.80161	1,933
D4		80.85	2.3 × 10 ⁴	0.86763	3,273	
F1		59.90	3.1 × 10 ⁴	0.93897	8,010	
F2		136.33	7.5 × 10 ⁷	0.95082	10,131	
A2		23.76	4.9 × 10 ⁶	0.90604	4,928	
A3		11.66	1.8 × 10 ⁷	0.8424	2,627	
R2		11.77	7.6 × 10 ⁵	0.84645	27,167	
R3		43.32	1.3 × 10 ⁶	0.88542	3,901	

**Fig. 7** Arrhenius plot of the best fitting function $g(z)$ for stage 1 (200–354 °C)**Fig. 8** Arrhenius plot of the best fitting function $g(z)$ for stage 2 (385–700 °C)

315 Conclusions

316 The study of the dielectric behaviour of ytterbium tartrate
 317 trihydrate crystals shows the strong dependence of dielectric
 318 constant on temperature. The dielectric constant (ϵ')
 319 varies with the temperature and attains a peak value around
 320 215 °C after which it decreases, thus establishing this
 321 temperature as the transition temperature of the material.

X-ray diffraction results suggest that the crystals belong to tetragonal system with cell parameters: $a = 5.885 \text{ \AA}$, $c = 35.80 \text{ \AA}$, $\alpha = \beta = \gamma = 90^\circ$, $V = 1239.86 \text{ \AA}^3$. Thermogravimetric analysis shows that the material is thermally stable up to a temperature of about 200 °C. Decomposition of ytterbium tartrate trihydrate occurs in two complete stages ultimately leading to the formation of ytterbium oxide. The reaction corresponding to stage 1 is governed by random nucleation model (F1) with activation energy

103.6 kJ/mol and frequency factor $1.73 \times 10^{-1} \text{ s}^{-1}$ whereas that of stage 2 by second order reaction model F2 with activation energy 136.33 kJ/mol and frequency factor $7.5 \times 10^{-7} \text{ s}^{-1}$.

Acknowledgement One of the authors (B. Waint) is thankful to the UGC, New Delhi and Department of Higher Education, Government of J & K for extending the tenure of the teacher fellowship. The corresponding author (PNK) is thankful to the All India Council of Technical Education, New Delhi for award of Emeritus fellowship. The authors are grateful to Professor T. K. Razdan of the Department of Chemistry, University of Kashmir, presently at the Department of Chemistry, University of Jammu, for his valuable suggestions.

References

- Torres ME, Lopez T, Peraza J, Stockel J, Yanes AC, Gonza Lez-Silgo C, Ruiz Perez C, Lozano-Luis PA (1998) *J Appl Phys* 84:5729
- Rahimkuty MH, Rajendra Babu K, Shreedharan Pillar K, Sudashana Kumar MR, Nair CMK (2001) *Bull Mater Sci* 24:249
- Torres ME, Yanes AC, Lopez T, Stockel J, Peraza JF (1995) *J Cryst Growth* 156:421
- Torres ME, Lopez T, Stockel J, Solans X, Garcia-Valles M, Rodriguez Castellon E, Gonza Lez-Silgo C (2002) *J Solid State Chem* 163:491
- Fousek J, Cross LE, Seely K (1970) *Ferroelectrics* 1:63
- Ivanov NR (1984) *Ferroelectric Letters* 27:45
- Jona F, Shirane G (1993) In: *Ferroelectric Crystals*. Dover Publications, Inc., New York, Ch VII
- Valasek J (1921) *J Phys Rev* 19:478
- Merz WJ (1949) *Phys Rev* 75:687
- Mathias B, Hulm JK (1951) *Phys Rev* 82:108
- Desai CC, Patel AH, Ramana MSV (1990) *Ferroelectrics* 23:102
- Abdel-Kader MM, El-Kabbany F, Taha S (1991) *J Mater Sci Mater Elect* 1:201
- Abdel-Kader MM, El-Kabbany F, Taha S, Abouseily A, Jahrom KK, El-Sharkawy A (1990) *J Phys Chem Solid* 52:655
- Gron HB (1990) *J Cryst Growth* 102:501
- Yanes AC, Lopez T, Stockel J, Peraza JF, Torres ME (1996) *J Mater Sci* 31:2683
- Lopez T, Stockel J, Peraza JF, Torres ME (1995) *Cryst Res Technol* 30:671
- Arora SK, Patel V, Patel RG, Amin B, Kothari A (2004) *J Phys Chem Solids* 65:965
- Arora SK, Patel V, Kothari A (2004) *Mater Chem Phys* 84:323
- Jain A, Bhat S, Pandita S, Kaul ML, Kotru PN (1997) *Bull Mater Sci* 20:1089
- Deb N (2004) *J Therm Anal Cal* 78:227
- Hensch HK (1973) In: *Crystal Growth in Gels*. Pennsylvania State University Press, University Park, PA
- Hensch HK (1988) *Crystals in gels and Liesegang rings*. Cambridge University Press, Cambridge
- Waint B, Ahmad F, Kotru PN (2006) *Cryst Res Technol* 41:1167
- Werner PE, Eriksson L, Westdahl M (1985) *J Appl Crystallogr* 18:367
- Hawthorne FC, Borys I, Ferguson RB (1985) *Acta Cryst C* 39:540
- Mathew JA, Michael GB, Morris DS, David AR (1996) *Polyhedron* 15:3377
- Chuan De W, Xiao-Ping Z, Can-Zhong L, Hong-Hui Z, Jin-Shun H (2002) *Acta Cryst E* 58:228
- Schuster P (1976) In: *The hydrogen bond—recent developments in theory and experiments*. North-Holland Publ. Co., Amsterdam, p 1142
- Mackenzie RC (1972) In: *Differential thermal analysis*. Academic Press, London, vol 2, Ch 44, p 500
- Manna SC, Zangrando E, Ribas J, Chaudhuri NR (2006) *Polyhedron* 25:1779
- Nakamoto K (1997) In: *Infrared and Raman spectra of inorganic and coordination compounds*. John Wiley & Sons, 5th edn, part B, Ch III, p 70
- Coats AW, Redfern JP (1964) *Nature* 201:68
- Straszko J, Olszak Humienik M, Mozejko J (2000) *J Therm Anal* 39:935

364
365
366
367
368
369
370
371
372
373
374
375
376
377
378
379
380
381
382
383
384
385
386
387
388
389
390
391
392
393
394
395
396
397
398
399
400
401
402



Journal 10553
Article No. 1907
ISSN Code 0907

Dispatch 25-6-2007

Page: 7

FT

EPRINT

PDF

DISK